

Modifications of PVDF-co-HFP membranes for desalination by direct contact membrane distillation

By

Minwei Yao

A Thesis submitted in fulfillment for the degree of
MASTER of ENGINEERING



**University of Technology Sydney
FACULTY OF ENGINEERING**

**School of Civil and Environmental Engineering Faculty of
Engineering and Information Technology**

University of Technology, Sydney (UTS),

New South Wales, Australia

November 2015

CERTIFICATE OF AUTHORSHIP/ORIGINALITY

I certify that this thesis has not previously been submitted for a degree nor has it been submitted as part of requirements for a degree except as fully acknowledge within the text.

I also certify that the thesis has been written by me. Any help that I have received in my research work and the preparation of the thesis itself has been acknowledged. In addition, I certify that all information sources and literature used are indicated in the thesis.

Signature of candidate

Minwei Yao

ACKNOWLEDGEMENT

With the support of my university colleagues, supervisors, and friends, I am able to complete the thesis efficiently for my Master research degree. I have lots of gratitude to express here for their generous support.

Firstly, I would like to express my deep gratitude to all the other members of my small but strong membrane distillation group, composed of my supervisor Associate Professor Ho Kyong Shon, Dr. Leonard Tijing, Dr. Wang-geun Shim and Mr. Yunchul Woo. Without their wise guidance and mentoring at all levels, I cannot achieve the academic results so smoothly.

Also, I would like to give my special thanks to all the other laboratory colleagues in our water technology center. Receiving so many generous helps, knowledge and insights, and encouragement, I start to think that these two years of master study experience are the best in my life. I am very pleased to put their names here for acknowledgement: MJ Park, Alex Phuong, Youngjin, Johir, Dr. Sherub Phuntsho, Danious, Sungil, Ruoshi, Cao and many others. I would like to extend my appreciation to all the school HDR staff as well, Viona, Phyllis and Craig. Their hard work saved me lots of efforts so that I could be focused on researches.

Moreover, I would like to express my gratitude to my families. Without their understanding and encouragement, I could not imagine the life of these two years research.

And, Last but not the least; I would also sincerely acknowledge the project funding provider here. This research was supported by the Ministry of Land, Infrastructure and Transport of the Korean government under the Industrial Facilities & Infrastructure Research Program.

LIST OF ABBREVIATIONS

MD: Membrane Distillation

LMH: Liter per Square Meter per Hour

FE-SEM: Field Emission Scanning Electron Microscopy

LEP: Liquid Entry Pressure

RO: Reverse Osmosis

FO: Forward Osmosis

DCMD: Direct Contact Membrane Distillation

AGMD: Air Gap Membrane Distillation

VMD: Vacuum Membrane Distillation

SGMD: Sweeping Gas Membrane Distillation

PVDF: Polyvinylidene Fluoride

NIPS: Non-solvent-induced Phase Separation

TIPS: Thermally Induced Phase Separation

VOC: Volatile Organic Compounds

PTFE: Polytetrafluoroethylene

PP: Polypropylene

PE: Polyethene

CA: Contact Angle

PVDF-co-HFP or PH: poly (vinylidene fluoride-co-hexafluoropropylene)

PVDF-co-CTFE: poly (vinylidene difluoride-co-chlorotrifluoroethylene)

NTIPS: Nonsolvent-thermally-induced Phase Separation

CPL: ϵ -caprolactam

PS: Polystyrene

PAN: Polyacrylonitrile

PET: Polyethylene terephthalate

DMAc: Dimethylacetamide

DMSO: Dimethyl sulfoxide

NMP: N-Methyl-2-pyrrolidone

THF: Tetrahydrofuran

RH: Relative Humidity

CBD: Chemical Bath Deposition

CVD: Chemical Vapor Deposition

PPFDA: poly (1H, 1H, 2H, 2H-perfluorodecyl acrylate)

LBL: Layer-by-layer

TFPTMOS: Alkoxides 3, 3, 3-trifluoropropyltrimethoxysilane

TMOS: Tetramethyl orthosilicate

i-pp: Polypropylene

SMM: Surface Modifying Macromolecules

PS μ M: Phase Separation Micromolding

PDA: Self-polymerized Polydopamine

NCC: Nanocrystalline Cellulose

PMMA: Poly (methyl methacrylate)

FPU: Fluorine End-capped Polyurethane

SLIPS: Slippery Liquid-infused Porous Surface

PCL: Poly (Caproectone)

PPFEMA: Polymerized Perfluoroalkyl Ethyl Methacrylate

DI: Deionized

PSD: Pore Size Distribution

TABLE OF CONTENTS

ACKNOWLEDGEMENT	ii
LIST OF ABBREVIATIONS	iii
TABLE OF CONTENTS	vi
LIST OF FIGURES	ix
LIST OF TABLES	xi
ABSTRACT	xii
1. Introduction	2
1.2 Need of membrane designed for MD	3
1.3 Fabrication and modification of membrane for high LEP.....	4
1.4 Heat-press on electrospun membrane.....	5
1.5 Research objectives and scopes.....	5
1.6 Outline of thesis.....	6
2. Literature review	8
2.1 Membrane distillation.....	8
2.1.1 MD configurations	8
2.1.2 Development history of MD	11
2.1.3 Mechanism and modeling of MD	12
2.1.4 Critical conditions in MD setup.....	13
2.1.5 Hydrophobicity of membrane and wetting	16
2.1.6 Other phenomenon of MD affecting permeation performance	18
2.2 Membrane fabrication	18
2.2.1 Requirement of MD membrane	19
2.2.2 Current commercial membranes used in laboratory	20
2.2.3 Laboratory membrane fabrication via phase inversion.....	20
2.2.4 Membrane fabrication via electrospinning for MD	22
2.2.5 Membrane fabrication via other methods	22

2.3 Electrospinning.....	23
2.3.1 Development of electrospinning.....	24
2.3.2 Mechanism of electrospinning process.....	25
2.3.3 Preparation of polymer solution for electrospinning.....	26
2.3.4 Crucial parameters in electrospinning.....	27
2.4 Membrane modification for wetting resistance.....	31
2.4.1 Top-down approaches.....	32
2.4.2 Bottom-up techniques.....	35
2.4.3 Combination of top-down and bottom-up.....	36
2.5 Case study: pilot-scale MD plant in Plataforma Solar de Almeria (PSA), Spain (Guillen-Burrieza et al. 2014).....	39
2.5.1 Background.....	39
2.5.2 Membrane and membrane modules.....	40
2.5.3 Effect of fouling on characteristics of the fouled membranes.....	40
2.5.4 Discussion of cleaning strategies.....	41
3. Materials and methods.....	44
3.1 Materials.....	44
3.2 Membrane fabrication by electrospinning.....	44
3.3 Heat-press post-treatment.....	44
3.4 Characterization.....	47
3.5 Direct contact membrane distillation (DCMD) test.....	48
4. Effects of heat-press conditions.....	51
4.1 Effect of heat-press temperature on the membranes.....	51
4.1.1 Effect of heat-press temperature on MD permeation flux.....	55
4.2 Effect of heat-press pressure on the membranes.....	56
4.2.1 Effect of heat-press pressure on MD permeation flux.....	60
4.3 Effect of heat-press duration on the membranes.....	61

4.3.1 Effect of heat-press duration on MD permeation flux.....	65
5. Influence of thickness on electrospun membranes.....	67
5.1 Influence of thickness on membrane characteristics.....	67
5.2 Effects of heat-press on characteristics on membrane with various thickness.....	68
5.3 MD permeation performance with membrane having various thickness before and after heat-press	72
5.4 DCMD performance comparison with other studies using heat-pressed membranes.....	75
6. Conclusion and recommendations	78
6.1 Conclusions	78
6.2 Recommendations	79
6.2.1 Further study on heat-press conditions.....	79
6.2.2 Superhydrophobic modification with aerogel powder	80
6.2.3 Optimization of support layer and its adhesion to active layer with electrospinning	80
APPENDIX.....	82
REFERENCE.....	83

LIST OF FIGURES

Figure 1-Current water treatment technology involving usage of membrane	2
Figure 2-Processes of various MD configurations: (a) DCMD and DCMD with liquid gap; (b) VMD; (c) SGMD and thermostatic SGMD; (d) AGMD (Khayet & Matsuura 2011).	9
Figure 3-Schematic diagram of MD mechanism	12
Figure 4-SEM images of supported layers: (a) scrim-backing; (b) non-woven. (Adnan et al. 2012).....	14
Figure 5-Variou states of wetting	16
Figure 6- Schematic of electrospinning process	24
Figure 7-Schematic diagram of taylor cone in electrospinning process	25
Figure 8-SEM images of PS fibers and beads electrospun with various solvents: (a) THF; (b) Chloroform; (c) CS ₂ ; (d) NMP; (e) DMF (Eda et al. 2007).	29
Figure 9- SEM images of PTFE foils: (a) untreated; (b) treated with oxygen plasma for 60 s; (c) 120 s; (d) 10 mins (Li et al. 2007).	33
Figure 10.Illustration of assumed mechanism of heat-press on PVDF electrospun membrane.....	34
Figure 11-Membrane modules used in pilot AGMD plant at PSA.....	39
Figure 12-Impact of fouling on the major parameters of MD membranes	40
Figure 13-Comparison of CA, LEP, and BP with various cleaning strategies	41
Figure 14-Schematic diagram of DCMD process used in this study.....	49
Figure 15- SEM images of as-spun and heat-pressed PH membrane at magnifications of 10 K and 50 K: (a)as-spun neat membrane (Neat); membranes heat-pressed under (b) 140 °C (M0); (c) 150 °C (M1); and (d) 160 °C (M2).	51
Figure 16- Pore size distributions of as-spun and membrane samples heat-pressed under various temperatures.	52
Figure 17- Effects of temperature on thickness, porosity and contact angle	53
Figure 18-Flux comparisons of electrospun membranes heat-pressed at various temperatures	56
Figure 19-SEM images of heat-pressed PH membrane at magnifications of 10 K and 50 K: membranes heat-pressed under (a) 0.7 kPa (M1-A); (b) 2.2 kPa (M1-B); (c) 6.5 kPa (M1-C), and; (d) 9.8 kPa (M1-D).....	57

Figure 20- Pore size distributions of as-spun and membrane samples heat-pressed under various pressures.	58
Figure 21-Effects of pressure on thickness, porosity and contact angle	58
Figure 22- Flux comparisons of electrospun membranes heat-pressed at various pressures.....	61
Figure 23- SEM images of heat-pressed PH membrane at magnifications of 10 K and 50 K: membranes heat-pressed for (a) 1 h (M1-B-1); (b) 2 h (M1-B-2); (c) 4 h (M1-B-3); (d) 8 h (M1-B-4).....	62
Figure 24-Pore size distributions of as-spun and membrane samples heat-pressed for various durations.	63
Figure 25-Effects of heat-press pressure on thickness, porosity and contact angle.....	63
Figure 26- Flux comparisons of electrospun membranes heat-pressed at various durations.....	65
Figure 27-Comparison of CA and porosity of electrospun membrane with various thicknesses	68
Figure 28-Representative SEM cross section images of as-spun, PH3 (a: 400 K) and heat-pressed membrane, PH3' (b: 350 K; c: 1500 K).....	69
Figure 29-Effects of heat-press with optimal conditions on porosity and contact angles of membranes with various thicknesses.....	71
Figure 30-Comparison of DCMD permeation performance of selected membrane samples.....	74

LIST OF TABLES

Table 1- Key parameters of membranes that affect MD permeation performance.....	19
Table 2-Key properties of the unused PTFE membranes	40
Table 3-Heat-press conditions and name conventions used in the present study.	46
Table 4- Characteristics of the membranes after heat-press at different temperatures	54
Table 5-Characteristics of the membranes after heat-press at different pressures.....	59
Table 6-Characteristics of the membranes after heat-press at different durations.....	64
Table 7-Comparison of membrane characteristics with various thicknesses.....	67
Table 8-Characteristics of the membranes with various thicknesses after heat-press	70
Table 9- Comparison of heat-pressed MD flat-sheet membranes for desalination with commercial PVDF membrane.....	75

ABSTRACT

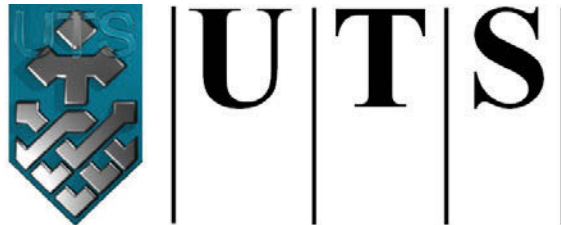
Membrane distillation (MD) has been considered as a promising next-generation technology for desalination because of its high efficiency regarding permeation performance and energy consumption. The foundation of MD mechanism is based on membrane contact rather than membrane permeation process. It means that only vapor molecular can pass through the membrane sheet rather than liquid water. In recent years, electrospun polymer fiber membranes are widely studied due to their high porosity, high hydrophobicity, controllable fiber distribution, and ease of fabrication and modification. However, because such membranes are susceptible to wetting in long-term operation, the robustness of these membranes are still not guaranteed, especially when the MD system is applied with relatively high feed temperature. Heat-press treatment is a simple and effective procedure to improve the morphology and thus characteristics of polymer membranes. More than 8 h stable MD performance with an average flux of 34 liters per square meter per hour (LMH) and 99.99% salt rejections may be achieved with heat-pressed membranes, while the membranes without the post-treatment can easily become wetted only in half an hour. In the current study, three controllable conditions during heat-press (which are temperature, pressure, and duration) were investigated, and their effects on the morphology and characteristics were carried out in separate stages, which would be addressed in detail in this report.

In stage 1, by applying heat-press on membrane with various temperatures, mechanical strength was proved to be improved greatly. Maximal stress of the electrospun membrane can be greatly increased from 11.7 to 103.9 MPa once samples were heat-pressed at 160 °C. However, the thickness of the membrane could be decreased significantly from 45 to 31 μm because of partially melting of the films, which could be observed through the relative FE-SEM images analysis. In stage 2, it was found out that increase in pressure from 0.7 to 9.8 kPa in heat-press process could result in the further reduction of surface pore size from 0.49 to 0.42 μm . Generally, heat-pressed membranes lost some hydrophobicity as the surface roughness decreased owing to premelting phenomenon, and the loss of hydrophobicity was confirmed by the reduction of contact angle. A decrease from 152° to 139° could be observed when membranes heat-pressed for 8 h. Nevertheless, the loss of hydrophobicity was offset by the increase in mechanical strengths. Impressive improvement of both tensile strength and LEP could be observed after heat-press. Therefore, based on the improvement of LEP and

mechanical, better resistance against wetting could be achieved in MD process. In stage 3, it was found that longer duration of heat-press could improve the membrane morphology and thus its characteristics as well. Membrane that had been heat-pressed for 8 h had smaller pore size and higher LEP than the ones heat-pressed for shorter duration. Furthermore, influence of membrane thickness was investigated, and optimum treatment conditions for the membrane were developed in the study. Then, the optimum conditions of heat-press were applied on the electrospun membranes with various thicknesses to verify whether the technique could be applied on thicker membranes and what was the degree of its effectiveness.

CHAPTER 1

INTRODUCTION



University of Technology Sydney
FACULTY OF ENGINEERING

1. Introduction

Water and energy has been recognized as the top two major challenges in today's and coming future's world. Nowadays, lots of freshwater resources are becoming unrenusable due to climate change and massive human activities. Moreover, the water shortage issues are much more serious in some countries with bad climate and poor economic conditions, so lack of clean water is a great threat to the hygiene of local residents (Tijing et al. 2014b).

Desalination is a viable option to obtain freshwater supply stably for coastal countries that are short of fresh water, and, currently, reverse osmosis (RO) is widely applied in desalination treatment plant due to its relatively high energy efficiency compared with thermal process. However, the capital and maintenance costs of RO plants are high and large amounts of electrical energy is required for generating high pressure in the process. In addition, RO has negative impact on global environment via carbon dioxide as the generation of electrical energy is very likely fossil-fuel based. RO brine disposal is another major issue which is widely concerned by the society due to their impact on the local ecological system. Therefore, development of new generations of technology is strongly needed for replacement of RO technology (Alkhudhiri et al. 2012).

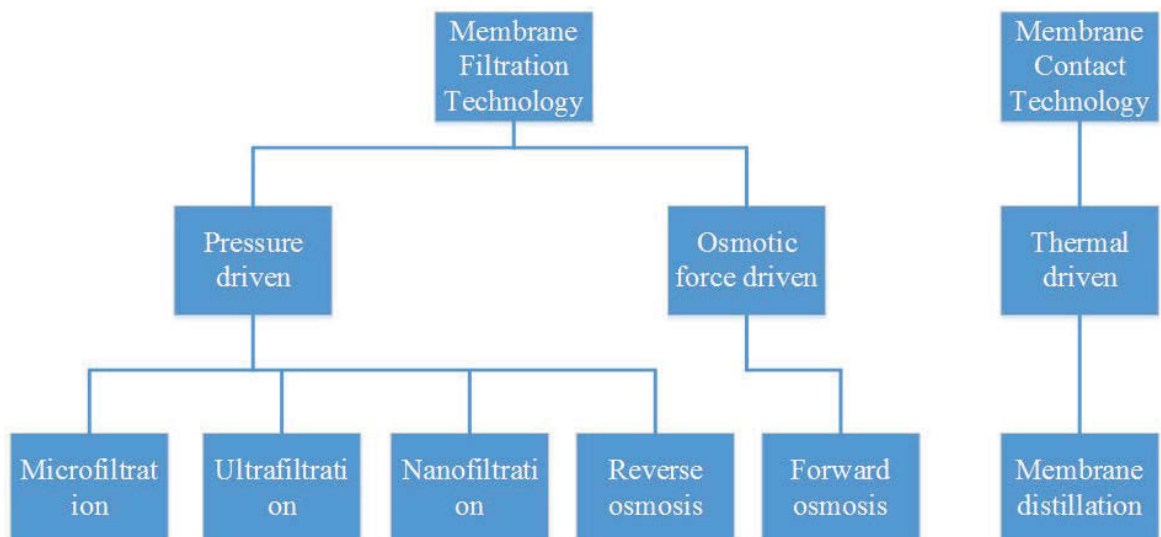


Figure 1-Current water treatment technology involving usage of membrane

Membrane distillation (MD) has been considered as a promising next-generation technology for desalination because of its higher efficiency and permeation performance

independent on the salt concentration. The potential usage of low grade heat such as industrial waste heat or solar heat makes it a very attractive option. Fig. 1 states that the MD process is a separation process based on evaporation through pores of a hydrophobic membrane (Tian et al. 2014b; Geng et al. 2014; Boubakri et al. 2014; Alkhudhiri et al. 2013), which is fundamentally different from the other membrane filtration technology (including the state-of-art RO and emerging FO). The driving force of the MD is generated by the pressure of vapor formed by a difference in temperature between solutions on both sides of a hydrophobic membrane (Fan & Peng 2012a). Evaporation of liquid water occurs at the membrane interface with the contact of hot solution (Dong et al. 2014). Under the pressure, the vapor then diffuses through the pores to the other side of interface where it condenses by cool permeate side (Tomaszewska et al. 1994).

MD is generally applied in four principal configurations: Direct Contact Membrane Distillation (DCMD), Air Gap Membrane Distillation (AGMD), Vacuum Membrane Distillation (VMD), and Sweeping Gas Membrane Distillation (SGMD) (Alkhudhiri et al. 2012; Fan & Peng 2012a; Geng et al. 2014; Koo et al. 2013). This research is focusing on DCMD configuration due to the convenience of setup and relatively stable performance regarding flux and salt rejections.

1.2 Need of membrane designed for MD

As an emerging technology, MD has not yet been widely applied in the global water industry due to lack of suitable membranes for long-term operation. Qualities such as strong resistance against wetting and fouling is lacking in current available membranes on the market (Francis et al. 2014). At the moment, membranes designed for microfiltration are utilized in MD and they are mainly made of polyvinylidene fluoride (PVDF) due to its high hydrophobicity, good solubility in common solvent, and high resistance against chemicals and heat (Liao et al. 2013b; Hwang et al. 2011; Dong et al. 2014). Non-solvent-induced phase separation (NIPS) and thermally induced phase separation (TIPS) are the two most common approaches exercised to fabricate membranes. However, these membranes are still not good enough for MD processes due to their low flux performance and susceptibility to wetting (Ge et al. 2014; Song & Jiang 2013; Nghiem & Cath 2011; Goh et al. 2013). Thus, recently there is an increasing trend of membrane fabrication with new approaches for MD. Zhang et al.

noted that the main challenges for membranes used in MD are to design features including both porous structure and superhydrophobic surface for good filtration performance and high LEP for long-term operation (Lalia et al. 2013; Francis et al. 2013; Song & Jiang 2013; Zhang et al. 2011). Electrospun membranes possess many appropriate advantages involving high hydrophobicity, high porosity, adjustable pore size, and membrane thickness, which make them attractive candidates as MD membrane (Feng et al. 2013; Francis et al. 2013; Alkhudhiri et al. 2012). Compared with NIPS and TIPS, electrospinning is a relatively simple technique to fabricate membrane. By applying high electric fields on a polymer solution, millions of fibers are formed joining together to become nonwoven membrane sheet, collected on the rotating collector (Tijing et al. 2014a; Feng et al. 2013). Though electrospun membranes have many attractive properties for MD, however, they had some drawbacks limiting its performance including relatively big pore sizes, low mechanical properties, and LEP compared with the membranes fabricated by casting methods. Therefore, there is a requirement to improve these characteristics without sacrificing high porosity and hydrophobicity through some membrane modification approaches.

1.3 Fabrication and modification of membrane for high LEP

To increase the resistance against membrane wetting in MD process in long-term operation, MD membranes should have higher LEP after fabrication or modification. Currently there are several ways to increase LEP of membranes. However, most of those approaches have some drawbacks which offset the benefits. Decrease in membrane pore size can greatly increase membrane LEP, but the pathway for vapor permeation is greatly narrowed and hence the mass transfer coefficient may be decreased, which is not favored. Increase in thickness of membrane can also increase the LEP value, but the permeation efficiency of MD may also be decreased (Guillen-Burrieza et al. 2015). Incorporation of some specific additives into the polymer solution such as graphene or carbon nanotube can increase LEP, but it may decrease the mechanical strength of the membrane as the additives particle usually have weak connection with the polymers. Another method of increasing LEP value is to enhance hydrophobicity of the membrane (Dong et al. 2014), which can be achieved by surface modification.

1.4 Heat-press on electrospun membrane

Apart from the methods indicated in last section, heat-press, a simple post-treatment method, can be applied to improve LEP of membranes. In practices, heat-press is a common polymer modification approach to improve the morphology and thus characteristics of the membrane to meet the requirement of the applications. It is found that successful application of heat-press on MD membrane can enhance its capability against wetting (Liao et al. 2014b; Lalia et al. 2013; Francis et al. 2013; Alkhudhiri et al. 2012). Liao and Tijing stated that heat-press could enhance the desalination performance by changing mechanical structure of the membranes into favorable way (Tijing et al. 2014a; Liao et al. 2013b). It was found that when the membrane was placed under a pressure for some time at certain temperature just below melting point of the polymer, the polymer nanofibers tends to fuse together at the interlay point, and the pore size tended to be decreased due to increase in fiber size. Therefore, the internal structure of membrane transformed from open network to dense porous structure, and it became hard for water molecular to penetrate the membrane matrix. It is expected that higher LEP, higher mechanical tensile strength, less thickness, smaller average pore size, and more uniform distribution of the pore size can be obtained via this technique. However, the conditions of the heat-process have not been fully investigated and optimized, and only few assumptions were given to explain the mechanism. In later sections of the thesis, effects of various conditions of heat-press, which are temperature, pressure, and duration, are examined and addressed, and the mechanism of heat-press is explored as well.

1.5 Research objectives and scopes

The main purpose of this study is to improve the electrospun membranes characteristics regarding both permeation flux and long term operation performance against wetting. Therefore, methods of membrane fabrication and modification have been fully researched and summarized in terms of obtaining a membrane with high LEP or hydrophobicity. Heat-press treatment has been carefully developed to improve the characteristics of membranes for better permeation performance. One of the main objectives of this study is to investigate effects of various heat-press conditions on the membrane characteristics, morphology of membrane surfaces and optimal heat-press parameters should be determined on the basis of the findings. Moreover, electrospun membranes with various thicknesses will be applied with the optimal conditions, and

best performance regarding permeation rate and salt rejection will be compared with commercial membranes and other heat-pressed electrospun membranes in previous researches.

1.6 Outline of thesis

This study is focusing on the improvement of electrospun membrane for higher LEP, hydrophobicity, and thus better MD permeation performance. Introduction in Chapter 1 describes the background and current trend of the MD process. Membrane fabrication and modification for higher hydrophobicity are also mentioned as the solution to solve the MD issues. It also states the scope and outline of this thesis. Chapter 2 is a mini summary of a literature review stating the history, mechanism, configuration, approaches, and dominant affecting parameters in MD, electrospinning, and membrane modification. Chapter 3 suggests the experimental materials, devices, relative models, and methods of experiments regarding both characteristics measurement and MD performance. Chapter 4 shows the experimental results and discussions in terms of effects of heat-press conditions on the electrospun membrane which is applied for desalination by DCMD. Before or after optimal heat-press treatment, influence of membrane thickness will be examined in Chapter 5. Chapter 6 is the conclusion of the thesis, stating the potentials of the approaches and future possible research development and their relative applications.

CHAPTER 2

LITERATURE REVIEW



University of Technology Sydney
FACULTY OF ENGINEERING

2. Literature review

2.1 Membrane distillation

Membrane distillation (MD), one of non-isothermal membrane separation technologies, has been developed for more than 50 years (Alkudhiri et al. 2012). However, MD is still lack of adequate industrial implementations and requires further studies (Tijing et al. 2014a). The separation of the liquid from the impurities are based on the vapor pressure caused by the difference of the temperature of the vapor between the feed side and the permeate side, and the mechanism will be further discussed in Section 2.1.2. Due to the uniqueness of this process, MD is fundamentally different from other membrane process in which liquid molecules passes through the membrane instead of vapor. Therefore, with these unique advantages (e.g., nearly 100% non-volatile impurities rejection), MD is widely accepted as the next generation membrane separation processes molecules (Peñate & García-Rodríguez 2012).

2.1.1 MD configurations

Four major MD configurations have been widely recognized, which are: (1) direct contact membrane distillation (DCMD), (2) sweeping gas membrane distillation (SWMD), (3) vacuum membrane distillation (VMD) and (4) air gap membrane distillation (AGMD) (Alkudhiri et al. 2012). Among all the configurations, the design of feed side in the membranes modules are similar, the difference varies in the setup of permeate side by how the condensations arranged. Driving force of the vapor molecules is the force generated from difference of temperature between the feed and permeate side. Different configurations of permeate side can have impressive effects on the MD process (Tijing et al. 2014a).

These four configurations have their own advantages and drawbacks, which means they have distinct application suitability (e.g., desalination, environmental/waste clean-up, food, medical, etc.). The processes of the four configurations are shown in Fig. 2 below.

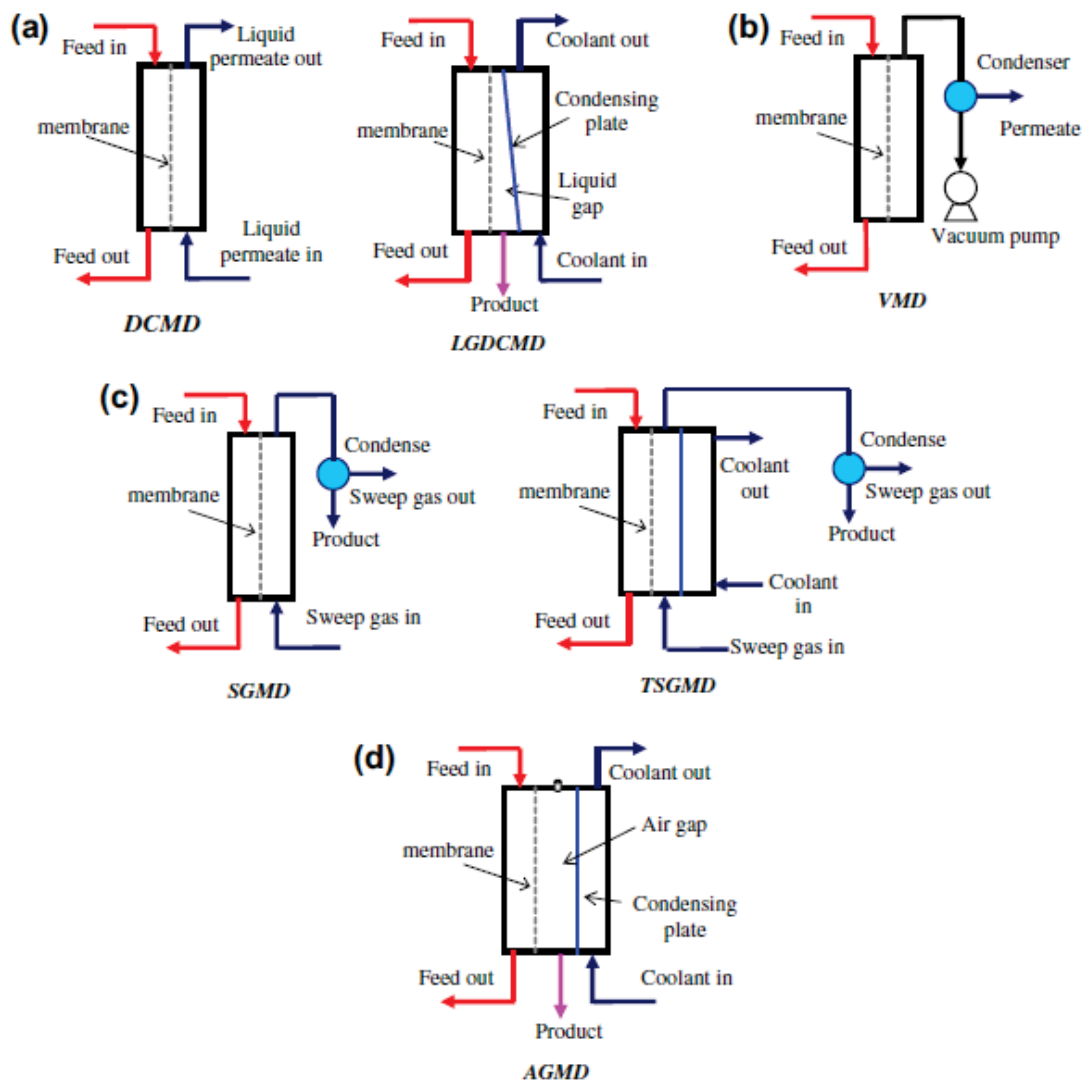


Figure 2-Processes of various MD configurations: (a) DCMD and DCMD with liquid gap; (b) VMD; (c) SGMD and thermostatic SGMD; (d) AGMD. (adapted from Khayet & Matsuura 2011).

Although SGMD was mentioned and patented in the earliest stage of studies in MD history, however, up to 2015, the number of papers published regarding application of SGMD is the lowest among all types of the configurations (Tijing et al. 2014a). The requirement of external condenser and additional cold sweeping gas source is account for the unpopularity as they can increase both cost and complexity of system design. Nevertheless, SWMD has a great perspective for the future research owing to tis advantages. It is noted that SWMD has higher mass transfer coefficient which can lead to higher permeate flux compared with DCMD while maintaining a relatively low conductive heat loss (HL) comparable to AGMD. The other benefit of SGMD is that

there is nearly no risk of pore wetting from the permeate side, when applied for removal of organic compounds from water.

Similar to SGMD, VMD configuration requires an external condenser, which can result in higher design complexity and costs. For that reason, VMD is the second least topics that have been studied. Because the air in the membrane pores is removed by applying a continuous vacuum on the permeate side, mass transfer resistance can be greatly reduced, as diffusion occurring inside the membranes pores at the feed/membrane interface is favored. The other benefit of VMD is its high thermal efficiency, that means conductive HL through the membrane is minimalized by applying vacuum on the permeate side which works as insulation (Fan & Peng 2012b). However, VMD requires the applied membrane to have much higher LEP than other configuration as vacuum applied on the membrane increases the pressure greatly on the membrane.

The most studied configuration till now is DCMD, due to its simple setup as both membrane and condensation plate can be incorporated into one single MD module. The mass transfer coefficient is usually higher than other configurations as there is no air, other gas, or gap in between condenser and membrane; therefore the vapor can condense directly after go through the membrane (Manawi et al. 2014). However, due to lack of insulation, DCMD has highest HL among all the configurations, and it result in higher requirement of membrane fabrication and module design to improve the thermal energy efficiency (Zhang et al. 2013a). Also, membrane pore wetting problems in DCMD is more severe than other configurations. Because permeate is in direct contact with the membrane, pore wetting can result in both impressive reduction of impurity rejection and permeation flux (Wang & Chung 2015).

The last configuration is AGMD, and it is secondary most studied among all. Similar to DCMD, the condenser plate can be installed in the same membrane module. The only difference between AGMD and DCMD is a narrow air gap between membrane and condensation plate. The vapor condenses by natural convection in the air gap after diffusion through the membrane (Alkhudhiri et al. 2013). The LEP requirement of AGMD membrane is higher because higher difference of temperature (for higher vapor force) is usually applied in this configuration due to its relatively low permeation efficiency. However, AGMD have some unique benefits that other configurations do not have. Firstly, AGMD has the most stable permeation performance regarding long-

term operation than other configurations (Tian et al. 2014a). The reason is that the external pressure applied on the membrane is relatively low, as the condenser is not in direct contact with the membrane and there is no external vacuum force applied on the membrane surface. Secondly, AGMD has lower HL due to the existing of stagnant air gap in the permeate side, improving the thermal efficiency greatly (Warsinger et al. 2015). The third advantage is that AGMD can be utilized in some applications, while DCMD are not able to, such as removal of volatile organic compounds (VOCs) from aqueous solution (Tijing et al. 2014a).

2.1.2 Development history of MD

In 1963, Bodell filed the first MD patent, and five years later, he developed another patents using SGMD for desalination with a novel apparatus. Both theoretical and experimental studies had been mentioned in his paper. Also, VMD was first time addressed in this paper as an alternative configuration where vacuum was applied on the permeate side (Khayet & Matsuura 2011).

In 1967, Findley tried various membrane materials including aluminum foil, cellophane, glass fibers, paper plate, diatomaceous earth mat, nylon, paper hot cup, and gum wood to coat on the membranes for a hydrophobic surface of the membrane. Hydrophobic materials such as Teflon and Silicone were examined as well. By doing these tests, he concluded that a long life membrane lasting in high temperature could be economical. Also, in this year, the concept of using waste heat and solar heat for MD was also proposed in the 2nd European Symposium on Fresh Water from the Sea held in Athens (Khayet & Matsuura 2011).

Soon after, MD lost lots of attention in research field due to its much lower permeation performance than reverse osmosis (RO) process. The interests in MD recovered in the early 1980s as novel membranes with better characteristics become available (e.g. Gore-Tex membrane). Innovative types of MD membranes designs and their relative apparatuses had also been developed, which included composite membrane comprising both hydrophobic and hydrophilic membranes. Later the same group of researchers improved the dual-layer apparatus by coating a thin non-porous hydrophilic layer on one side of the hydrophobic membrane. Also, fluoro-substituted vinyl polymers such as polytetrafluoroethylene (PTFE) and polyvinylidene fluoride (PVDF) were mostly proposed for the hydrophobic layers (Khayet & Matsuura 2011).

After that time, the interests in MD grew rapidly while most of them were academic oriented, which was obvious with the increasing number of papers referenced in MD reviews. There were only 87 papers referenced in the 1997 MD review by Lawson and Lloyd, and just in ten years, the numbers increased to 168 in the MD review by El-Bourawi (2006). Currently, the actually number of published paper regarding MD in international journals was more than 500 (Khayet & Matsuura 2011).

2.1.3 Mechanism and modeling of MD

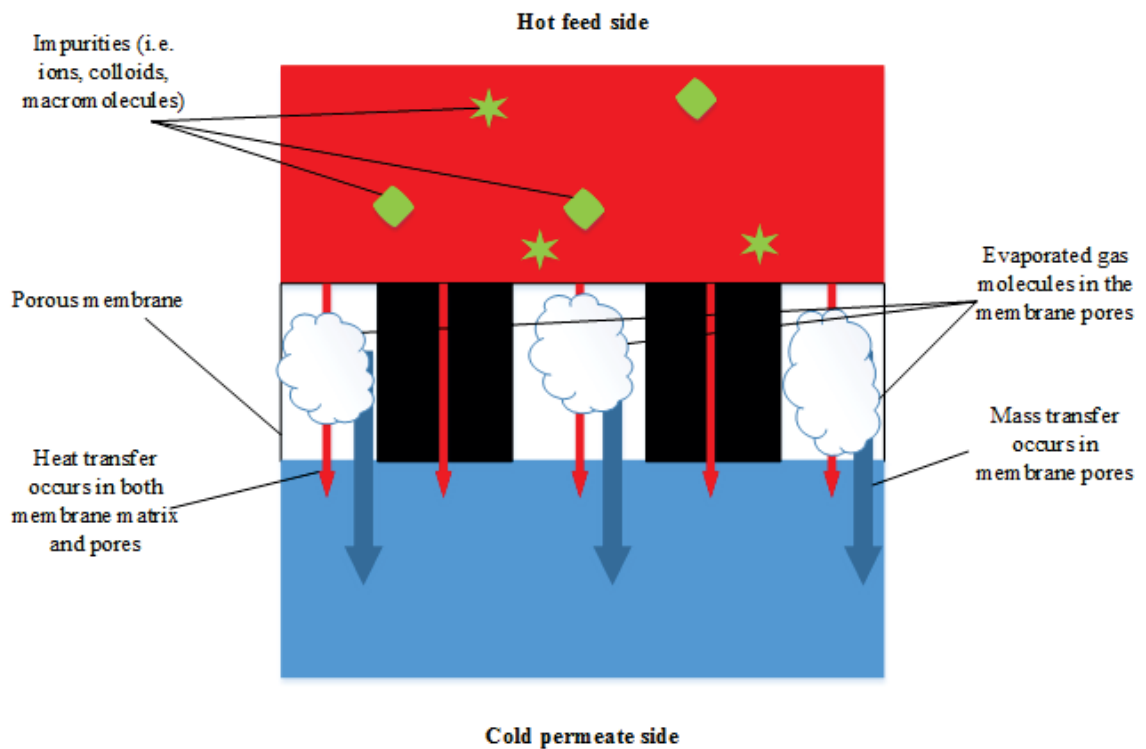


Figure 3-Schematic diagram of MD mechanism

Fig. 3 showed the mechanism of MD (DCMD, specifically). In process of MD, both mass and thermal transfers occur simultaneously. While mass of vapor is transferring through the pores of the membrane only, heat in the feed side is transferring through both the membrane matrix and its pores by conduction (Alkudhiri et al. 2012). It is worth mentioning that only water vapor or volatile compounds are transferred through the membrane from the feed side to the permeate side, and the liquid water molecular is blocked by the hydrophobic membrane on the feed side. The mechanism is fundamentally varied from other membrane processes (e.g. microfiltration) in which the feed water passes through the membrane pores of small sizes for filtering the impurities.

The other difference is that MD is a non-isothermal process which means that the temperatures in feed and permeate sides are not identical.

Transport of gases and vapors through porous membranes have been extensively studied and various models have been developed to understand and estimate the performance of mass transfer with different mechanisms. Depending on the ratios between free paths of specific vapor molecules and mean membrane pore sizes, several different types of mechanism models can be used for analysis and prediction, including Knudsen flow model, viscous or flow model, ordinary molecular diffusion model, and/or dusty gas model (which are a summary of above models) (Wu et al. 2014; Fan & Peng 2012a). It is worth noting that different equations and their relative parameters were used in various MD configurations. For instance, due to the existing of stagnant air gap in AGMD, Stefan-Maxwell equations were used to describe this multicomponent mass transfer in the systems.

Heat transfer occurs by conduction through both membrane matrix and vapor molecules in the pores. The heat transfer is found to be driven by latent heat. Extensive researches have been carried out and models have been developed, and the equation for heat transfer is displayed below in various studies:

$$Q_m = \frac{k_m}{\delta} (T_{m,f} - T_{m,p}) + \sum_{i=1}^s J_i^t \Delta H_{v,i}$$

where k_m is the thermal conductivity of the membrane, δ is the membrane thickness, $\Delta H_{v,i}$ is the evaporation enthalpy of the species i of the transmembrane flux J_i^t , s is the number of permeated components, $T_{m,f}$ is the temperature of the feed aqueous solution at the membrane surface and $T_{m,p}$ is the temperature of the permeate aqueous solution at the membrane surface (Chen et al. 2014; Fard et al. 2015).

2.1.4 Critical conditions in MD setup

For optimizing the permeation performance of MD and energy efficiency, operational parameters have been comprehensively studied. It is found that feed temperature, permeate temperature, temperature difference, flow rate, current mode, and usage of support layer and space play important roles in membrane permeation performance (Manawi et al. 2014). Normally, increasing temperature difference between the permeate side and feed side can resulting in higher flux performance and energy

efficiency. However, when temperature difference is maintained same, compared with decreasing the permeate temperature, increasing feed temperature may improve the flux and energy efficiency much more (Francis et al. 2014). Flow rate also has strong effect on the permeation performance and energy efficiency. Increasing flow rate can increase the permeate flux greatly due to reduction of both thermal and concentration polarizations (Hwang et al. 2011). However, the energy efficiency improvement is not as obvious as flow rate. Performance of MD running in co-current and counter-current were also compared. Although minor difference had been observed between the two running mode (Hwang et al. 2011), counter-current had slightly better overall performance and even distribution of thermal pressure through the membranes, which made it more favorable in the MD researches (Manawi et al. 2014). Besides, using support layer could decrease the permeation flux and energy efficiency, because additional layer could lead to increase in reduction of porosity (Francis et al. 2014).

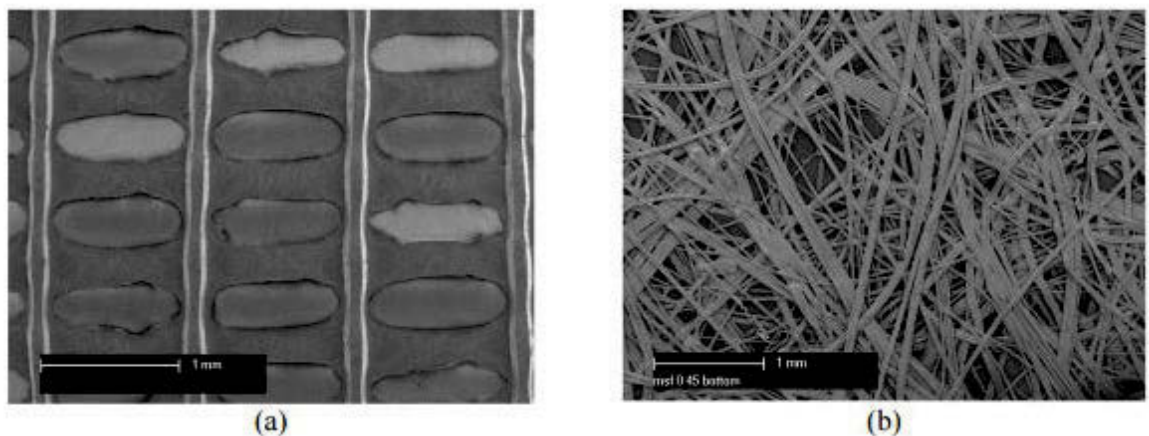


Figure 4-SEM images of supported layers: (a) scrim-backing; (b) non-woven. (adapted from Adnan et al. 2012)

Further researches on support layer found that supporting layer with different materials and microstructure had very distinct effects on the permeation performance and energy efficiency (Fig. 4). Regarding the microstructure of membrane, some researchers claimed that support layers with fiber structures had better effects on performance than non-woven fabric and scrim structures (Shirazi et al. 2014). Some other researcher agreed that support layer with scrim-back could increase temperature polarization more than non-woven support layer, and thus it had lower permeation performance and energy efficiency (Adnan et al. 2012). Polymer material of support layer can affect the permeation performance as well. Due to its higher heat coefficient, support layer made

of polypropylene (PP) had better performance and energy efficiency than the one made of polyethylene (PE) (Jeong et al. 2014). Whatever the microstructure and material of the support layer, it is recognized that the MD module using support layer has lower performance and energy efficiency than the one without support layer when other conditions kept same. Spacer was mentioned in literature as well. Some researchers claimed that by using spacers in the MD modules, the permeation flux improved greatly. It was found that spacer was able to destabilize the flow and create eddy currents in the laminar regime, so the momentum, heat, and mass transfer would be enhanced (Manawi et al. 2014; Razmjou et al. 2012). Hwang argued that the salt concentration can decrease the flux greatly due to the polarization layers formed on the membranes (Hwang et al. 2011), while Fard stated that, in larger scale plant, the feed salinity had little effects on the permeation performance over extended range of feed temperature (40 – 80°C) (Fard et al. 2015).

2.1.5 Hydrophobicity of membrane and wetting

Based on the unique mechanism of MD, membrane with hydrophobic surface is required for the process as only water vapor should pass through it rather than liquid water. Whether the membrane is hydrophobic is mainly decided by the surface tension of the materials, while high roughness of surface morphology can greatly increase the hydrophobicity (or hydrophilicity if the materials have high surface tension). Based on the effect of both roughness and surface energy, there may be two distinct states, which are Wenzel and Cassie-Baxter (Li et al. 2007), and an intermediate state between them may exist (Fig. 5).

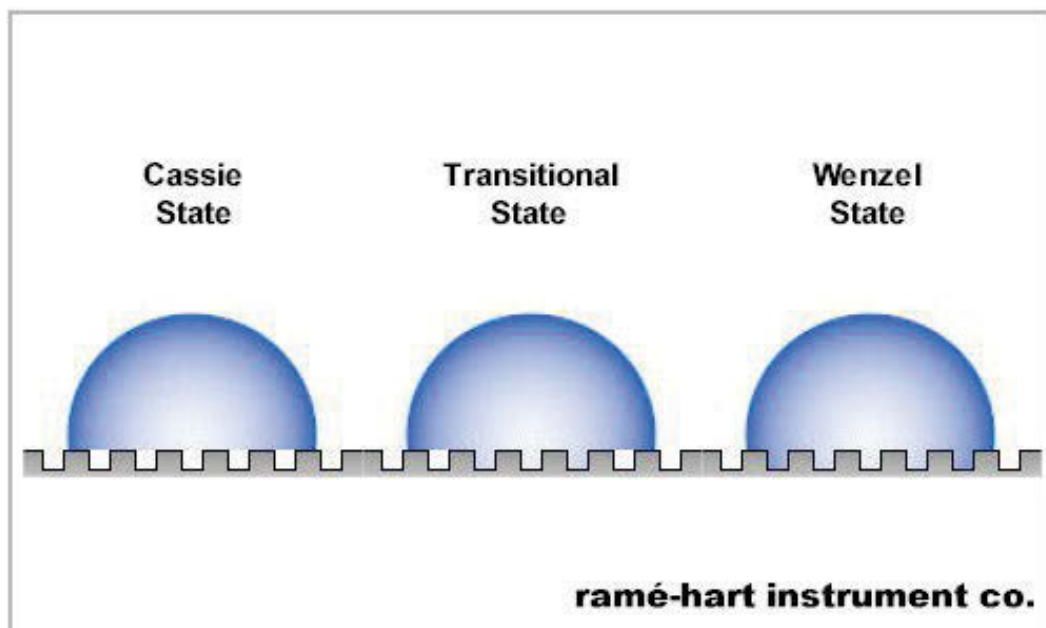


Figure 5-Variou states of wetting

While Cassie-Baxter state means the suspension of the water droplets on the asperities, Wenzel state means penetration of the asperities. Therefore, Cassie-Baxter surface has higher contact angle (CA) and the water droplet on the surface can slide away easily, while Wenzel surface has lower CA and a much higher sliding angle. The difference of two states is caused by the much higher roughness of the Cassie-Baxter surface. Usually, Cassie-Baxter is composed of both micro and nano scale structures and thus lots of air pocket can exist on the surface, leading to great decrease in the water-solid interface area. It is also worth noting that under high pressure, some Cassie-Baxter state may be converted to Wenzel state as the trapped air may be released, leading to increase in interface area between water-solid (Acatay et al. 2004).

In MD, wetting is recognized as one of top challenges (Wang & Chung 2015). When liquid water molecules pass through the membrane in long-term operation under both hydraulic and vapor pressure, the phenomenon is defined as “pore wetting” (Guillen-Burrieza et al. 2015). When wetting occurs, permeation of MD will increase greatly, and quality of permeate deteriorate rapidly. It is because that liquid has much high mass transfer rate than vapor molecules, and when wetting occurs, the feed water can pass through the wetted membrane directly. Also, the impurities dissolved in feed solution can pass across the membranes to the permeate side within the feed water (Wang & Chung 2015). This phenomenon only occurs in MD because mass transfer is expected to be based on the movement of vapor molecules rather than liquid.

Usually, membrane wetting occurs after long-term operation, as the trapped air on the membrane surface may be gradually released under the pressure induced by the thermal difference. Risks of wetting come from both liquid penetration and vapor condensation in the membrane.

Except surface roughness and liquid entry pressure (LEP), fibers, pores, and their ratio play important role in the wetting patterns as well (Guillen-Burrieza et al. 2015). Due to its relatively large pore size and low tensile strength (weak against deformation which may result in larger pores), electrospun membrane without treatment tends to become wetted easily. It was found that PVDF membrane without any modification could suffer wetting only in an hour after operation started (Liao et al. 2013a) It was also mentioned that increase in thickness could increase wetting resistance, because LEP would be increased when membrane thickness increased .

At high feed temperature, incorporation of fouling and wetting is another challenge in MD. Due to the hydrophobic adsorption between organic foulants and membrane, a cake fouling layer, the dominant fouling type, can be easily formed on the MD membrane in seawater desalination (Zhang et al. 2013b). Ironically, the cake fouling layer could prevent partially wetting for some extent although it decreased the flux. When Calcium ion was introduced into the feed solution, however, the membrane would suffer more aggravated wetting due to the formation of calcium-humic complexes which formed a tighter bridge between the membrane surface and humic acid. When partially wetting occurs, the permeate quality could be worsened rapidly,

due to an assumed “adsorption-desorption” mechanism (Meng et al. 2014). Also, crystallization of salts might occur when slower wetting happened.

Modification of membrane for better wetting resistance will be extensively discussed in later sections.

2.1.6 Other phenomenon of MD affecting permeation performance

Often occurring simultaneously, there are two types of phenomenon which can affect the performance of membrane in negative ways: temperature and concentration polarization, and inorganic, organic and bio fouling (Adnan et al. 2012). Similar to other membrane processes, there will be an adjoining fluid boundary layers next to the membrane surface in both permeate and feed sides. Along the boundary from inlet to outlet of the flow, the temperature will decrease gradually on the feed side and increase on the permeate side, leading to the decrease of vapor pressure force (Chen et al. 2014; Francis et al. 2014). This is called temperature polarization. Also, the concentration of salts on the feed side may be increased as impurities become accumulated, and it is assumed that it will affect the evaporation rate of liquid in a negative way, leading to decrease in vapor flux and drive force (Ge et al. 2014; Hwang et al. 2011; Fard et al. 2015). This is called concentration polarization. Both temperature and concentration polarization will decrease the permeation performance in MD, so the phenomenon should be minimized by both engineering design and control.

Inorganic, organic, and bio fouling are expected to be less severe in MD than in RO and other pressure driven membrane technologies for water treatment as no external high pressure is applied on the membranes in the feed side. However, due to hydrophobicity of the membranes, foulant is more easily getting attached on the membranes than their hydrophilic counterparts (Kang & Cao 2014; Ge et al. 2014; Meng et al. 2014). Moreover, fouling and pore wetting may interact with each other and make severity and complexity of the phenomenon higher (Ge et al. 2014). Therefore, fouling control is a major challenge in the progress of MD commercialization and requires great amounts of further research.

2.2 Membrane fabrication

Due to the shortage of suitable membrane for MD process, currently membrane fabrication has become one of major focuses in research field regarding MD (Khayet &

Matsuura 2011; Tijing et al. 2014b). Researchers are working hard on fabricating and modifying the membranes to achieve required properties via their newly developed or improved approaches.

2.2.1 Requirement of MD membrane

To achieve good permeation performance, the membranes used in MD should have characteristics distinguished from the ones used in other membrane process. These properties and their relative purposes are summarized in the Table 1 (Khayet & Matsuura 2011).

Table 1- Key parameters of membranes that affect MD permeation performance

Characteristics	Requirement	Purpose
Surface hydrophobicity	Higher is better	Prevent membrane wetting
Porosity	Higher is better	Wider gas pathway for better permeation performance
Surface pore size	Higher is better	Increase evaporation rate for better permeation flux
Pore size distribution	Narrow	Prevent wetting; Obtain stable flux
Average pore size	Appropriate (0.1 – 0.8 μm)	When pore size is too big, it will be easily wetted; when pore size is too small, the permeation flux will be very low as water vapor becomes hard to pass through.
Thickness	Appropriate (30-150 μm)	When membrane is too thin, it will be wetted easily; when membrane is too thick, the permeation flux will be very low due to narrower average pore size and longer gas pathway.
Liquid entry pressure (LEP)	Higher is better	Prevent water molecular penetrating the membranes owing to vapor pressure
Mechanical strength	Higher is better	Improve robustness for long-term operation
Thermal resistance	Higher is better	Improve thermal efficiency to reduce operational cost

2.2.2 Current commercial membranes used in laboratory

Hydrophobic commercial membranes have been widely used in MD system although their origin purpose is for microfiltration. As mentioned in previous section, fluoro-substituted polymer, such as PVDF and PTFE, is widely used as the membrane matrix material due to their low surface tension, which can form hydrophobic surface provided the surface has high enough roughness (Alkhudhiri et al. 2012). Also, membranes made of PVDF and PTFE have very high resistance against heat and chemical, and they have good mechanical properties as well, making them suitable for being used in long-term MD operation process (Feng et al. 2013).

Currently, there are a range of commercial hydrophobic membranes available on the market, manufactured by Millipore, Gore-Tex, Gelman, and etc. (Khayet & Matsuura 2011). Although all of these membranes are designed for the use of microfiltration, a wide range of pore size, porosity and thickness can be selected, which means that some of them, with or without modification might, be fit for MD. Usually, commercial membranes are composed of an active and a support layer for better mechanical strength.

2.2.3 Laboratory membrane fabrication via phase inversion

Due to its low surface tension and thus high hydrophobicity, PVDF, along with its copolymer such as poly (vinylidene fluoride-co-hexafluoropropylene) (PVDF-co-HFP), poly (vinylidene difluoride-co-chlorotrifluoroethylene) (PVDF-co-CTFE), and etc., has become the major semi-crystalline organic polymer used for membrane fabrication and are being extensively studied in the laboratories (Liu et al. 2011). With PVDF solution, phase inversion (i.e. phase separation), one of the major fabrication methods, are applied to obtain the PVDF membrane with required properties. The process of phase inversion can be described as that the polymer molecular solved in homogenous solutions change state from liquid to solid through certain controllable methods. Currently, there are two common methods, which are non-solvent induced phase separation (NIPS) and temperature-induced phase separation (TIPS), and they are extensively used and researched in industry and laboratory (Liu et al. 2011; Wang & Chung 2015).

Kang and Cao (2014) stated that most new MD membrane currently fabricated in the lab was via NIPS process where phase inversion is achieved by demixing the solution with sufficient amounts of non-solvent liquid (e.g., water). Through this method,

PVDF membrane is relevantly easy to be fabricated because most polar aprotic solvent could dissolve the polymer without difficulty by mechanical stirring only. By varying the concentration of polymer solution, temperature, and exposure time, the macro structure and relevant morphology properties of the polymer film can be manipulated. Solvent plays an important role in affecting the membrane morphology and thus its characteristics, and combination of a weak solvent and strong solvent (e.g. Trimethylphosphate - dimethylsulfoxide) is widely applied for optimal results (Liu et al. 2011). Evaporation time, coagulation bath medium, temperature of coagulation bath, and non-solvent additives also has strong effects on the crystallization process and the resulting morphology of membrane.

Generally, increasing viscosity by increasing concentration and reducing temperature can reduce the formation of thick skin layer and thus result in smaller pores which are called sponge shaped macro voids (Francis et al. 2013). By using “softer” non-solvent such as alcohol, we can reduce the liquid-liquid demixing rate and thus promoting sponge shape structure as well. However, this type of macro structure was not favorable in MD as it can decrease the pore size, and thus result in lower mass transfer coefficient. Liu et al. (2011) stated that some additives such as lithium chloride could increase the precipitation rate and induce larger pore size as well. In addition, it is believed that the crystallinity, crystal phase, and hierarchical structure of fibers are able to affect the experimental parameters.

TIPS is another popular fabrication method in industry (Liu et al. 2011). Phase inversion is achieved by removing the thermal energy in the homogeneous solution that comprises polymer solute and diluent. The selection of diluent is essential as it can affect the process of polymer crystallization and the resulting morphology greatly, and thus it can determine the membrane characteristics such as porosity, pore size, strength, flux, and etc. (Wang & Chung 2015; Khayet & Matsuura 2011). Compared to NIPS solvent optimizing, mixed diluents of good and poor ones have also been applied to optimize the morphology of membrane (e.g. dibutyl phthalate/dioctyl phthalate). Other conditions, such as cooling rate, quenching condition, and additives in the diluent, also play important roles in determining the final morphology of the TIPS membranes (Xiao et al. 2015).

2.2.4 Membrane fabrication via electrospinning for MD

In recent years, there are increasing numbers of papers regarding utilizing electrospinning technique to fabricate membranes for MD. Electrospun membranes have some superior properties which are naturally fit for MD. These properties include high porosity, high contact angle, large pore size, and narrow pore size distribution (Francis et al. 2013).

Mechanism of electrospinning and major parameters affect membranes characteristics will be fully discussed in next sections.

2.2.5 Membrane fabrication via other methods

In recent years, many new techniques have been developed to fabricate MD membranes. Xiao developed new fabrication method called nonsolvent thermally induced phase separation (NTIPS) (Xiao et al. 2015). PVDF polymers were firstly dissolved completely in water soluble solvent (i.e., ϵ -caprolactam (CPL)) and form homogenous solution by stirring mechanically at temperature of 130 - 150 °C for 2 h. Then the homogenous solution were casted onto the glass plate with an automated high temperature casting machine, and the glass plates were straightaway immersed into water coagulation bath at temperature of 20 °C. By combining the advantages of both techniques, NTIPS membranes had increased porosity, LEP, and mechanical strength compared with NIPS and TIPS membranes, which were desirable properties for MD applications.

In addition, dual layer and triple layer membranes fabrication techniques, which comprised multiple layers fabricated through various fabrication methods, were also developed to improve MD permeation performance. A three-layer membrane had been successfully fabricated (Prince et al. 2014), which comprised a thin superhydrophobic top layer fabricated by electrospinning, a thick hydrophobic middle layer fabricated by NIPS, and a thin hydrophilic bottom layer fabricated by electrospinning. The LEP and mechanical strength of membrane increased greatly with the three-layer structure, and better flux and salt rejection performance could be achieved.

Other approaches of membrane fabrication, such as molecular layer-by-layer assemble, had great potentials for MD application although they had only been used to fabricate FO membranes (Kwon et al. 2015).

2.3 Electrospinning

Sharing the same equipment setup, electrospinning is considered as a special state of electrospraying when certain conditions are met (Ahmed et al. 2015). Electrospinning involves applying high voltage electric field on the polymer solution or melted polymer to form solution jet. Fibers ranged from few micros to nanometer scale can be obtained after the “whipping” process when the jet is being elongated and the solvent is evaporating, and the nanofibers are collected on the grounded collector and form non-woven mats. The electrospun membranes can provide very large specific surface area, high porosity (> 80%), and high degree of interconnection, which make them very suitable for MD process (Lalia et al. 2013). Moreover, the properties of electrospun membrane, such as thickness, pore size, porosity, and etc. can be controlled by changing the parameters in the electrospinning process (Liao et al. 2014a). Furthermore, additional required characteristics for the specific applications are easy to be applied onto the membrane by membrane modifications during or after fabrication process (Frenot & Chronakis 2003). Fig. 6 shows the setup of a typical electrospinning device. There are three major components, which are high voltage power supply unit, grounded collector, and syringe containing the polymer solution (or melted polymer) with metallic spinneret, and a syringe pump is used to push the liquid out of spinneret.

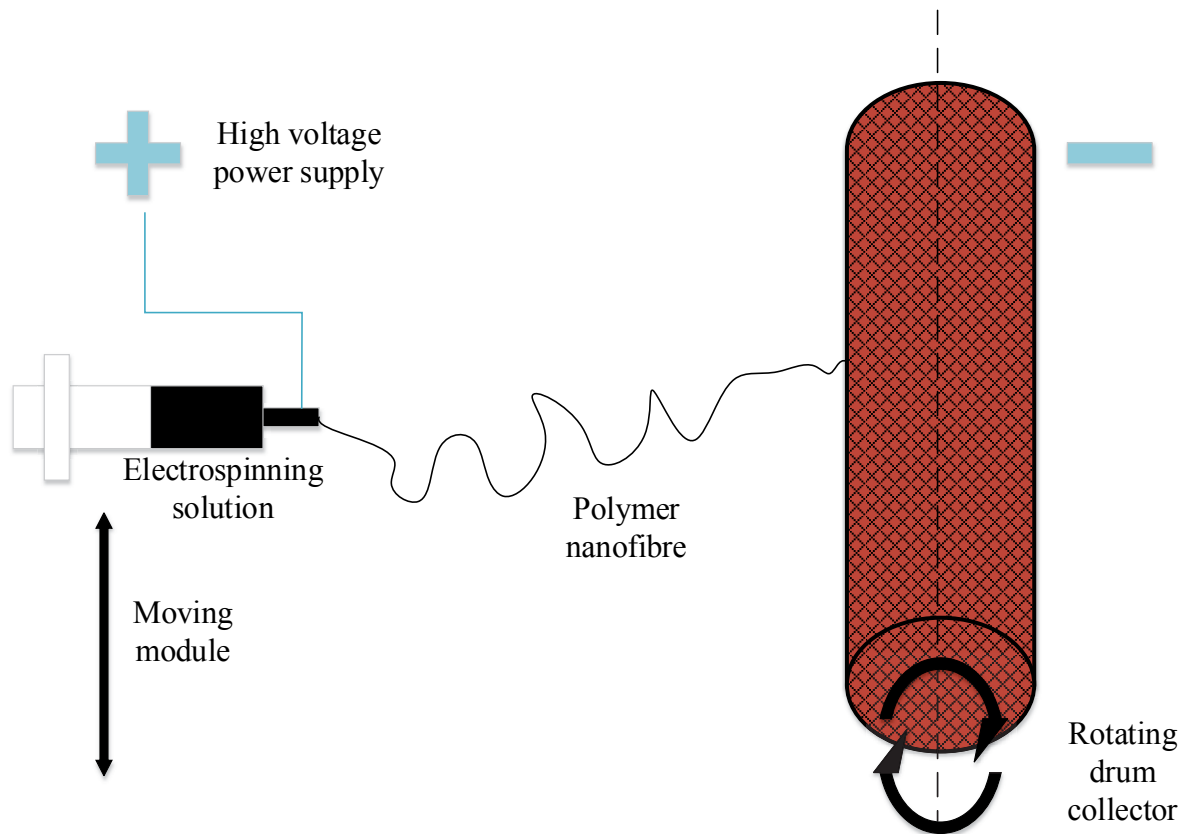


Figure 6- Schematic of electrospinning process

2.3.1 Development of electrospinning

Tracking back to 16th century, phenomenon of electrospaying was found by William Gilbert when he placed an electrically charged piece of amber close to a droplet of water. Electrospinning started to be extensively studied regarding both practice and theory from the beginning of 20th century and went to commercialization soon after when several important patents were registered from 1934 – 1944. It is interesting to mention that the former Soviet Union had applied the electrospinning technique to fabricate battlefield smoke filter for gas masks in military equipment from 1940s. In 1960s, Sir Geoffrey Ingram Taylor developed the mathematical models of electrospinning; therefore, the shape of extended fluid in the front of the spinneret was named after him to honor his contributions (Frenot & Chronakis 2003; Ahmed et al. 2015).

In 1990s, some research groups found that many organic polymers could be electrospun into micro- or nano-fibers. Hereafter, electrospinning gained huge attentions as it had been recognized as a versatile technique for a broad range of applications. Since then, the number of paper regarding electrospinning increased greatly each year (Zhang et al. 2014).

2.3.2 Mechanism of electrospinning process

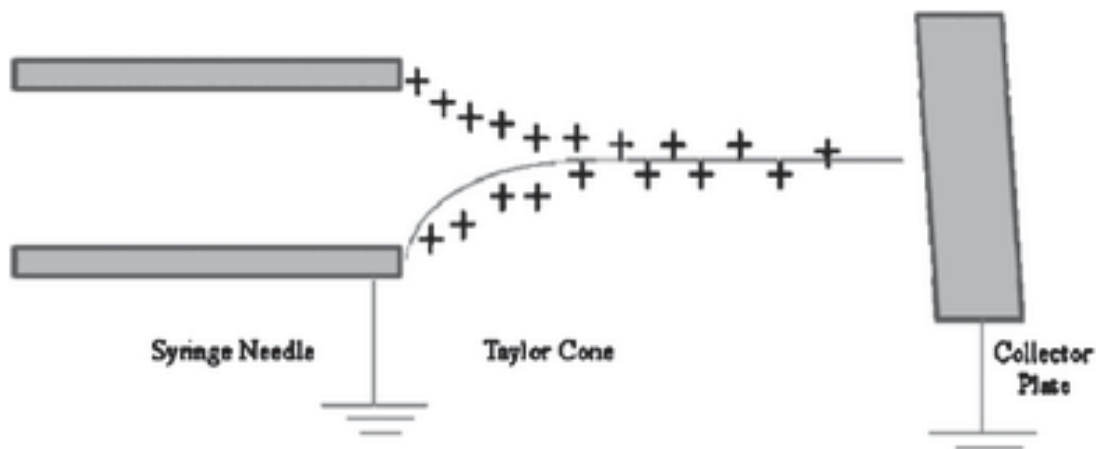


Figure 7-Schematic diagram of Taylor cone in electrospinning process

When the polymer solution is pushed out of spinneret under the pressure generated by the syringe pumps, the droplet at the tip of the spinneret will be applied with electrostatic repulsion force, which was caused by the electrostatic field provided by high voltage power supply, and a cone (conical shape distortion of the droplet) can be formed at the tip of the spinneret owing to the balance between solution surface tension and electrostatic repulsion force. Fig. 7 showed when the electrostatic repulsion is high enough to overcome the surface tension, a polymer jet can be ejected from the cone (at certain whole angles depending on the solutions), and the shape of solution on the tip is called Taylor cone (Frenot & Chronakis 2003).

Under high electrostatic field, The polymer jet can turn into a state of instability and experience stretching and whipping (Tijing et al. 2014a). If the cohesion of polymer solution is high enough, there will be no breakup in the jet stream so that the electrospinning will not occur, and continuous solution fiber can be obtained. The solvent in the polymer jet will evaporate during the whipping process, and the evaporation rate is greatly affected by the solution properties and relative humidity (Eda

et al. 2007). If the solvent evaporates adequately before the jet reaches the collector, the polymer string will eventually change from liquid homogeneous solution into solid polymer nanofibers during the process of stretching and whipping, and non-woven nanofibers membranes can be formed on the collector which are made of enormous amounts of nanofibers after several hours' electrospinning operation.

2.3.3 Preparation of polymer solution for electrospinning

Feng stated that several types of polymers worked well with electrospinning (Feng et al. 2013). The most common ones are Polystyrene (PS), Polyvinylidene fluoride (PVDF), Polyacrylonitrile (PAN), Polyethylene terephthalate (PET) and Nylon 6. In the application of MD process, hydrophobicity is an essential requirement for membranes; therefore, membrane with low surface energy is more favorable. PVDF has relatively low surface energy, and is easy to dissolve in common organic solvents, while other hydrophobic polymer such as PTFE cannot. Moreover, it is common to introduce copolymer into the PVDF polymer chains to further decrease the surface energy of the material, thus the hydrophobicity of the membranes may be further increased. Recently, PVDF-co-HFP is widely researched in electrospinning process because PVDF-co-HFP membranes has better hydrophobicity and porosity compared to PVDF ones, and the copolymer remains high solubility in common organic solvents (Lalia et al. 2013; Ataollahi et al. 2012). PVDF-co-HFP has some other advantages such as high stability and resistance against chemical backwashing, and these benefits cannot be obtained through modification methods, such as blending of inorganic materials into solutions, surface chemical modifications, and grafting (Kang & Cao 2014; Lee 2011). Furthermore, it is more convenient to use copolymer in electrospinning as it requires much less resources and procedures than other modification techniques (Lalia et al. 2013).

Solvent choice is a significant part in electrospinning process as well because it can affect the viscosity of the membrane and thus its morphology greatly. Generally, solvents can be classified into two types: Strong solvent, such as Dimethylacetamide (DMAc), Dimethylformamide (DMF), Dimethyl sulfoxide (DMSO) and N-Methyl-2-pyrrolidone (NMP), are the ones have higher boiling point and dielectric constant (Liu et al. 2011; Eda et al. 2007), while weak solvent, such as acetone and Tetrahydrofuran (THF), are the ones have lower boiling point and dielectric constant. By controlling the

ratio between the strong and weak solvents, the researcher can precisely control the viscosity of the polymer and thus indirectly control the diameters of the electrospun fibers. Moreover, morphology of the electrospun membranes can be controlled in that way either as whether beads and droplets are formed with or without polymer strings is depending on the viscosity of electrospinning solution significantly (Tijing et al. 2014a).

2.3.4 Crucial parameters in electrospinning

Electrospinning is a versatile technique which is utilized in many diverse industry fields. In recent years, Membrane fabrication via electrospinning has become a new trend, and more and more research groups pay attention to this area. Thus, parameters that can significantly affect the polymer morphology and characteristics have been extensively studied for understanding and improvement of MD membrane (Tijing et al. 2014a). In Liao's paper, parameters that affected properties of the nanofibers and membranes could be mainly classified into three groups, which were: Solution parameters, Experimental parameters, and External environmental parameters (Liao et al. 2013b). How each parameters affect morphology and characteristics of the electrospun membranes are summarized below.

2.3.4.1 Effect of solution parameters on membrane morphology and characteristics

Viscosity of solution plays an important role in the effect on the morphology and characteristics of the electrospun membranes. Generally, lower viscosity will result in increase in nanofiber size and hence larger pore size, while higher viscosity can result in lower smaller pore size (Liao et al. 2013b). However, too high viscosity can prevent membrane forming. Therefore, by using acetone as co-solvent with DMF, solution viscosity can be decreased and thus fibers can be formed due to less instability of whipping process and higher evaporation rate of the acetone (Eda et al. 2007).

Regarding effect of viscosity, there are exceptions when change of polymer concentration and molecular weight are involved. Increasing concentration of polymer can increase the viscosity of the solution, but it can increase the fiber size rather than decrease it (Frenot & Chronakis 2003; Lalia et al. 2013). However, too high polymer concentration often makes polymer plugs up the needle easily and interrupt the process of continuous electrospinning, and too low polymer concentration viscosity can increase the tendency of forming beads and droplets (Pelipenko et al. 2013; Liu et al. 2011).

High surface tension can decrease the surface area per unit mass of fluid and affect the morphology and characteristics of membranes in the same way as viscosity. Increasing surface tension can result in decrease in membrane nanofiber diameter and membrane pore size. However, surface tension should be low enough to prevent the jet from collapsing to droplets before the solvent has evaporated (Frenot & Chronakis 2003).

High solution conductivity leads to higher charges in the electrospinning, which has a similar effect as power supply; thus, the fiber diameter will be decreased due to additional stretching and elongation during the whipping process. Moreover, secondary jets can be formed as a result of increase in the conductivity of polymer solution and thus the electrospun nanofiber size will be further decreased due to decrease of solution volume in main jet (Pelipenko et al. 2013).

With solvents of low dielectric constant, such as THF and chloroform, large extensional flow, low instabilities, large number of secondary jets, and constant flow rate can be obtained. On the contrary, with solvents of high dielectric constant, such as DMF and NMP, limited extensional flow, high instabilities, small number of secondary jets, and decreasing flow rate can be achieved. Moreover, higher dielectric properties can prevent the formation of beads and droplets on the electrospun membranes (Fig. 8).

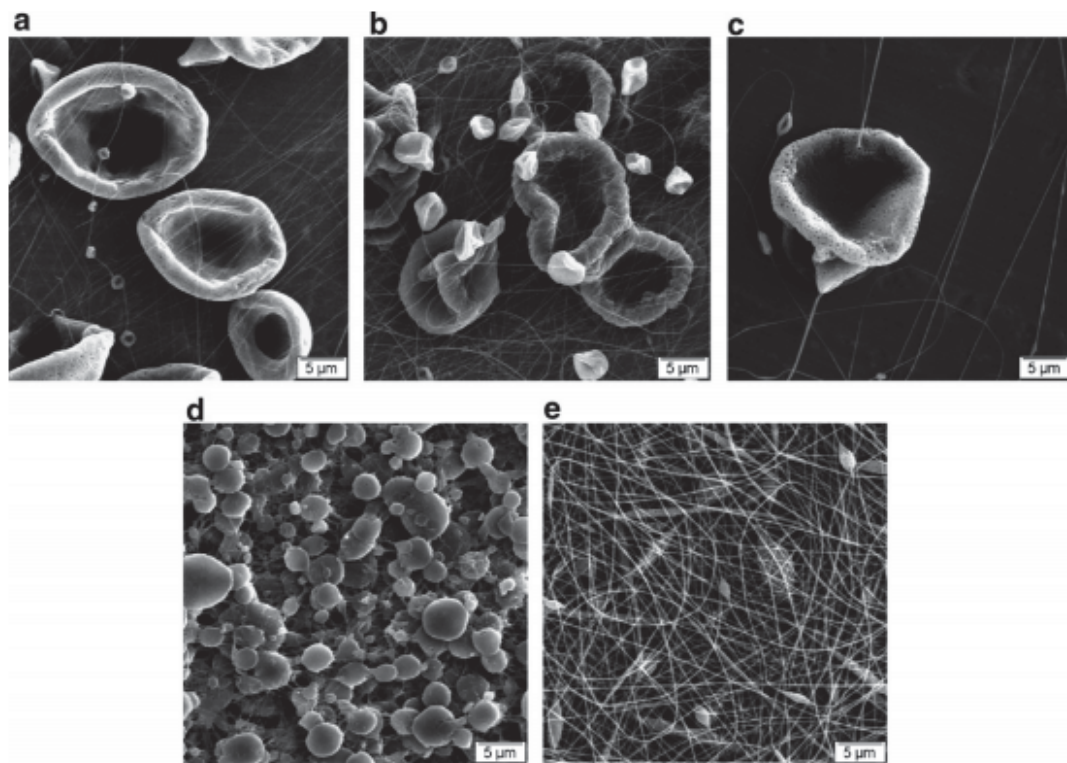


Figure 8-SEM images of PS fibers and beads electrospun with various solvents: (a) THF; (b) Chloroform; (c) CS₂; (d) NMP; (e) DMF. (adapted from Eda et al.

2.3.4.2 Effect of experimental parameters on membrane morphology and characteristics

Low voltage may be not strong enough to form polymer solution jet, and increasing voltage can reduce the diameter of solution fibers. However, too high voltage above critical value may cause high frequency droplets due to greater pulling force on solution, and beads will be formed on the membranes. For some polymer, high voltage can increase the instabilities of jet, and, with certain solutions parameters, porous fibers can be formed. For example, fluffy network of polystyrene nanofibers can be formed due to increased bending instabilities at higher voltage (Ahmed et al. 2015)

Decreasing internal diameter of spinneret theoretically can result in smaller diameter of nanofibers. However, if the internal diameter is too small, the polymer solution may easily block the spinneret, and electrospinning jet cannot be formed (Tijing et al. 2014a).

Tip-collector distance has a direct influence on the electric field strength and the flight time of the solution jet (Frenot & Chronakis 2003). When the distance is too narrow, solvent may not evaporate timely, and it may result that the fibers fuse to each other and the nanofiber structures can be lost. If the distance is too wide, the electric field can

become too weak to form continuous electrospinning jet, and beads and droplets may be the dominant morphology features on the membranes.

Depending on the viscosity of the solution, syringe pump feeding rate can affect the morphology of electrospun membrane greatly, and the change can be resulted in two opposite directions. When the polymer solution has relatively low viscosity (e.g., polymer dissolved in weak solvent acetone), increasing feeding rate can decrease average nanofiber diameters and increase tendency of forming beads owing to large amounts of new secondary jets formed (although total supply of solution increased). When the polymer solution has relatively high viscosity (e.g., polymer dissolved in strong solvent DMF), increasing pump rate can also increase average nanofiber diameters, because very few or no additional secondary jets are formed and thus each solution jets have more supply of polymer solution (Eda et al. 2007).

Temperature of solution plays important role as well, because it can affect the viscosity of solution. Generally, increase temperature of solution can decrease the viscosity of the solution due to the increase in solubility of solvent at higher temperature. According to the effect of viscosity in section 2.3.4.1, increase in the viscosity may result that the fiber size may reduce, and beads and droplets may be formed on the membranes (Tijing et al. 2014a).

2.3.4.3 Effect of external environmental parameters on membrane morphology and characteristics

Due to their strong effect on the solvent evaporation rate, relative humidity (RH) can affect the morphology and characteristics greatly. Interestingly, RH has opposite effects on aqueous-solvent and organic-polymer-solvent solutions (Pelipenko et al. 2013).

For aqueous polymers solution, it is found that decreasing RH will result in increase in nanofiber diameter and pores size. It is assumed that when the RH is very low, the rate of solvent evaporation will be high, so it will result in a fast increase in the local polymer concentration and thus decrease in the stretching of polymer chains (due to less time for stretching). Thus, large diameters of nanofiber can be obtained when RH is low. Another assumption of mechanism is addressed to explain the effect of RH on the aqueous polymer solution in electrospinning, that decrease in fiber diameter can be caused by the formation of secondary jets due to increase in conductivity at higher RH.

However, the second assumption cannot fully explain the formation of beads and droplets on the membranes (Pelipenko et al. 2013).

Explanation of mechanism of aqueous solvent solution can be applied to organic-polymer-solvent based solutions. Similar as aqueous-solvent solution where evaporation rate and nanofiber morphology can be controlled by manipulating RH, vapor pressure in the environment can be controlled by changing RH.

In organic-polymer-solvent solutions, increase in RH can enhance the rate of process of precipitation (phase inversion), and this will result in increase in local polymer viscosity. According to effect of polymer concentration discussed in last section, increase in polymer concentration can result in large fiber diameter and pore size. Another supporting assumption of mechanism was addressed, that the presence of more water molecular in the electrospinning chamber will decrease the excess charges on the nanofibers owing to molecular polarization. Therefore, the nanofibers will have a lower self-repulsion force to stretch fibers, and it will result in larger nanofiber diameter and membrane pore size (Pelipenko et al. 2013).

Temperature of electrospinning chambers has effects on the membrane morphology and thus characteristics. Increasing temperature will decrease the local polymer viscosity and thus increase the elongation time, resulting in a smaller nanofiber and pore size (Tijing et al. 2014a).

2.4 Membrane modification for wetting resistance

To improve the MD performance and stability for desalination, membranes should be modified to obtain higher hydrophobicity or LEP without reduction of porosity and mechanical strength. Also, high hydrophobicity and LEP can help against membrane wetting, which is the top challenge in MD. Generally, high hydrophobicity can be obtained by greatly increasing the roughness of the membrane surface at nano and micro scale provided low surface tension materials is used as the membrane material. Till now, quite a few amounts of membrane modification methods have been developed. Kang and Cao illustrated that the modification methods could be classified into two stages, depending on whether it was prior to or after membrane fabrication (Kang & Cao 2014). Some other researchers categorized the approaches for superhydrophobic surface modification into three groups, depending on the degree of self-assembly

process involved in the fabrication and modification process. The three approaches groups were named top-down, bottom-up, and combination of bottom-up and top-down (Li et al. 2007). In this thesis, all the summarized approaches are sorted into these three groups according to Li's classification method.

2.4.1 Top-down approaches

Top-down approaches is the methods to fabricate material with specific features by carving, molding, or machining bulk materials with tools, lasers, and other external objects, and self-assembly is not involved in this types of fabrication process (Li et al. 2007).

2.4.1.1 Templatation

This method involves the use of a template masters with the desired features. The replication features can be achieved by molding and subsequent lifting off the replica or dissolution of the templates. Polymeric superhydrophobic coating is obtainable with the templatation approaches. One major advantages of this method is that many materials can be used as the template master, including natural lotus leaves, template mold prepared by a lithographic process, commercial inorganic membranes, and etc. With this approach, generally, hydrophobic surface with a contact angle more than 120 degree can be obtained. However, few of them can achieve superhydrophobic (contact angle $>150^\circ$) (Ma & Hill 2006), and even few among them had a low sliding angle, indicating the technique limitation of templatation. Another drawback is that not every material that required modification is suitable for templatation.

2.4.1.2 Photolithography

In this technique, light is irradiated through a mask with desired features to the substrate with a photoresist, and the desired patterns were developed through the etching steps. Generally, silicon is used as the substrate, and x-ray or e-beam can be used as light source in photolithography process. High hydrophobicity of material surface can be achieved with proper setting of spacing and pillar size. However, similar to templation, superhydrophobicity are rarely achieved on the modified surface via photolithography (Fürstner et al. 2005; Martines et al. 2005).

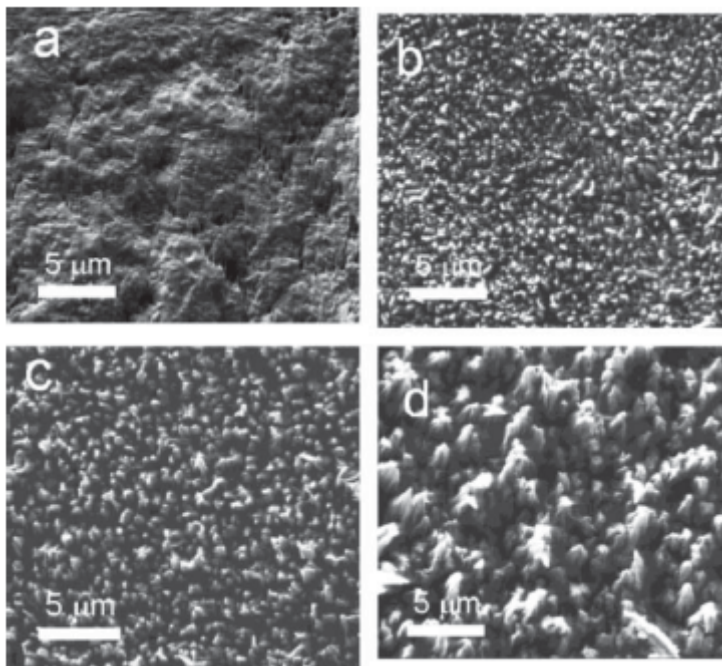


Figure 9- SEM images of PTFE foils: (a) untreated; (b) treated with oxygen plasma for 60 s; (c) 120 s; (d) 10 mins. (adapted from Li et al. 2007).

2.4.1.3 Plasma treatment

Plasma treatment is always involving the use of plasma etching. It is a dry etch technique where reactive atoms or ions are produced on the membrane surface by the discharged gas. The ions generated during the process are accelerated in the boundary layer between the plasma and substrate with high directivity, and thus they may penetrate and be grafted on the membrane surface. Fig. 9 illustrated that the process can affect the surface of the material and has great impact on both chemical composition and physical morphology. For various functions, different chemical gases are used in the plasma treatment. CF_4 and fluorine are widely applied in plasma treatment

modification for superhydrophobicity. Yang successfully obtained superhydrophobic PVDF membrane with ultra-low sliding angle through CF₄ plasma modification (Yang et al. 2014) owing to F's low surface energy and increase in roughness. In the best scenario, contact angle increased from 133° to 155° after 5 m process. The LEP of the membrane was increased greatly while pore size was slightly increased after the CF₄ treatment. MD performance regarding flux and salt rejection was also improved successfully.

2.4.1.4 Heat-press treatment

Heat-press treatment is a simple but effective method to improve LEP and mechanical strength, with little sacrifice of hydrophobicity and porosity. The assumption of heat-pressing mechanism was addressed by Liao (Fig. 10) (Liao et al. 2013b). Some other researches had applied this method on their home-made PVDF membranes and

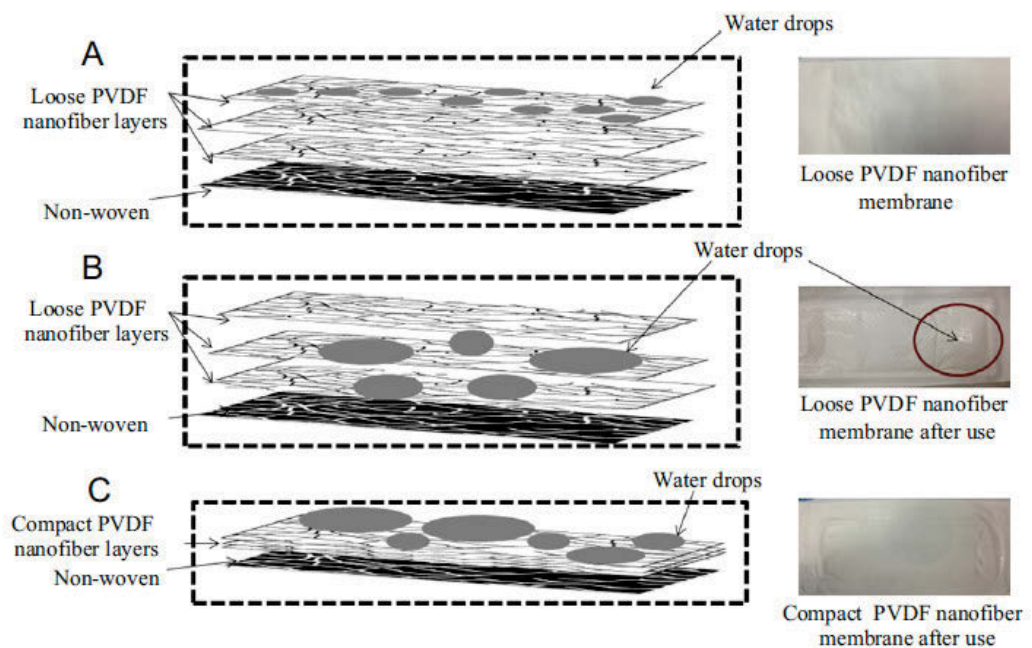


Figure 10. Illustration of assumed mechanism of heat-press on PVDF electrospun membrane. (adapted from Liao et al. 2013b)

successfully improved their characteristics and thus MD performance. However heat-press treatment has still not been fully investigated, as there were no studies on the effects of heat-press conditions reported yet. Therefore, in this study, the candidate is focusing on the effects of conditions in the heat-press process on the electrospun membrane, and MD performance with optimally heat-pressed membrane was also

compared with the commercial membranes (Zhang et al. 2007; Liao et al. 2013b; Wu et al. 2014).

2.4.2 Bottom-up techniques

Different from the top-down techniques, the bottom-up techniques do not involve external tools or lasers to achieve high roughness at nano and micro scale. On the contrary, the nanostructure should be obtained with self-assembly and self-organization, so larger complex objects were formed of smaller building blocks or components spontaneously. In some of the techniques, the small polymer blocks are kept being assembled in solution or at gas phase, until they reach the minimal energy when whole molecular structures turn into solid form.

2.4.2.1 Chemical deposition

The chemical deposition approach involves the chemical reaction on the surface of suitable substrate, so the product self-assembles and deposits and a thin film can be formed on top of the substrate. Usually, crystalline inorganic materials (e.g. ZnS) are utilized in the self-assembled film. However, in some cases, semicrystalline polymer materials can be used in the chemical deposition for specific features and properties. There are three major types of chemical depositions, which are chemical bath deposition (CBD), chemical vapor deposition (CVD), and electrochemical deposition, and the three types differs from each other based on deposition conditions. Commonly, CBD are applied to create nanopin or nanorod films on top of the substrate, and a contact angle from 150 up to 178 ° can be achieved. However, highly porous electrospun membrane is not suitable for CBD. Therefore, lots of researchers used CVD instead of other chemical deposition methods to modify their membranes. Guo applied poly(1H,1H,2H,2H-perfluorodecyl acrylate) (PPFDA) coating on poly(trimethyl hexamethylene terephthalamide) membrane via CVD, and the contact angle increases from 0 to 151 ° at maximum. Also, the LEP of membrane improved dramatically from 15 to 373 kPa (Guo et al. 2015).

2.4.2.2 Layer-by-layer deposition

By exploiting the mechanism of electrostatic charge interactions between different layers such as polyanion and polycation, layer-by-layer (LBL) is a rather easy approach to fabricate membrane, and membrane thickness can be precisely controlled by selecting number of LBL circles (Kwon et al. 2015). Due to the mechanism of LBL mechanism,

polyelectrolyte, a hydrophobic polymer, is necessary for this process, so a hydrophobization is always required for superhydrophobic modification process. In addition, to enhance the roughness of the material surface, either acid treatment or nanoparticles are essential for the LBL process. With various simplified approaches of LBL, multiple researchers have successfully fabricated superhydrophobic surface, where high contact angle around 170° and low sliding angle less than 1° can be obtained (Han et al. 2005b; Jisr et al. 2005).

2.4.2.3 Sol-gel methods

Sol-gel has potentials to fabricate superhydrophobic membrane, which can be used to dip coat on the substrate to fabricate the membrane with desired properties. By controlling the process of hydrolysis and condensation reactions of various silica precursors, microstructures of the sol-gels surface can be manipulated and thus high roughness can be obtained. Although superhydrophobic can be obtained without incorporation of nanoparticles during sol stage, the superhydrophobic surface usually has high hysteresis which is not favorable (Shang et al. 2005). Incorporated with certain silica nanoparticles, such as alkoxides 3,3,3-trifluoropropyltrimethoxysilane (TFPTMOS) and tetramethylorthosilicate (TMOS), superhydrophobic surface with CA up to 170° can be achieved and low hysteresis can be obtained (Doshi et al. 2005).

2.4.3 Combination of top-down and bottom-up

To achieve superhydrophobic surface, combination of top-down and bottom-up, a technique consisted of both processes, has been considered as the most viable approach. This method, having advantages of both top-down and bottom-up approaches, can produce membrane surface structures with two scales of roughness which can lead to high contact angle and low sliding angles (i.e. lotus effect). Usually, top-down process is utilized to obtain rough structure in micro scale, and bottom-up process is applied to obtain rough structure in nano scale. It is worth noting that, in most cases, although stage of top-down process may be followed by stage of bottom-up process, the two stages might occur simultaneously.

2.4.3.1 Combinations methods based on CVD

On silicon substrates quadrate micro pillar arrays prepared by photolithography, aligned carbon nanotubes were arranged to obtain hydrophobic surface in microstructure. Then, a fluorinated layer of (2-(perfluorooctyl) ethyl) trimethoxysilane was coated on the film

through CVD. Sliding angle could be decreased to less than 1° after CVD although CA was significantly increased after CVD process (Zhu et al. 2005).

2.4.3.2 Combinations methods with phase inversion methods

As a viable approach utilized by many researchers, phase inversion techniques were fully discussed in section 2.2.3. Normally, with low surface tension polymer (e.g. PVDF and PS), by controlling the solvent, nonsolvent, and temperature, it is possible to obtain membranes with hydrophobic surface having high LEP. However, further increasing CA and reducing sliding angle requires incorporation of nanoparticles or nanosolvent. By using polypropylene (i-PP) as solute, Xylene as solvent, and Methyl ethyl ketone as nonsolvent, a CA up to 160° could be obtained (Lu et al. 2005) .

Incorporation of additional polymer materials with low surface tension energy macromolecules can lead to superhydrophobicity and high LEP, such as surface modifying macromolecules (SMM), which was used as additive in Prince's research (Prince et al. 2014). Due to similar mechanism, it had been proved that PTFE particles blending in PVDF solution was able to increase CA (Dong et al. 2014)

For micro scale surface roughness, some other group prepared a template through photolithography firstly; then, solution of Hyflon AD was casted on the substrate, which was named as phase separation micromolding ($PS_{\mu}M$) (Vogelaar et al. 2006).

2.4.3.3 Utilizing micelles

Micelles are basically surfactants in solution, which are often association colloids, and they tend to form aggregates in equilibrium. Compared to phase separation, micelles have similar mechanism of forming membranes. Films fabricated with PtBA-b-PDMS-b-ptBA micelle solution could have a CA up to 163° . In addition, if hydrophobic nanoparticles were added into the solution, the CA of the surface could be further increased to 170° , and the sliding angle could be as low as 2° (Han et al. 2005a).

2.4.3.4 Crosslinking hydrophobic nanoparticles on the surface

Recently, a new physical modification practice, using innovative crosslinking agent to coat super hydrophobic layer firmly on the membrane surface, is gaining increasing attentions (Jiang et al. 2011; Liao et al. 2013a). Regardless whether the substrate fabricated by electrospinning, phase inversion, or some other approaches, this

modification can be applied on various surfaces. The crosslinking agent, self-polymerized polydopamine (PDA), was applied as adhesive film on top of the membrane surface. Then, particles with very low surface energy were placed on top of the thin PDA film to form a superhydrophobic top layer (Jiang et al. 2011). With this method, high CA of 158° and sliding angle lower than 10° can be achieved (Liao et al. 2013a).

2.4.3.5 Electrospinning with addition of nanoparticles

Electrospinning has been discussed extensively in previous sections. It is found that electrospun membrane that has bead-dominant morphology is much more hydrophobic than membranes formed of nanofibers. That means that polymers with lower molecular weight and thus lower viscosity tended to have higher CA. The highest static CA that could be achieved with electrospun membranes is 167° (Acatay et al. 2004).

Introduction of inorganic nanoparticles such lithium chloride into polymer can also improve hydrophobicity of membrane surface fabricated via electrospinning. It is proved that nanocrystalline cellulose (NCC), clay, tetramethyl orthosilicate (TEOS), and modified silica nanoparticles could increase the CA of membrane surface although the sliding angle is still high. (Ahmed et al. 2015; Park et al. 2010; Razmjou et al. 2012; Liao et al. 2014a)

Besides, two-polymer materials technique had been developed for superhydrophobic membrane fabrication. By using poly (methyl methacrylate) (PMMA) and fluorine end-capped polyurethane (FPU), the membrane fabricated via electrospinning had two scales roughness, and thus it has high CA of 166° and a low sliding angle, which was able to exhibit lotus effect (Xie et al. 2004). Block copolymer poly (styrene-block-dimethylsiloxane) was used in electrospinning solution for its low surface tension. It is found that the CA could reach up to 163° with a sliding angle of 15° (Ma et al. 2005a).

Distinct from those researches inspired from lotus effect, recently, slippery liquid-infused porous surface (SLIPS) is invented with fundamentally different mechanism. Usually, a hierarchical structure was created on the film surface, followed by infusing liquid chemical substance with ultra-low surface tension (e.g. FAS-17) into the surface pores of the films (Zhang & Lv 2015). However, this approach of membrane

fabrication may not be applicable to MD because the membrane pores that water vapors pass through may be blocked by the slippery liquid.

For better control of membrane parameters, some researchers combined electrospinning with other modification approaches, such as iCVD (Guo et al. 2015). Along with a high surface roughness inherent to the poly (caproectone) (PCL), the electrospun films coated with polymerized perfluoroalkyl ethyl methacrylate (PPFEMA) could achieve a very high CA of 175° and a low sliding angle less than 2.5° . Moreover, the resulting surfaces not only show superhydrophobicity but also high oleophobicity (118° for decane) (Ma et al. 2005b).

2.5 Case study: pilot-scale MD plant in Plataforma Solar de Almeria (PSA), Spain (Guillen-Burrieza et al. 2014)

2.5.1 Background

For fully utilizing the MD technology, the pilot scale plant was built at PSA in 2010, and three AGMD modules manufactured by Scarab AB Company (Sweden) were installed in the plant (Fig. 11). From 2010 to 2013, three major operations have been carried out to investigate greatly concerned issues in full scale desalination plant for long-term operation, which are wetting, fouling, and recovery of the membrane quality after cleaning. Moreover, cleaning strategies for mitigating fouling were also required.

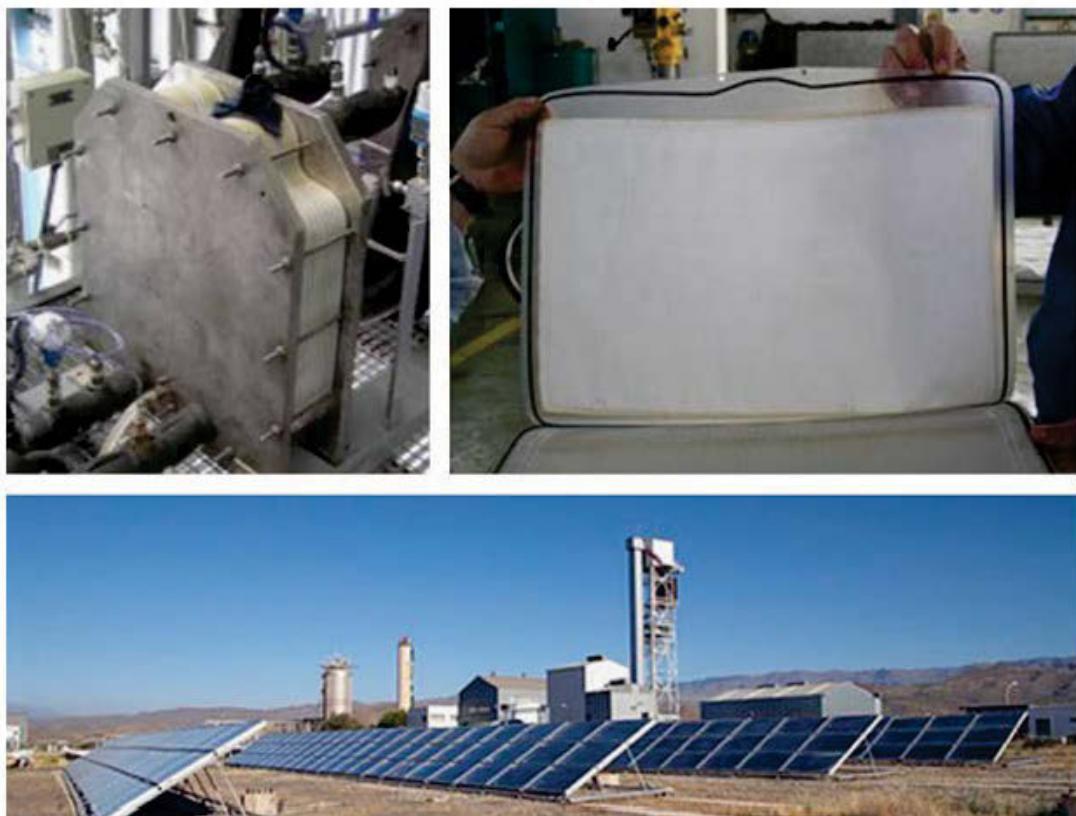


Figure 11-Membrane modules used in pilot AGMD plant at PSA. (adapted from Guillen-Burrieza et al. 2014)

2.5.2 Membrane and membrane modules

Fig.11 showed that the membranes were thermally sealed to PP frames in a size of 30 cm by 35 cm. The membranes material was PTFE, and the membrane was supported by non-woven PP support layer. Key properties of the brand new membrane were addressed in Table 2 below. Fig. 11 also illustrated that the solar heat was being incorporated to increase the temperature of the salt solution in the feed side.

Table 2-Key properties of the unused PTFE membranes

Average pore size (mm)	0.18 ± 0.003
Largest pore size (bubble point, BP) (μm)	0.45 ± 0.003
Total thickness (μm)	241.67 ± 15.04
Top(active) surface thickness (mm)	54 ± 2.0
Porosity (onlyactivesurface)	$64.05\% \pm 2.4$

2.5.3 Effect of fouling on characteristics of the fouled membranes

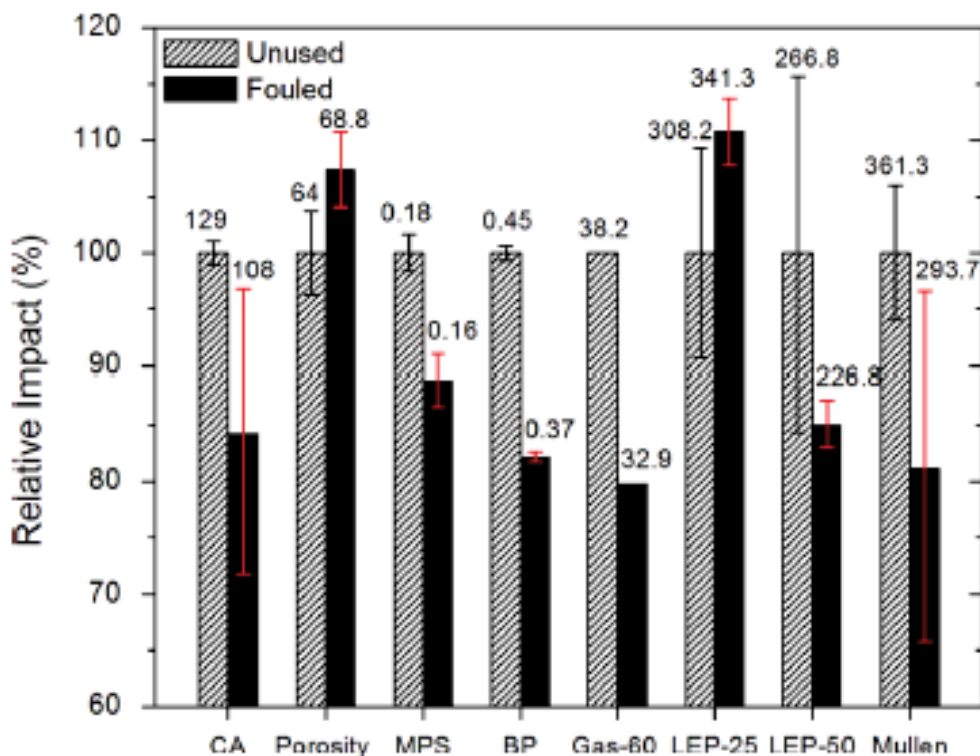


Figure 12-Impact of fouling on the major parameters of MD membranes. (adapted from Guillen-Burrieza et al. 2014)

From Fig. 12, we can observe that the fouling had strong impact on the characteristics of the membranes which was used in PSA MD plants. The reduction of CA meant that

the membrane had become less hydrophobic after being fouled, and it became more easily wetted and suffered more severe concentration polarization. Generally, all the parameters were worsened except porosity and LEP 25. Although the BP (pore size) decreased, the increase of porosity in the fouled membrane could be caused by the cake fouling layer which was highly porous. Revealed in the SEM image, the porous cake fouling layer increased the porosity of the membrane. After being fouled, the decrease in BP led to an increase in LEP at 25°C. However, the LEP of fouled membranes at 50°C become lower than the LEP of new membranes, indicating that the pore size and structure of the fouling cake layer was sensible to the solution temperature and the underneath polymer fibrils had been damaged by the foulant.

2.5.4 Discussion of cleaning strategies

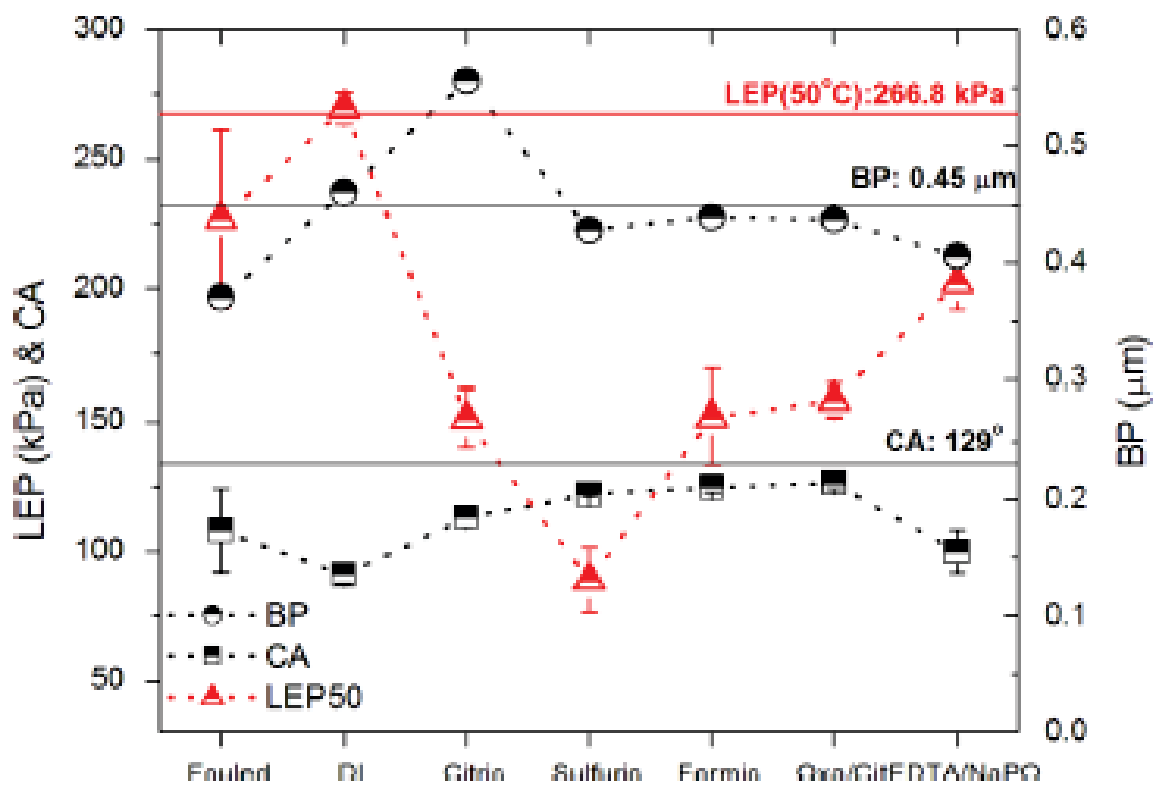


Figure 13-Comparison of CA, LEP, and BP with various cleaning strategies. (adapted from Guillen-Burrieza et al. 2014)

CA, LEP and BP had been measure after the fouled membranes were cleaned with DI water, citric acid, sulfuric acid, formic acid, oxalic +citric acid, and EDTA + Na₅P₃O₄ (Fig. 13). Although the author claimed that “0.1% oxalic followed by 0.8% citric acid”

had the best cleaning efficiency for MD performance recovery, the LEP at 50°C was still much lower than the one of the fouled membranes which was itself lower than the virgin membrane's LEP. It meant that all the fouled membrane cleaned by the chemical reagents had much lower wetting resistance than the unused membranes due to the structure damage caused by either the fouling layer and/or cleaning process itself. Therefore, the chemical-cleaned membranes' capacity for long-term operation was questionable. Actually, based on Fig. 13 alone, it could be argued that cleaning strategy with DI water had the best cleaning results as its LEP at 50°C increased and CA reduced slightly.

It is worth to note that, during the inactive periods, the saline feed solution could cause wetting which might be as worse as the membrane exposed to the structural damage after cleaning. Hence, a good shut-down protocol should be designed including rinsing the membrane with DI water and complete drying of them (Guillen-Burrieza et al. 2014).

CHAPTER 3

MATERIALS AND METHODS



University of Technology Sydney
FACULTY OF ENGINEERING

3. Materials and methods

3.1 Materials

The polymer used for the fabrication of membranes was polyvinylidene fluoride-co-hexafluoropropylene (referred herein as PH, MW = 455,000), and it was purchased from Sigma-Aldrich, USA. Acetone (ChemSupply, Australia) and N, N dimethylacetamide (DMAc, Sigma, USA) were used as solvent. All the chemicals were used as received without further purification. A polypropylene (PP) filter layer purchased from Ahlstrom was applied in each MD experiment as support layer. Commercial microfiltration membrane (pore size = 0.22 μm , porosity = 70%, GVHP) bought from Millipore was used for MD test as a reference.

3.2 Membrane fabrication by electrospinning

PH at 20 wt% was dissolved in a mixed solvent consisting of acetone and DMAc (1:4 ratio of acetone/DMAc). To obtain homogenous polymer solution, the mixture was magnetically stirred for 24 h. The prepared PH solution was then stored in a 12 ml plastic syringe fitted with a 21G nozzle (internal diameter = 0.51 μm). Fig. 6 illustrates the configuration of the electrospinning device used in this study. The polymer solution was pulled out of the syringe by the syringe pump and formed whipping fibers within a high voltage electrical field (applied voltage = 21 kV). Then fibers were collected onto the rolling drum after most contained solvent evaporated during the whipping process. During electrospinning process, the nozzle was continuously moving inwards and outwards parallel to the axis of the rotation of the drum. The setting operation conditions for electrospinning were constant throughout the study in all the experimental stage: The distance between the nozzle tip and collector was set at 20 cm. The syringe pump had a pushing rate of 1 ml/h and had been running continuously for 6 h for each membrane sample from Stages 1-3 (see Table 3). In Stage 4, longer durations of electrospinning were utilized for thicker membrane.

3.3 Heat-press post-treatment

After electrospinning, the as-spun membranes were removed from the collector and initially dried at 50 °C for 2 h inside an air flow oven (OTWMHD24, Labec, Australia). Membranes were then fully covered by foils, placed between flat metal plates with dead weight placed on the top plate, and put in a pre-heated oven. In each stage, various

conditions (heat-press temperatures of 140, 150, 160, 170 °C; pressing pressure (i.e., dead weight on top of the membrane) of 0.7, 2.2, 6.5, and 9.8 kPa; and heat-press duration of 1, 2, 4 and 8 h were applied to the membrane as detailed with their name conventions in Table 3. The samples were investigated and compared separately in three consecutive stages classified by the conditions for deeply understanding their effects.

As shown in Table 3, the experiments could be classified into four stages in this study. In Stage 1, four various temperatures were selected and tested. The applied pressure was pre-set to be 2.2 kPa (7 kg dead weight using metal plates over a 15 mm x 20 mm membrane) and 2 h was selected as the duration of the process. Then, in Stage 2 (i.e., effect of heat-press pressure), the treatment temperature was fixed at 150 °C; then four various pressures were chosen in a wide range to check their effects. The duration of heat-pressure was pre-set to be 2 h. In Stage 3, the temperature and pressure was set at 150 °C and 2.2 kPa respectively, and the duration varied from 1 h to 8 h. Characteristics of post-treated membranes in each stage were addressed and compared. In Stage 4, optimal heat-press conditions were applied on the membranes with various thicknesses, in the range between 103 to 395 μm . Both as-spun and heat-pressed membranes were characterized. Selected as-spun and heat-pressed membrane samples from Stage 4 were applied in the DCMD for desalination, and their permeation performances (flux and salt rejection) were compared with the commercial membranes (GVHP, 0.22 pore size, and 110 μm thickness).

Table 3-Heat-press conditions and name conventions used in the present study.

Electrospun membrane samples		Heat-press conditions			
		Temperature (°C)	Pressure (kPa)	Duration (h)	Thickness (µm)
As-spun	Neat	-	-	-	45
Stage 1	M0	140			43
	M1	150	2.2	2	39
	M2	160			31
	M3	170			melted
Stage 2	M1-A		0.7		40
	M1-B	150	2.2	2	38
	M1-C		6.5		37
	M1-D		9.8		37
Stage 3	M1-B-1			1	38
	M1-B-2			2	38
	M1-B-3	150	2.2	4	37
	M1-B-4			8	36
Stage 4	PH1	-	-	-	103
	PH2				147
	PH3				224
	PH4				395
	PH1'				90
	PH2'				129
	PH3'	150	6.5	8	195
	PH4'				343

3.4 Characterization

The morphologies of all membrane samples were examined by a scanning electron microscope (SEM, Supra 55vp from Carl Zeiss AG). ImageJ software (National Institutes of Health, USA) was used to analyze the SEM images to work out the average fiber diameter, surface pore size and their distributions, and three SEM images from different spots of the membrane samples were used for each fiber and pore size analysis. The pore size counting method was consistent through all the experiments, and the surface pore size could be defined as the area between the electrospun fibers on the top three layers in the SEM images. Membrane thickness was measured with digital micrometer (IP65, Mitutoyo) and the average value of ten randomly picked spots was calculated for each sample.

Contact angles (CA), a major indicator of hydrophobicity, were measured by Theta Lite 100 (Attension) following sessile drop method (Liao et al. 2014b; Woo et al. 2015). A water droplet around 5~8 ml was released from a needle tip onto the membrane surface. A motion camera was mounted to capture the images at a rate of 12 frames per second. Through the recorded videos, contact angles were analyzed with the aid of specific software. To ensure experimental reproducibility, each set of samples were measured in triplicate and the average value of them was taken.

Mechanical properties including maximum stress, strain, and Young's modulus were measured with bench-type tensile tester (Lloyds). Average values of three runs were taken for each sample.

LEP test was carried on the as-spun and heat-press membrane samples with a homemade setup. A digital gauge was connected to a hollow stainless plate with a pipe, and nitrogen gas was released from the other end of pipe. On the stainless plate, there was a stainless cylinder container that was filled up with deionized (DI) water. The setup had an effective surface area of 7 cm². The samples were fixed on the top of cylinder by a stainless cap and a lock catch was used to secure the set-up. Pressure displayed on the gauge was recorded when water droplets came out through the membrane during the process of steadily releasing out nitrogen gas. Each sample was tested in triplicate and average data was recorded.

Membrane porosity was defined as the volume of the pores divided by the total volume of the membranes. It was determined by a gravimetric method in this study. After the membranes were immersed in ethanol (Univar 1170 from Ajax Finechem Pty. Ltd.) for adequate time to ensure that the pores fully filled up, the weight (w_1 , g) of membrane with ethanol was measured after the residual liquid on the surface was removed. Then the membrane samples were left still in the open air for some time and got weighed (w_2 , g) when all the ethanol within them had fully evaporated (i.e., dry condition). The porosity then could be worked out with the following equation:

$$\varepsilon_m = \frac{(w_1 - w_2)/\rho_e}{w_1 - w_2/\rho_e + w_2/\rho_{ph}}$$

where ρ_e was the density of the ethanol (g/cm^3) and ρ_{ph} was the density of the PH (g/cm^3) (Tijing et al. 2014b)

3.5 Direct contact membrane distillation (DCMD) test

MD is normally applied in four principal configurations: direct contact MD (DCMD), air gap MD (AGMD), vacuum MD (VMD), and sweeping gas MD (SGMD) (Geng et al. 2014; Fan & Peng 2012a). This study is focusing on DCMD configuration due to its higher permeation performance and relative ease of set up. The electrospun membranes were tested in DCMD setup shown in Fig. 14. All the membrane samples were supported by a nonwoven PP filter layer. The PP filter was placed on the bottom side of the electrospun membrane and fixed firmly in the module which was tightened with nails. The length and width of both feed and permeate channels were 77 mm and 26 mm respectively, making up an effective membrane area of 20 cm^2 . The module was placed horizontally and ran in counter-current mode with feed flow on top side (Tijing et al. 2014b; Woo et al. 2015). Sodium chloride (NaCl) at a concentration of 3.5 wt% in water was used in the feed side, and its temperature was being maintained at $60 \text{ }^\circ\text{C}$ by a heating bath. Deionized (DI) water was used in the permeate side, and its temperature was being kept at $20 \text{ }^\circ\text{C}$ by a chiller. The mass flow rates in both permeate and feed sides were being maintained at 400 ml/min via a gear pump. The running conditions and parameters of DCMD were being kept unchanged in the whole experiment, and each condition of heat-press was tested three times with a new sample for ensuring experimental reproducibility. A desktop computer was set-up to collect the data of temperatures in both feed and permeate sides automatically via thermocouples

connected to the flow lines. The flux was calculated by dividing the change of mass in the permeate container by the duration of change while the reading of mass was collected automatically once every minute on the linked electronic balance.

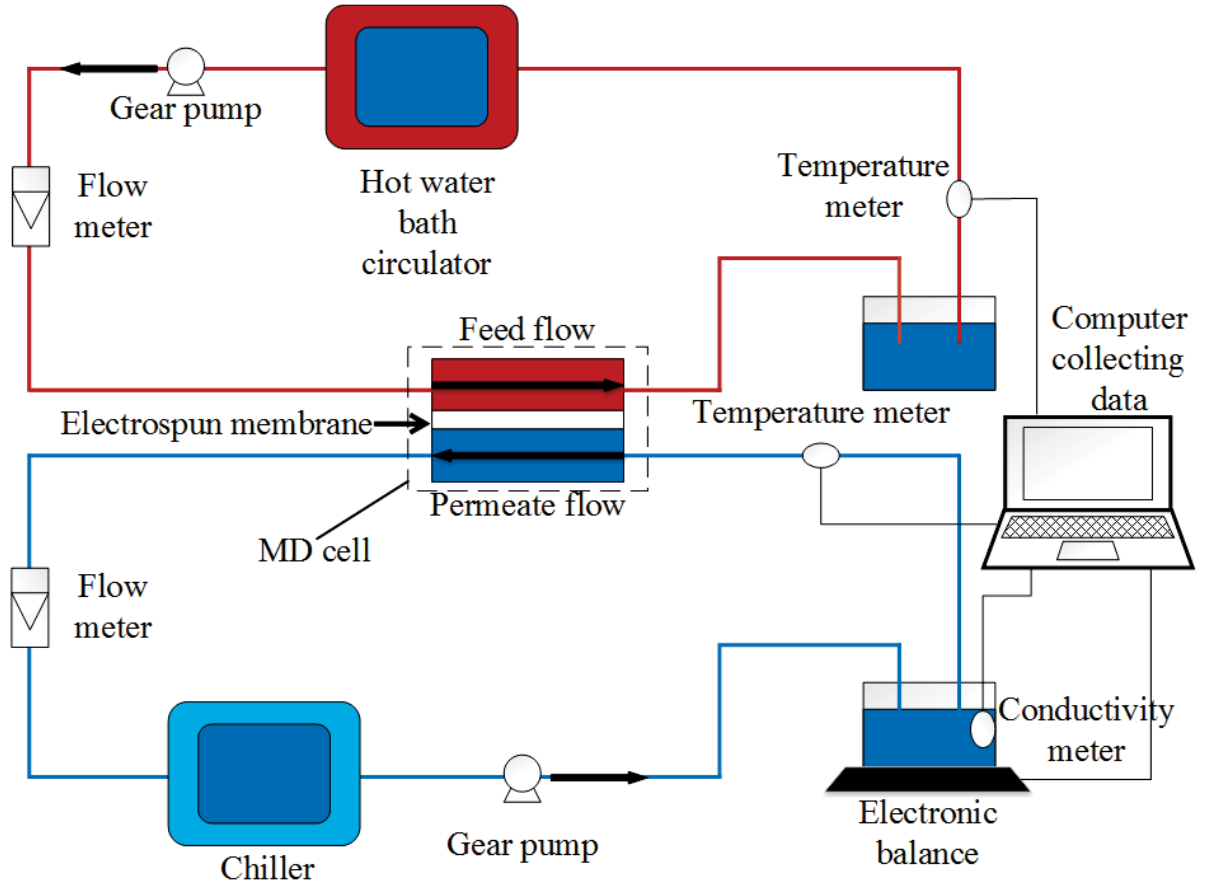


Figure 14-Schematic diagram of DCMD process used in this study

CHAPTER 4

EFFECT OF HEAT PRESS CONDITIONS



University of Technology Sydney
FACULTY OF ENGINEERING

4. Effects of heat-press conditions

4.1 Effect of heat-press temperature on the membranes

PH was used in this study with a melting point of 155-160 °C as described by the manufacturer (*Properties* 2015). The existence of co-polymer (HFP) reduced the melting point of the PH hence it had a slightly lower melting temperature than pure PVDF.

In Stage 1, various temperatures were applied on the membranes samples separately. The samples were named as M0, M1 and M2, corresponding to the applied heat-press temperatures of 140, 150 and 160 °C to the electrospun membranes, respectively.

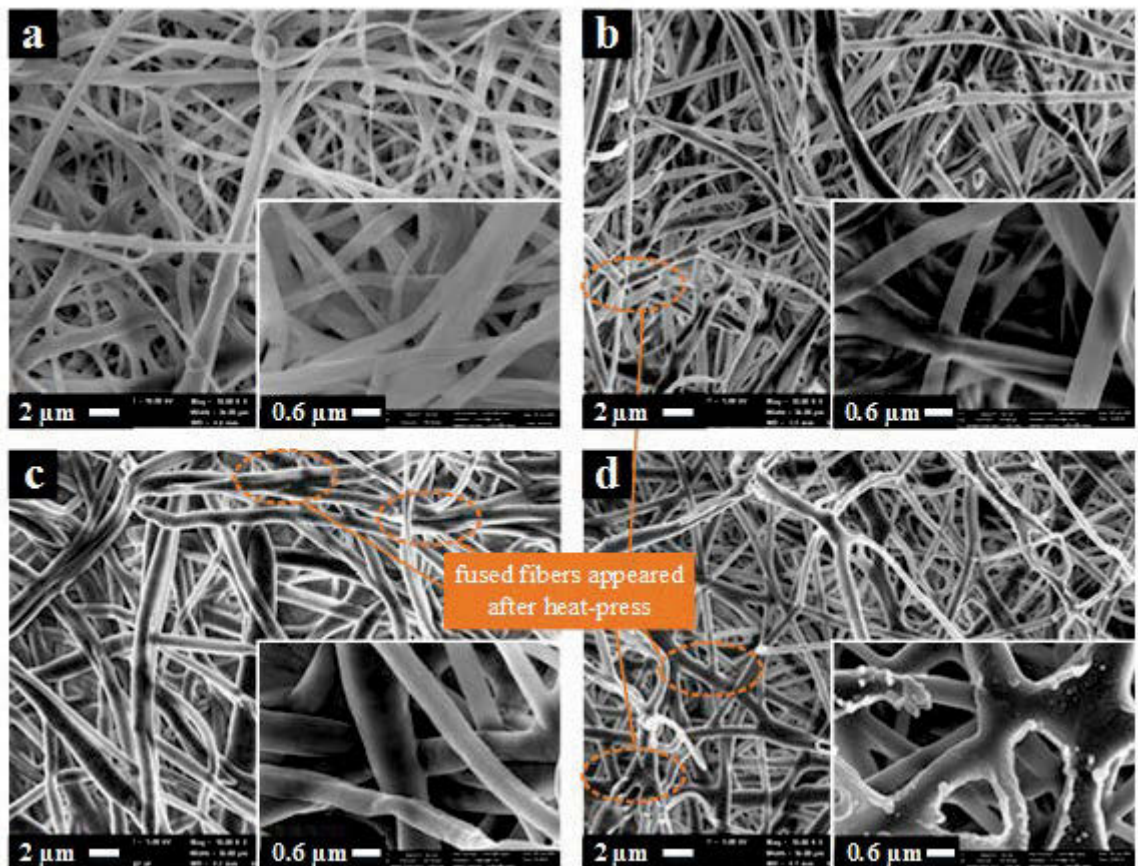


Figure 15- SEM images of as-spun and heat-pressed PH membrane at magnifications of 10 K and 50 K: (a)as-spun neat membrane (Neat); membranes heat-pressed under (b) 140 °C (M0); (c) 150 °C (M1); and (d) 160 °C (M2).

Fig. 15 shows the morphologies of as-spun and heat-pressed membrane under various temperatures (at 140, 150 and 160 °C) at low and high magnifications. It could be observed that some of the fibers fused together after heat-press treatment was applied,

and there were increasing numbers of fused fibers with the increase of the heat-press temperature. From the SEM images, the heat-pressed electrospun fibers were obviously larger than as-spun membranes, and the average surface pore size decreased as the fibers widened, which was also observed by other researchers (Wu et al. 2014). The measured surface pore size distributions (PSD) displayed in Fig. 16 showed an obvious trend. It was found that increasing the heat-press temperature could narrow the PSD and decrease the average pore size (Table 4). Similarly, Liao et al. and Wu et al. applied heat-press treatment with similar processes and conditions on PVDF electrospun membranes and obtained smaller pore size of electrospun membranes (Liao et al. 2013b; Wu et al. 2014).

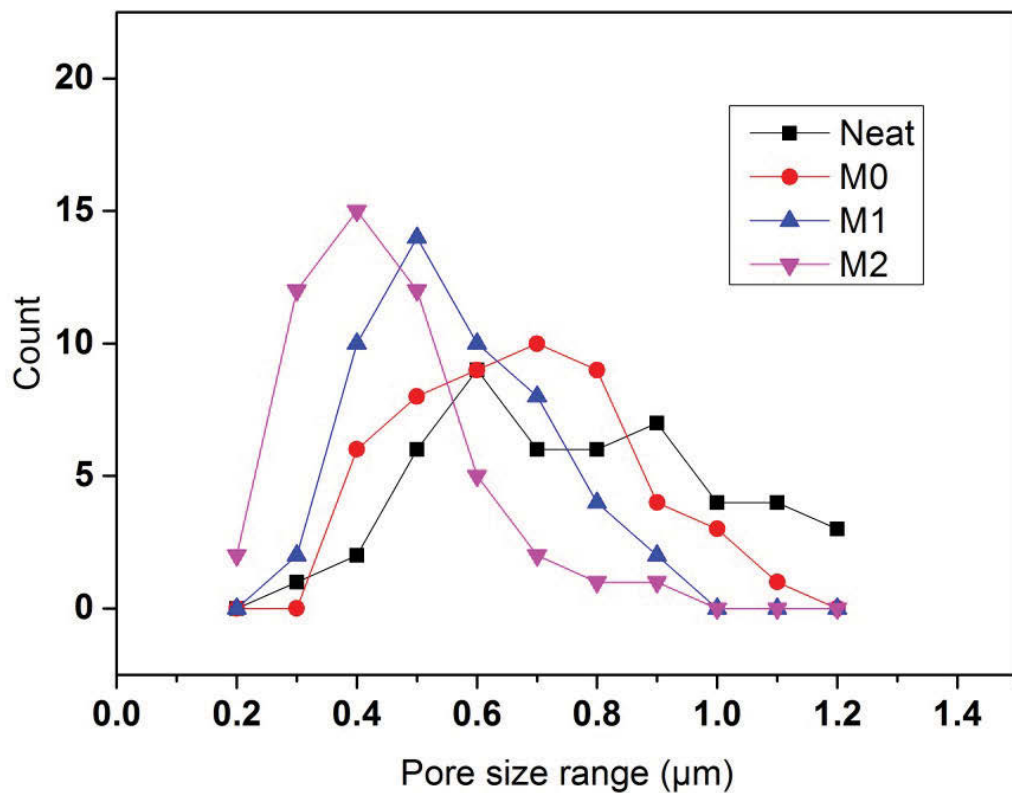


Figure 16-Pore size distributions of as-spun and membrane samples heat-pressed under various temperatures.

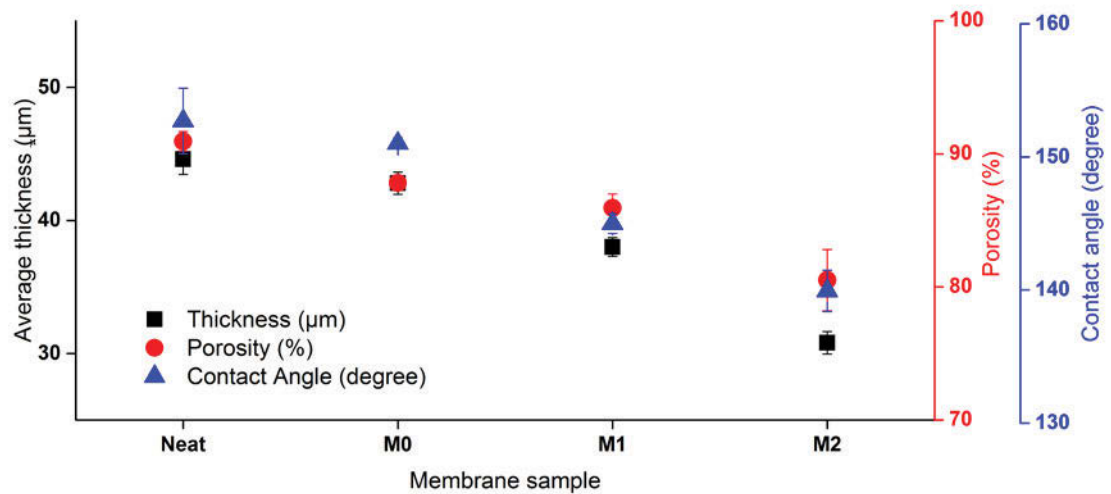


Figure 17-Effects of temperature on thickness, porosity and contact angle

Details of average fiber and surface pore sizes can be found in Table 4 that clearly shows an increase of fiber size and decrease of surface pore size when heat-press temperatures were raised.

The thickness of the heat-pressed membranes was affected by the temperature in an inverse manner, i.e., at higher temperature, thinner membranes were obtained. Membranes without heat-press treatment (i.e., neat or as-spun) had a thickness of 46 µm. After being heat-pressed at 140 °C, the membrane's thickness decreased to 41 µm. Further increase of the heating temperature to 150 °C could make the membrane even thinner. It was assumed that at high temperature multiple layers of fiber in membrane fused together and formed much denser structures, so the membrane became thinner. And further increasing temperature could increase the compaction level (Tijing et al. 2014b). However, when the temperature reached 160 °C, the thickness decreased sharply to 31 µm. It was believed that partial melting had occurred as some regions of the internal fibrous network melted together (Liao et al. 2013b). Some white residues can be found on the electrospun fibers, which are polymer fragments that the partially molten polymer fibers solidify again when the environmental temperature decreased back to room temperature from 160 degree. The white residue could not be other substance as no nanoparticles had been added into the electrospinning solutions. When heat-press temperature reached 170 °C (higher than the melting temperature), the phenomenon of total melting of the membrane samples could be observed by the naked

eyes. Therefore, temperatures over 160 °C was not applied in Stage 1 experiments. Porosity of membrane shared a similar trend of the thickness. Neat PH had the highest porosity of 92% and the M2 had the lowest porosity of 80% (Table 4). The reduction of the porosity after heat-press was on account of the loss of some voids by compaction.

Fig. 17 shows that the contact angle decreased steadily with the increase in applied heat-press temperature. At the highest tested temperature, i.e. 160 °C (M2), the CA dropped significantly to 140.0°, indicating that a partial melting of polymer on the surface has occurred (see Fig. 15). Generally, the surface of the membranes became less rough at higher heat-press temperature when the membrane started melting and fusing. It meant that the membrane surface would become less hydrophobic (Lalia et al. 2013; Liao et al. 2013b).

Table 4-Characteristics of the membranes after heat-press at different temperatures

Parameter/Sample	Neat	M0	M1	M2
Fiber size (µm)	0.39 ±0.12	0.55 ±0.19	0.69 ±0.24	0.75 ±0.30
Surface pore size (µm)	0.50 ±0.21	0.48 ±0.10	0.45 ±0.09	0.41 ±0.10
Young's modulus (MPa)	11.7 ±5.4	31.1 ±5.8	40.9 ±2.6	103.9 ±8.2
Stress at break (MPa)	3.09 ±0.18	10.64 ±0.55	12.11 ±0.35	16.09 ±1.26
Strain at break	0.66 ±0.05	1.30 ±0.08	1.56 ±0.19	0.84 ±0.15
LEP (kPa)	71 ±9	65 ±7	83 ±4	64 ±6

At higher treating temperatures, more fibers could be observed to be fused at interlay points, and they could contribute to both decreased pore size and increase of mechanical strengths. It was found that maximum stress and Young's modulus increased when temperature was raised. Higher tensile strength and Young's modulus could be achieved with higher heat-press temperature. Especially, M2 had a much higher Young's modulus than other samples, due to its greatly changed morphology. The membrane fibers partially melted, fused together, and formed layers of bulk polymer. LEP was greatly improved after heat-press, and the membranes would have better resistance against wetting and improved robustness (Ahmed et al. 2015). LEP of M0 was found to be lower than neat membrane. It was because the membrane was not sufficiently heat-pressed so the morphology such as surface pore size was not adequately enhanced (or narrowed). However, the membrane thickness had decreased and it contributed to a

smaller LEP (Guillen-Burrieza et al. 2015). On the other hand, M2, which had the smallest average pore size, had a decreased LEP as well. It was believed that the cause was significant reduction in thickness due to partial melting. The highest LEP among the tested membranes in this stage was found to be M1 and its value was 83 kPa. The improvement was attributed to its adequate fusion of fiber nodes and hence narrower PSD and smaller pore sizes. Additionally, the CA and thickness of M1 was just slightly reduced.

Based on Stage 1 results, the optimum heat-press temperature condition was found to be at 150 °C. Thus in Stage 2, we utilized and fixed this condition to check the effect of heat-press pressure.

4.1.1 Effect of heat-press temperature on MD permeation flux

In Fig. 18, it is found that membrane heated at various temperatures had distinctive MD flux performance. In addition to getting wetted quickly, neat membrane had a much lower initial permeation flux than the modified membranes and had a rapidly increasing flux afterwards due to wetting. On contrast, membrane heat-pressed at 140°C had much improved initial flux performance, increase from 18 to 28 LMH. Further increase in heat-press temperature could improve the MD performance. When membrane heat-pressed at 150°C, a higher flux of 30 LMH could be obtained. According to the observations addressed in previous section, the improvement of the permeation flux was caused by the improvement of LEP as strong fusion among overlapping electrospun fibers had been formed, increasing resistance against wetting. However, when the heat-press temperature was set above its melting point, 155-160 °C, the membrane would become partially melted, and the permeation flux could be decreased from 30 to 26 LMH, which was even lower than the flux of membrane heat-pressed at 140 °C. The salt rejection of MD with heat-pressed electrospun membranes was all over 99.99% in 8 h operation, while the neat membrane had a much lower salt rejection of 80% due to the fast partial wetting of the membranes.

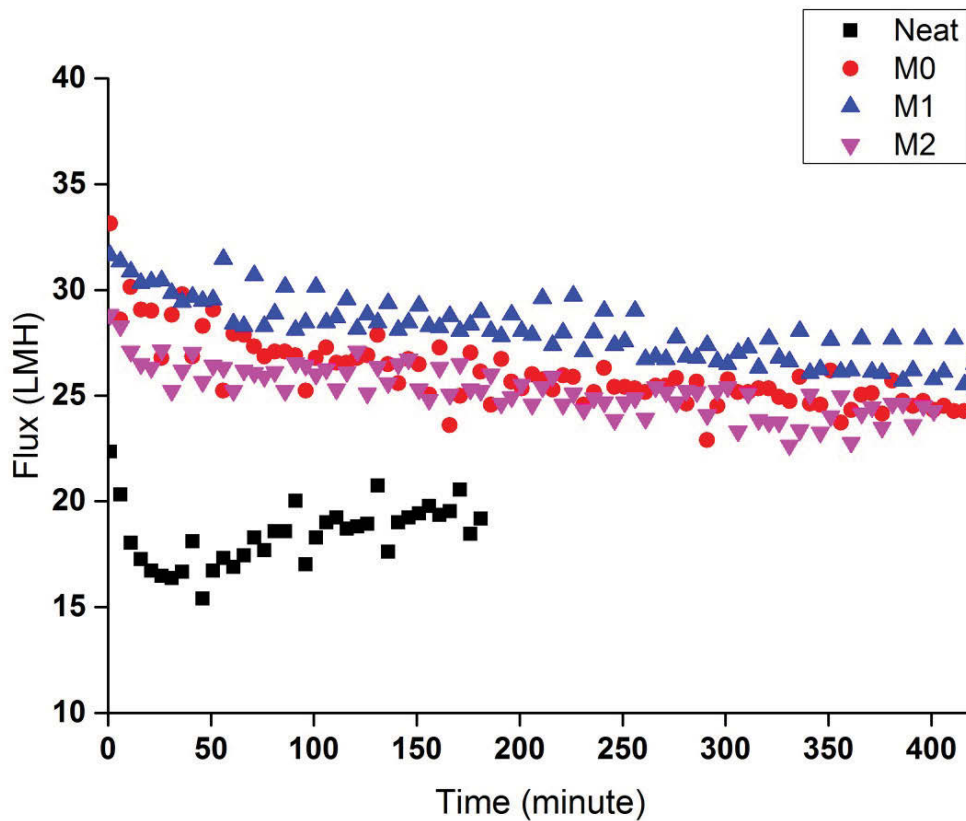


Figure 18-Flux comparisons of electrospun membranes heat-pressed at various temperatures

4.2 Effect of heat-press pressure on the membranes

Heat-press pressure plays an important role in affecting the morphology and characteristics of the membrane, and increasing pressure in heat-press process is expected to influence the membrane properties in a favorable way.

Keeping the heating temperature at 150 °C and treatment duration for 2 h, four metal plates with mass of 2, 7, 20 and 30 kg were applied on the membrane samples individually, which were equivalent to heat-press pressures of 0.7, 2.2, 6.5 and 9.8 kPa, respectively. The samples were then named as M1-A, M1-B, M1-C and M1-D, respectively.

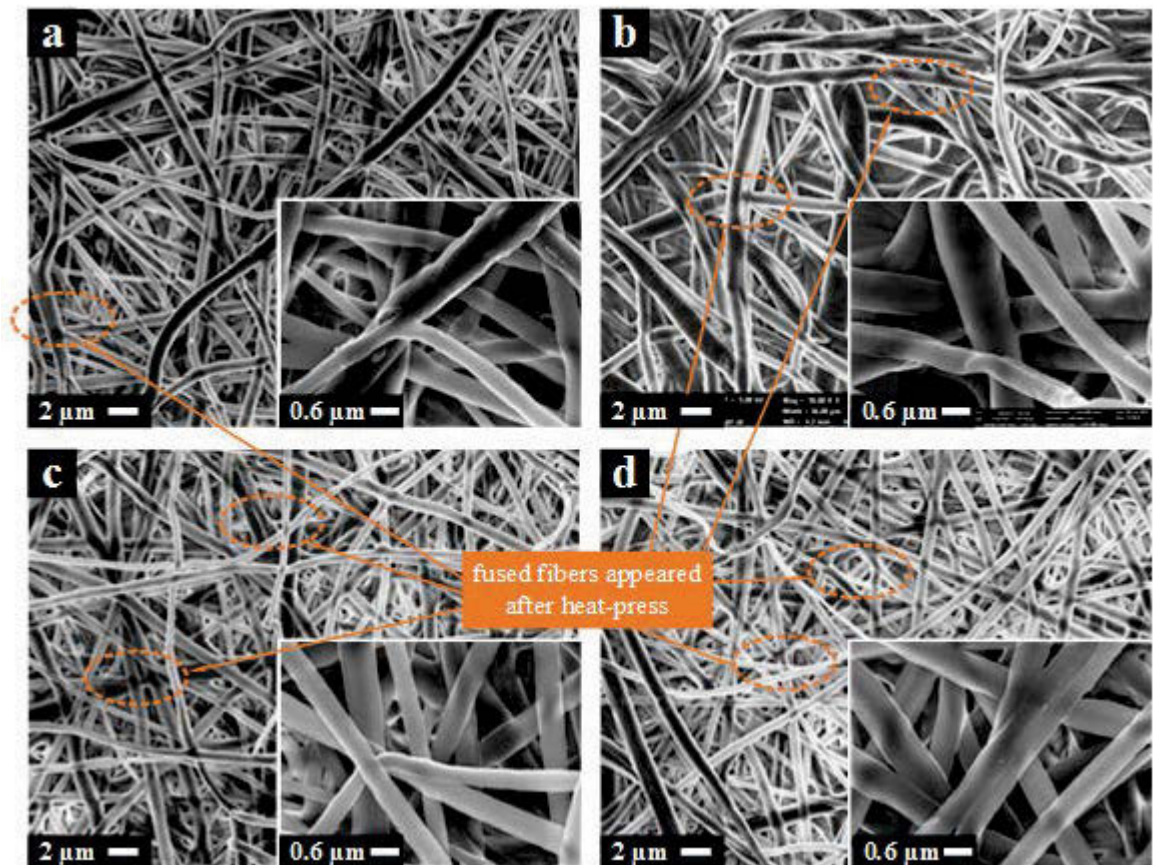


Figure 19-SEM images of heat-pressed PH membrane at magnifications of 10 K and 50 K: membranes heat-pressed under (a) 0.7 kPa (M1-A); (b) 2.2 kPa (M1-B); (c) 6.5 kPa (M1-C), and; (d) 9.8 kPa (M1-D).

Fig. 19 shows the morphologies of heat-pressed membranes under various pressures. It could be seen that although their surface structures shared similar features and fiber sizes looked nearly identical, more fused joints could be found in heat-pressed membranes under higher pressures. It was assumed that the external pressure could help the fibers fusing with each other. Analysis of surface pore sizes (Fig. 20) indicated that further increasing the pressures could narrow the PSD and reduce the average pore size. However, the samples M1-C and M1-D shared identical PSD and average pore size, and both had more favored morphologies than the other two samples.

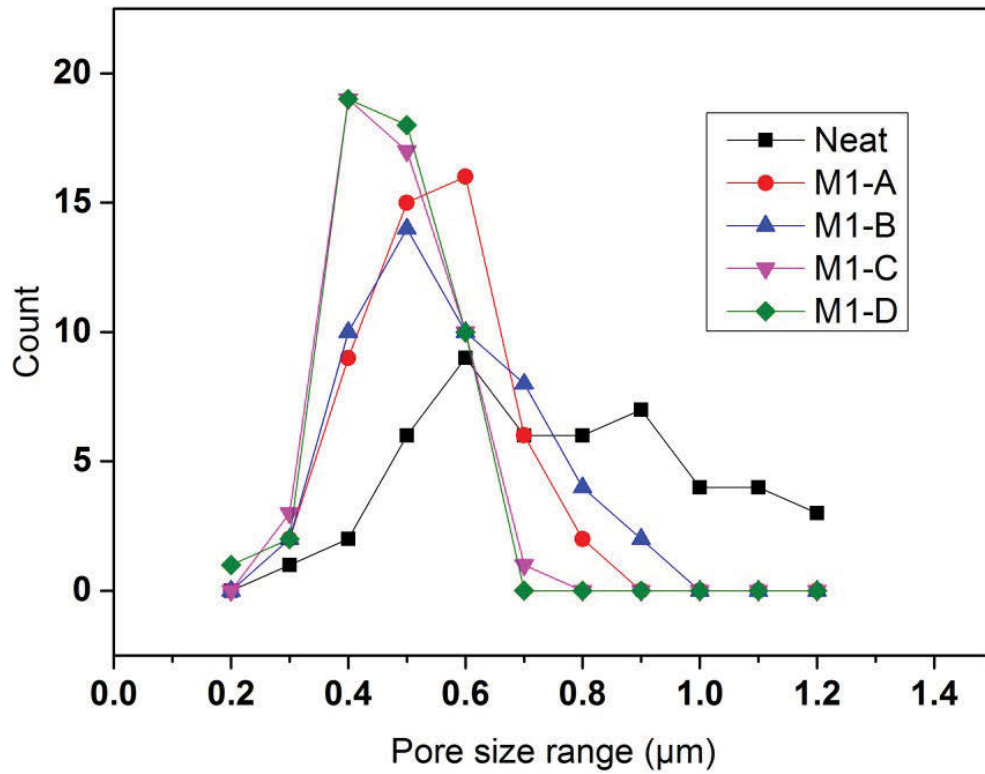


Figure 20-Pore size distributions of as-spun and membrane samples heat-pressed under various pressures.

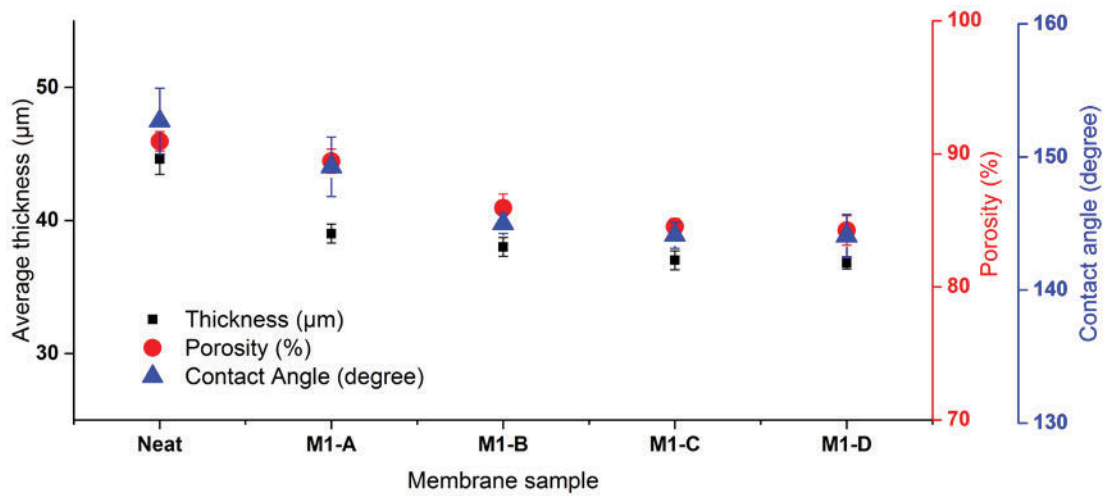


Figure 21-Effects of pressure on thickness, porosity and contact angle

It was observed that increasing pressure resulted in larger fiber size and smaller surface pore size. However, when the applied pressure was further increased beyond the value of 2.2 kPa, the effect of heat-press pressure on fiber sizes tended to become minimal (Table 5). It was also found that the difference of fiber size between M1-C and M1-D was insignificant. The two membrane samples shared very similar average size of 0.70 and 0.73 μm respectively, and their surface pore size was nearly identical (at 0.42 and 0.42 μm , respectively). It could be concluded that further increasing the pressure beyond certain values (6.5 kPa in this study) had no benefits on the characteristics of the membranes. In previous studies, heat-press pressures applied on the samples were also mentioned. Although we could find that only glass plates were applied on the membranes, increase of fiber size and decrease of pore size could be noticed (Lalia et al. 2013; Liao et al. 2013b). This meant that a moderate pressure higher than certain values should be sufficient for the heat-press treatment.

As displayed in Fig. 21, heat-press pressure had similar effects on thickness, porosity and contact angle, as all of three characteristics decreased when the applied pressure increased. However, the degree of the decrease was not as large as the tone affected by temperatures discussed in the last section. Additionally, M1-C and M1-D shared very similar values of thickness, porosity and contact angle, which meant that the membranes might have reached its maximum compaction level.

Table 5-Characteristics of the membranes after heat-press at different pressures

Parameter/Sample	Neat	M1-A	M1-B	M1-C	M1-D
Fiber size (μm)	0.39 \pm 0.12	0.63 \pm 0.18	0.69 \pm 0.24	0.70 \pm 0.20	0.73 \pm 0.20
Surface pore size (μm)	0.50 \pm 0.21	0.49 \pm 0.11	0.45 \pm 0.09	0.42 \pm 0.09	0.42 \pm 0.13
Young's modulus (MPa)	11.7 \pm 5.4	36.5 \pm 6.6	40.9 \pm 2.6	48.5 \pm 4.0	48.7 \pm 6.0
Stress at break (MPa)	3.09 \pm 0.18	11.90 \pm 1.21	12.11 \pm 0.35	13.29 \pm 1.85	13.50 \pm 0.85
Strain at break	0.66 \pm 0.05	1.30 \pm 0.08	1.56 \pm 0.19	1.42 \pm 0.38	1.38 \pm 0.19
LEP (kPa)	71 \pm 9	73 \pm 8	83 \pm 4	93 \pm 4	89 \pm 3

Table 5 also shows that increasing pressure could enhance the mechanical properties greatly. M1-C had a Young's modulus of 48.5 MPa which was much higher than M1-A. M1-C also had a higher tensile stress, which was the result of the changed morphology after heat-press (Tijing et al. 2014b). However, when the pressure was further increased beyond 6.5 kPa, the increase of both Young's modulus and maximum stress was found

to be negligible. Effect of heat-press pressure on LEP shared similarities with effect of pressure on tensile strength. Although increasing pressure could increase LEP to some degree. However, further increasing pressure beyond 6.5 kPa did not improve LEP significantly because we could see M1-C and M1-D had very similar LEP values. Based on Stage 2 results, a pressure of 2.2 kPa was decided to be used (i.e., M1-B) for next stage experiments.

4.2.1 Effect of heat-press pressure on MD permeation flux

After fixing the modification temperature at 150 °C, membranes heated-pressed at various pressures were tested with MD. Generally, increase in heat-press pressure could result in increase in flux (Fig. 22). However, membranes heat-pressed less than 6.5 kPa had slightly higher flux than less than 9.8 kPa, and hence it had highest flux performance in this stage. According to the findings in previous stages, increase in heat-press pressure could decrease the membrane thickness and increase the LEP, which could improve the flux significantly in terms of long-term operation. In this stage, membrane heat-pressed under 0.7 kPa had lowest MD flux performance, which could be due to insufficient compaction. Regardless of the heat-press pressures, all the post-treated electrospun membranes had salt rejection more than 99.99% in 8 h DCMD test.

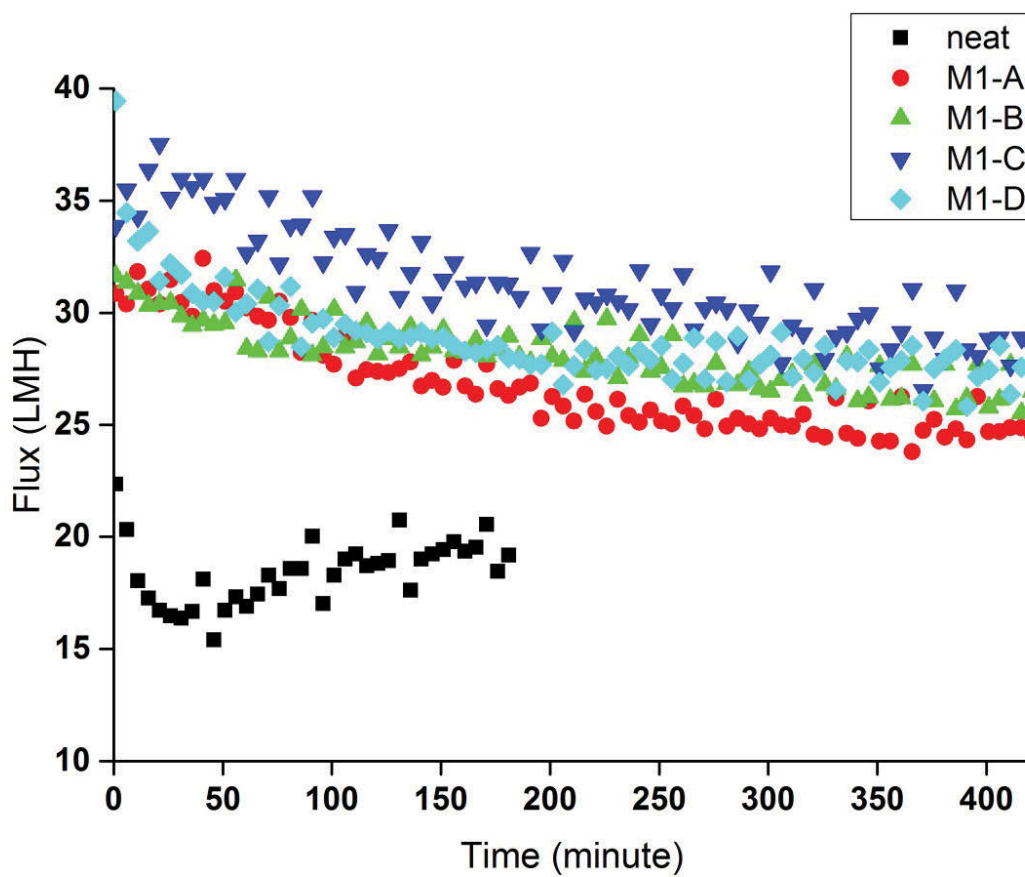


Figure 22-Flux comparisons of electrospun membranes heat-pressed at various pressures

4.3 Effect of heat-press duration on the membranes

Heat-press duration has not been extensively studied in previous studies (Wu et al. 2014). In recent relevant studies, there were two common approaches of heat-press process: the membrane samples were (1) placed in a pre-heated oven for 1 h (Liao et al. 2013b; Ma et al. 2005a); or (2) heat-pressed by extremely hot home iron for very short periods (e.g. 1-2 s) (Lalia et al. 2013; Na et al. 2008). Hence, there was a strong need to explore the effect of durations comprehensively. It was expected that the electrospun fibers could be better fused if the polymer films were heat-pressed for a longer duration, so both the morphology and characteristics might be improved. Thus four durations: 1, 2, 4 and 8 h were applied in post-treatment and their effects were investigated. The relevant samples were named M1-B-1, M1-B-2, M1-B-3 and M1-B-4, respectively.

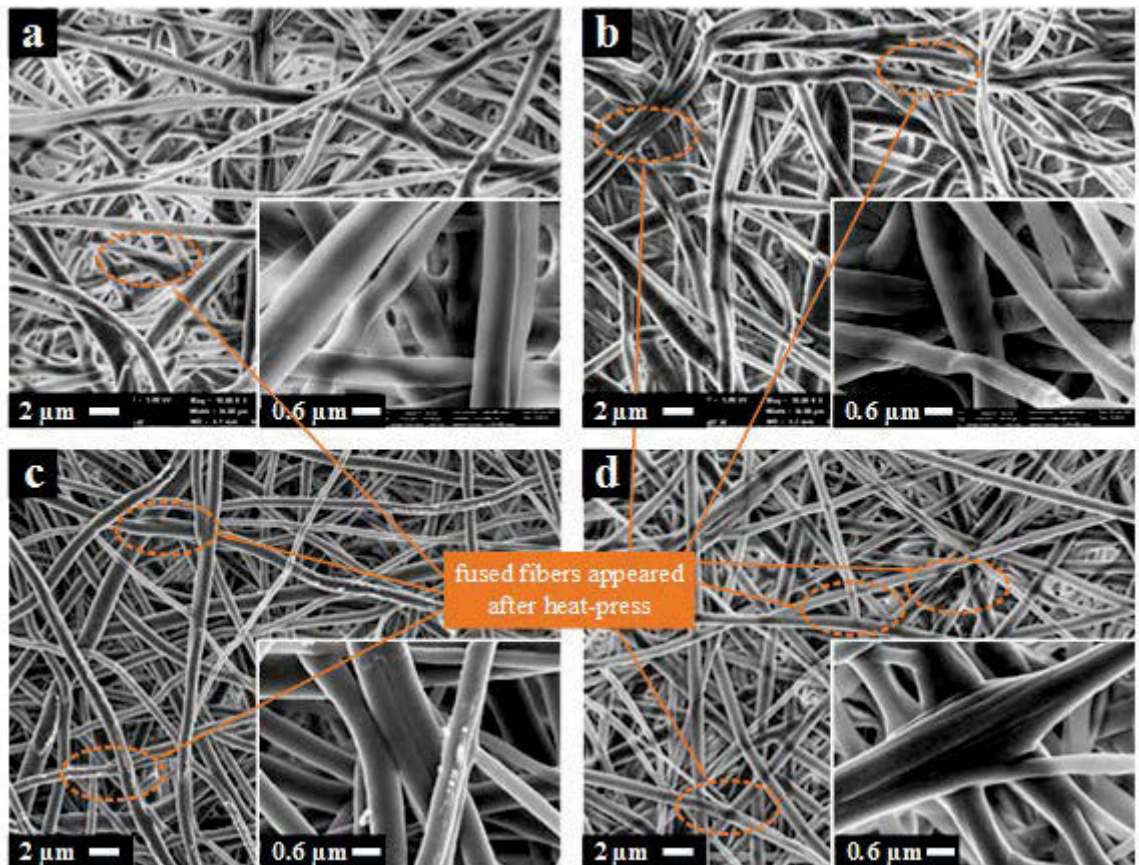


Figure 23-SEM images of heat-pressed PH membrane at magnifications of 10 K and 50 K: membranes heat-pressed for (a) 1 h (M1-B-1); (b) 2 h (M1-B-2); (c) 4 h (M1-B-3); (d) 8 h (M1-B-4).

In Fig. 23, it can be found that when increasing the durations of heat-press, there would be more fiber fused with each other based on the observations of the changes in morphology. M1-B-4 had most fused fibers than the other samples and a large fused joint could be seen in 50 K magnifications of Fig. 23d, which was rarely found in other samples. Also, heat-pressed membrane for longer duration tended to have larger fiber size and hence smaller surface pore size. It was clearly displayed in Fig. 24 that membranes heat-pressed for 8 h had the narrowest PSD and smallest average pore size.

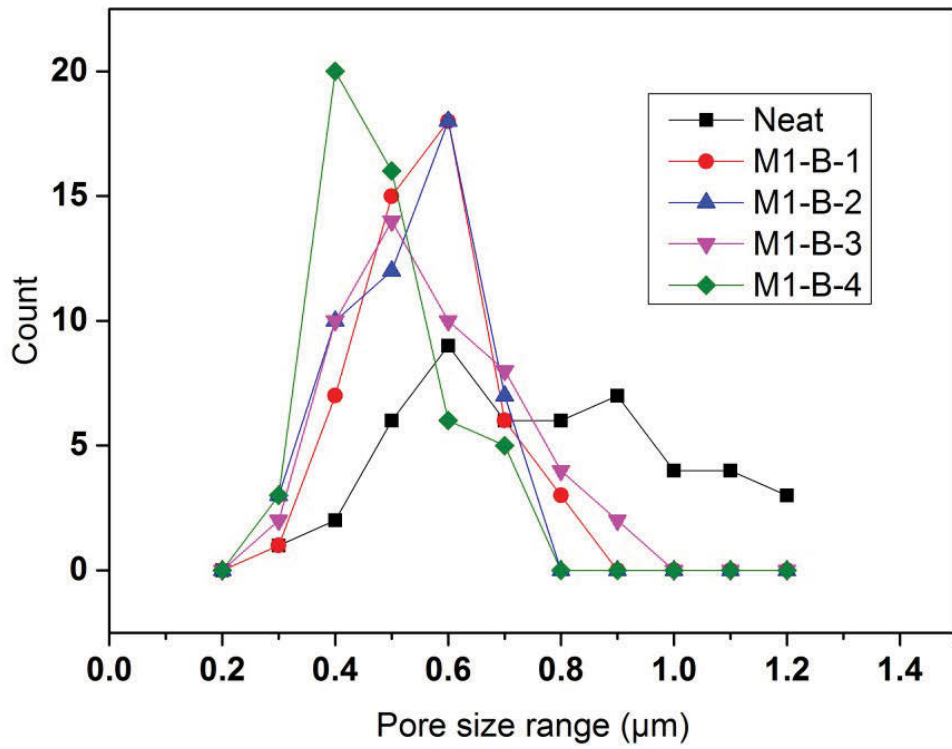


Figure 24-Pore size distributions of as-spun and membrane samples heat-pressed for various durations.

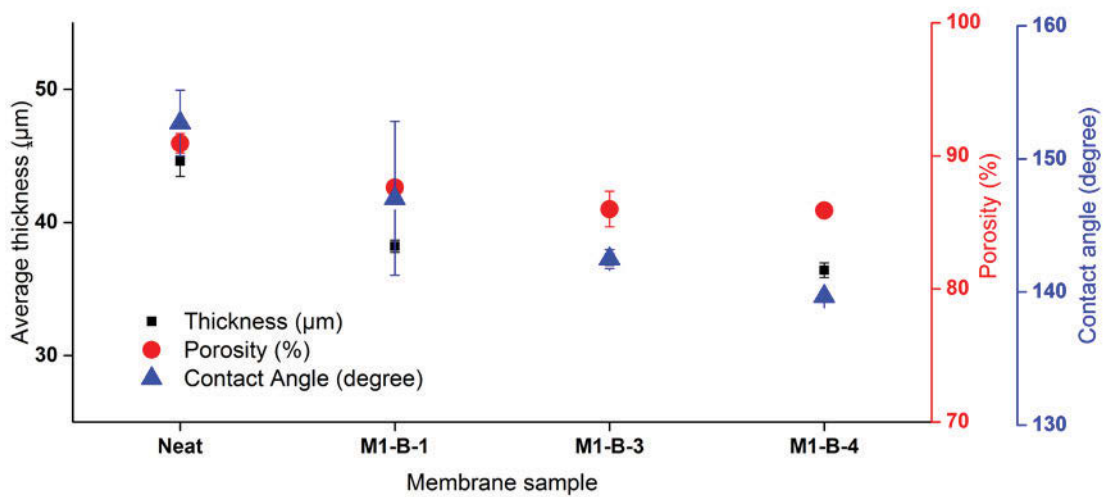


Figure 25-Effects of heat-press pressure on thickness, porosity and contact angle.

Fiber and surface pore size were strongly affected by the duration of the heat-press. It was observed that when membrane samples had been heat-pressed for 8 h, it had the largest fiber size of 0.80 μm and smallest surface pore size of 0.40 μm (Table 6).

Contact angle, porosity and thickness of membranes samples heat-pressed for various durations shared comparable trends. When the durations increased, the values of these characteristics decreased. Thickness and contact angle were affected by the duration more severely. However, it was interesting to point out that further increase of duration beyond 2 h had minimal influence on the porosity (Fig. 25). The reason might be that the membrane could not be further fused at the intersection points when the duration was increased beyond 2 h.

Table 6-Characteristics of the membranes after heat-press at different durations

Parameter/Sample	Neat	M1-B-1	M1-B-2	M1-B-3	M1-B-4
Fiber size (μm)	0.39 \pm 0.12	0.66 \pm 0.21	0.69 \pm 0.24	0.69 \pm 0.26	0.80 \pm 0.29
Surface pore size (μm)	0.50 \pm 0.21	0.48 \pm 0.12	0.45 \pm 0.09	0.45 \pm 0.12	0.40 \pm 0.10
Young's modulus (MPa)	11.7 \pm 5.4	27.9 \pm 4.8	40.9 \pm 2.6	41.8 \pm 7.9	45.7 \pm 7.6
Stress at break (MPa)	3.09 \pm 0.18	11.26 \pm 0.52	12.11 \pm 0.35	12.55 \pm 0.16	13.28 \pm 0.65
Strain at break	0.66 \pm 0.05	1.54 \pm 0.11	1.56 \pm 0.19	1.55 \pm 0.08	1.39 \pm 0.26
LEP (kPa)	71 \pm 9	58 \pm 4	83 \pm 4	82 \pm 4	90 \pm 7

The mechanical properties were also affected by the heat-press duration in a positive way. M1-B-1 had a lower tensile strength, indicating that the membrane was not sufficiently compacted and the electrospun fibers were not fully fused. Table 6 shows that M1-B-4 had the highest Young's modulus and maximum stress. It meant that longer heat-press duration could increase the mechanical properties impressively. Heat-press duration could affect the LEP as well as we could see that M1-B-4 had the highest LEP of 90 kPa. It is interesting to state that M1-B-1 had LEP lower than neat membrane. It could be explained by the fact that the decrease of thickness affected the LEP of membrane negatively and the membrane fibers did not have sufficient time for being fused together to deliver higher resistance against fiber deformations under high pressures which could lead to enlarged pores (Lalia et al. 2014).

4.3.1 Effect of heat-press duration on MD permeation flux

Fig. 26 showed that increase in heat-press durations could improve the permeation flux in 8 h DCMD test. In this stage, membrane heat-pressed for 1 h had the lowest permeation flux due to insufficient compaction in such a short time. Especially, a sharp decline in flux had been observed in electrospun membranes that had been heat-pressed for 1 h, which could be attributable to its much lower LEP. In long-term operation, membranes with lower LEP had more risks of exposing to partially wetting which could result in fast decline in permeation performance, so that adequate duration for heat-press is necessary. Long enough duration in heat-press can guarantee that the electrospun membranes had sufficient time for material changes from soft fluffy structures to some tough plastic matrix. Compared with membrane heat-pressed for 1 and 2 h, membrane heat-pressed for 8 h had significantly higher performance regarding flux. As there was minor flux improvement when membrane heat-pressed for more than 4 h, 8 h was considered as the optimal duration for sufficiently heat-pressing on electrospun PH membranes with relative thickness. The founding of improved performance with increased heat-press duration was novel for MD membrane modification as no previous researchers had tried to heat-press membranes for more than 1 h.

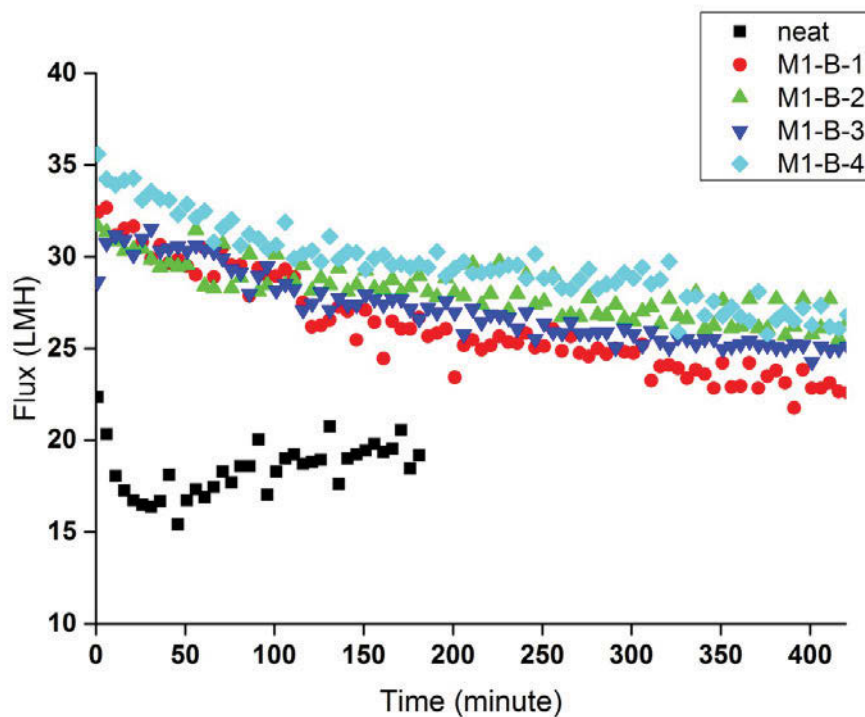


Figure 26-Flux comparisons of electrospun membranes heat-pressed at various durations

CHAPTER 5

INFLUENCE OF THICKNESS ON ELECTROSPUN MEMBRANES



University of Technology Sydney
FACULTY OF ENGINEERING

5. Influence of thickness on electrospun membranes

5.1 Influence of thickness on membrane characteristics

Table 7-Comparison of membrane characteristics with various thicknesses

Parameter/Sample name	PH1	PH2	PH3	PH4
Fiber size (μm)	0.43 \pm 0.24	0.45 \pm 0.29	0.43 \pm 0.26	0.40 \pm 0.23
Surface pore size (μm)	0.65 \pm 0.29	0.62 \pm 0.24	0.61 \pm 0.25	0.61 \pm 0.16
Thickness (μm)	103.4 \pm 1.1	146.8 \pm 3.0	224.4 \pm 4.4	395.2 \pm 3.5
Young's modulus (MPa)	15.7 \pm 9.4	16.2 \pm 1.8	16.4 \pm 5.9	20.6 \pm 0.6
Stress at break (MPa)	6.74 \pm 0.32	6.60 \pm 0.13	6.31 \pm 0.38	10.13 \pm 0.47
Strain at break	1.54 \pm 0.08	1.20 \pm 0.02	1.25 \pm 0.12	1.87 \pm 0.01
LEP (kPa)	76.5 \pm 2.2	79.0 \pm 1.2	88.0 \pm 2.0	93.0 \pm 2.5

Membrane thickness had strong influence on some characteristics of membranes including mechanical strength and LEP. Increase in the membrane thickness could result in increase in the LEP (Guillen-Burrieza et al. 2015). Membranes with thickness of 395 μm had 25% higher LEP than the ones with thickness of 103 μm (Table 7). Except the membranes with thickness of 395 μm , increase in thickness had minor effects on the mechanical strengths. Membranes with thickness of 103, 147, and 224 μm had nearly identical Young's modulus, stress, and strain at break. Similarly, membrane thickness had insignificant effects on fibers and surface pore size. Fig. 27 showed that thickness of electrospun membranes had no effects on CA and porosity because the increase in thickness was only caused by longer duration of electrospinning process,

thus not affecting the morphology and structure of the membranes.

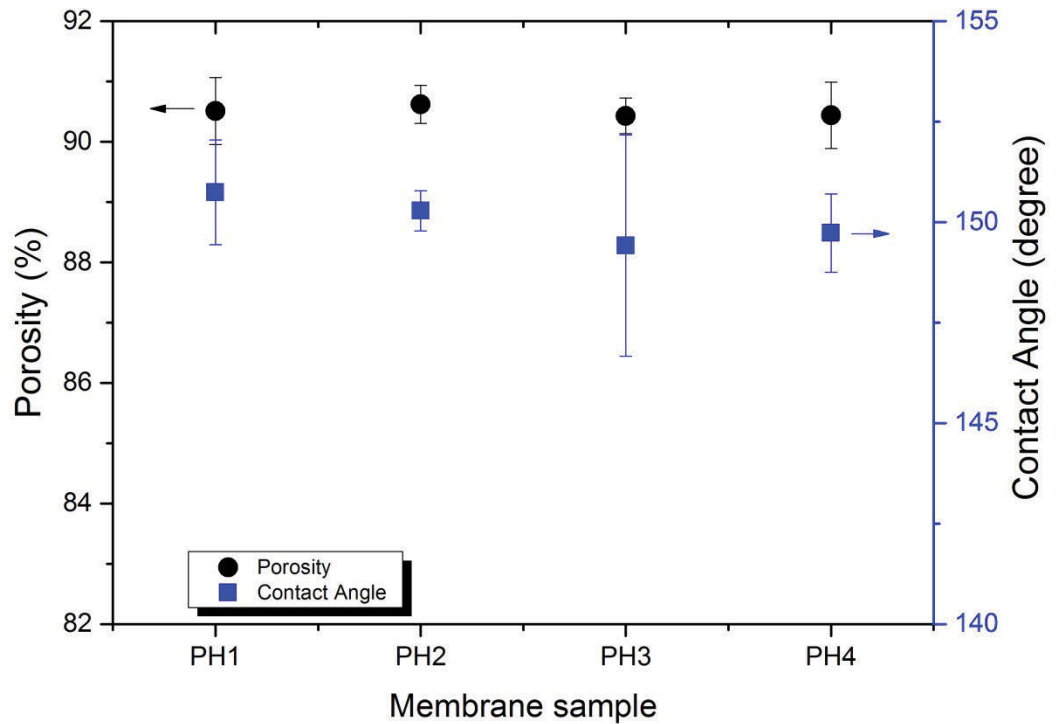


Figure 27-Comparison of CA and porosity of electrospun membrane with various thicknesses

5.2 Effects of heat-press on characteristics on membrane with various thickness

In the previous stages (1-3), it could be found that samples of M1, M1-C and M1-B-4 had better PSD, LEP and mechanical properties in each of their belonging group, and their relative controllable conditions were temperature of 150 °C, pressure of 6.5 kPa and duration of 8 h, respectively. It was assumed that the optimal heat-press condition could be achieved with the combination of the individual optimal conditions. Hence, the combination of 150 °C, 6.5 kPa and 8 h was considered as the optimal heat-press condition set in this study. In Stage 4, four membranes samples with different initial thicknesses from 103 to 395 μm were exposed to the optimal heat-press conditions. The as-spun membranes were named as PH1, PH2, PH3 and PH4 corresponding to initial membrane thicknesses of 103, 146, 224 and 395 μm , respectively and their corresponding heat-pressed conditions were named as PH1', PH2', PH3' and PH4'.

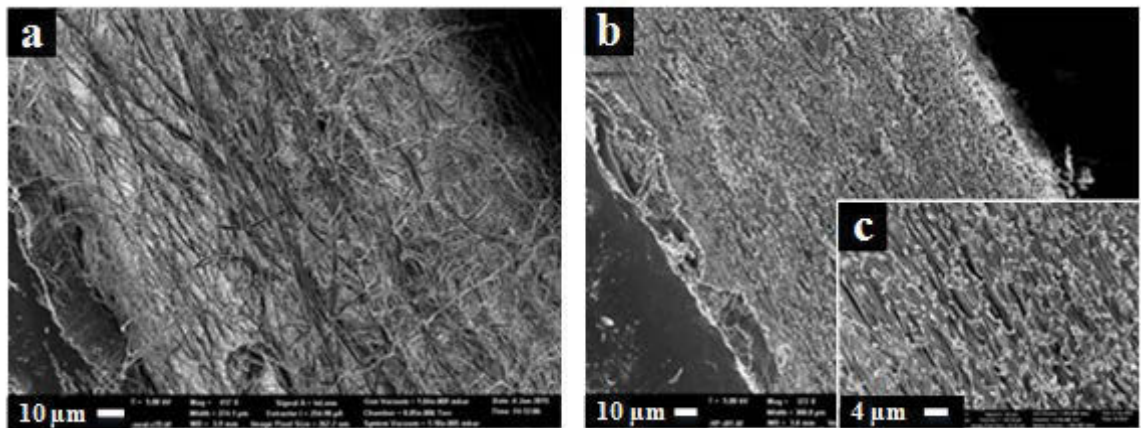


Figure 28-Representative SEM cross section images of as-spun, PH3 (a: 400 K) and heat-pressed membrane, PH3' (b: 350 K; c: 1500 K).

Fig. 28 shows representative cross-section SEM images of membranes before and after heat-press with optimal conditions. The as-spun membrane (Fig. 28a) showed more fluffy structure and thicker thickness while the heat-pressed membrane was thinner and more compact. Generally, more uniform and denser morphology can be observed in heat-pressed membranes and it could contribute to higher LEP, even though the thickness of heat-pressed membrane was obviously lower. The as-spun membranes (PH1 to PH4) have very similar membrane properties except for surface pore size and LEP as lower pore sizes and higher LEP values were obtained with thicker membranes (Table 8). The decreased pore size could be attributed to the increased overlapping, random orientation, and non-woven effect of fibers at higher thickness. Thus, the decrease in pore size would lead to increase in LEP. The trends of fibers and pore size change were similar with Wu et al.'s study (Wu et al. 2014).

Table 8-Characteristics of the membranes with various thicknesses after heat-press

Parameter/Sample name	PH1	PH1'	PH2	PH2'	PH3	PH3'	PH4	PH4'
Fiber size (μm)	0.43 \pm 0.24	0.68 \pm 0.26	0.45 \pm 0.29	0.76 \pm 0.27	0.43 \pm 0.26	0.70 \pm 0.24	0.40 \pm 0.23	0.64 \pm 0.22
Surface pore size (μm)	0.65 \pm 0.29	0.42 \pm 0.21	0.62 \pm 0.24	0.39 \pm 0.16	0.61 \pm 0.25	0.38 \pm 0.17	0.61 \pm 0.16	0.35 \pm 0.14
Thickness (μm)	103.4 \pm 1.1	89.8 \pm 1.1	146.8 \pm 3.0	129.0 \pm 2.9	224.4 \pm 4.4	194.8 \pm 1.9	395.2 \pm 3.5	343.2 \pm 2.3
Reduction percentage after heat-press from initial thickness		13.15%		12.13%		13.19%		13.16%
Young's modulus (MPa)	15.7 \pm 9.4	44.7 \pm 12.9	16.2 \pm 1.8	36.4 \pm 12.2	16.4 \pm 5.9	30.6 \pm 4.0	20.6 \pm 0.6	40.0 \pm 2.3
Stress at break (MPa)	6.74 \pm 0.32	13.29 \pm 0.33	6.60 \pm 0.13	13.61 \pm 1.07	6.31 \pm 0.38	14.23 \pm 1.89	10.13 \pm 0.47	15.91 \pm 1.04
Strain at break	1.54 \pm 0.08	0.86 \pm 0.01	1.20 \pm 0.02	1.09 \pm 0.03	1.25 \pm 0.12	0.95 \pm 0.42	1.87 \pm 0.01	1.40 \pm 0.16
LEP (kPa)	76.5 \pm 2.2	97.0 \pm 1.4	79.0 \pm 1.2	99.5 \pm 0.7	88.0 \pm 2.0	108.5 \pm 1.5	93.0 \pm 2.5	116.0 \pm 2.4

From Table 8, it could be observed that the percentage reduction in thickness (around 13%) of heat-press membrane was consistent regardless the membrane thicknesses. The results agreed with the experiment in the previous stages. Membrane with thickness of 45 μm was heat-pressed into 37 μm , indicating a reduction of around 15% from the initial thickness. However, the reduction percentage was relatively smaller than the ones in other studies. For example, Wu et al. reported a reduction of around 25% (Wu et al. 2014), and the reduction was over 50% in Liao et al.'s and Lalia et al.'s studies (Liao et al. 2014b; Lalia et al. 2013). The variations in results could be attributed to the differences of heat-press approaches (ironing or weight pressing in the hot oven) and polymer material used (PVDF or PH).

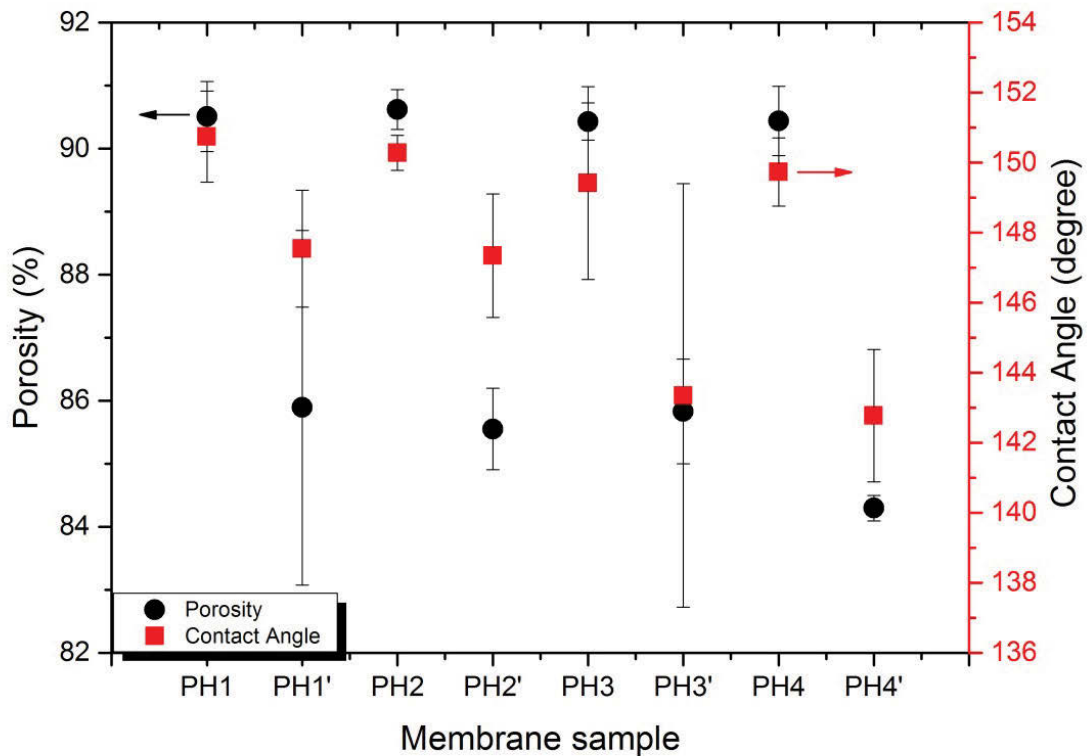


Figure 29-Effects of heat-press with optimal conditions on porosity and contact angles of membranes with various thicknesses

Fig. 29 indicates that porosity and contact angle share similar trend after heat-press treatment. Samples with various thicknesses had decreased porosity and contact angle with respect to increased initial membrane thickness. After heat-pressing, PH1' had a decreased CA from 151 to 148°, and a decreased porosity from 91 to 87%. PH4' had a

decreased CA from 150 to 143°, and a decreased porosity from 90 to 84%. . It can be concluded that heat-pressing slightly decreased the porosity and CA of the membranes, but the initial membrane thickness had little effect on porosity and CA.

It was also observed that increasing thickness of membranes could slightly enhance the mechanical strengths of the membranes, and the mechanical properties could be enhanced greatly after heat-pressing method. The maximum stresses at break increased by 57-125% after heat-press compared to their corresponding as-spun membranes. However, the maximum strains at break decreased, which indicated that the polymers turned from elastic to more plastic materials. Also, heat-press could improve the LEP of membranes with various thicknesses. The improvement was consistent, which was around 25% from their as-spun membrane counterpart. The highest LEP of 116 kPa was obtained with PH4'.

5.3 MD permeation performance with membrane having various thickness before and after heat-press

Selected heat-pressed electrospun membranes (PH1', PH2' and PH3') and commercial membrane samples were tested and compared in terms of permeation flux and salt rejection in DCMD module for desalination, with feed (3.5 wt% NaCl) and permeate (DI) temperature of 60 °C and 20 °C, respectively. Since the heat-pressed membranes had improved characteristics and properties, they are selected for the DCMD tests. **Fig. 30** shows the DCMD performance of commercial and heat-pressed membranes. The commercial membrane (GVHP, total membrane thickness of 107 µm) showed a stable flux of 22 L/m²h (LMH) and salt rejection of 99.98% after 8 h of test. On the other hand, the heat-pressed electrospun membranes showed varying results as PH1' and PH2' posting higher flux performance (28 and 26 LMH, respectively) compared to commercial membrane, while PH3' (17 LMH) had lower flux. The main reason for the low flux of PH3' was its much thicker thickness compared to other samples, which increases the passage length of the vapor through the membrane and thereby added mass transfer resistance. Similarly, the thinner thickness of PH1' (i.e., after heat-press and compaction) improved its flux performance without sacrificing the salt rejection which was maintained at 99.99% (Wu et al. 2014). Improvement of PSD, thinner thickness and higher LEP contributed more to the enhanced permeation and salt rejection performance. Besides, it was considered that the improvement of mechanical

strength could help electrospun membranes being more robust against deformation during long-term operation (Essalhi & Khayet 2013). Further, the better mechanical strength could reduce the tendency of membrane pores to expand, so it could prevent water being captured in the pores between the fiber layers and lead to an increase in mass transfer resistance (Liao et al. 2013b)

Generally membranes after heat-press treatment at optimal settings had much better performance than the ones before heat-press. Heat-pressed membranes had a stable performance of flux and salt rejection while as-spun had rapidly decreasing in flux and salt rejection in short time. In this study, thickness of heat-pressed electrospun membrane beyond 200 μm was not favored for DCMD due to its greatly decreased permeability.

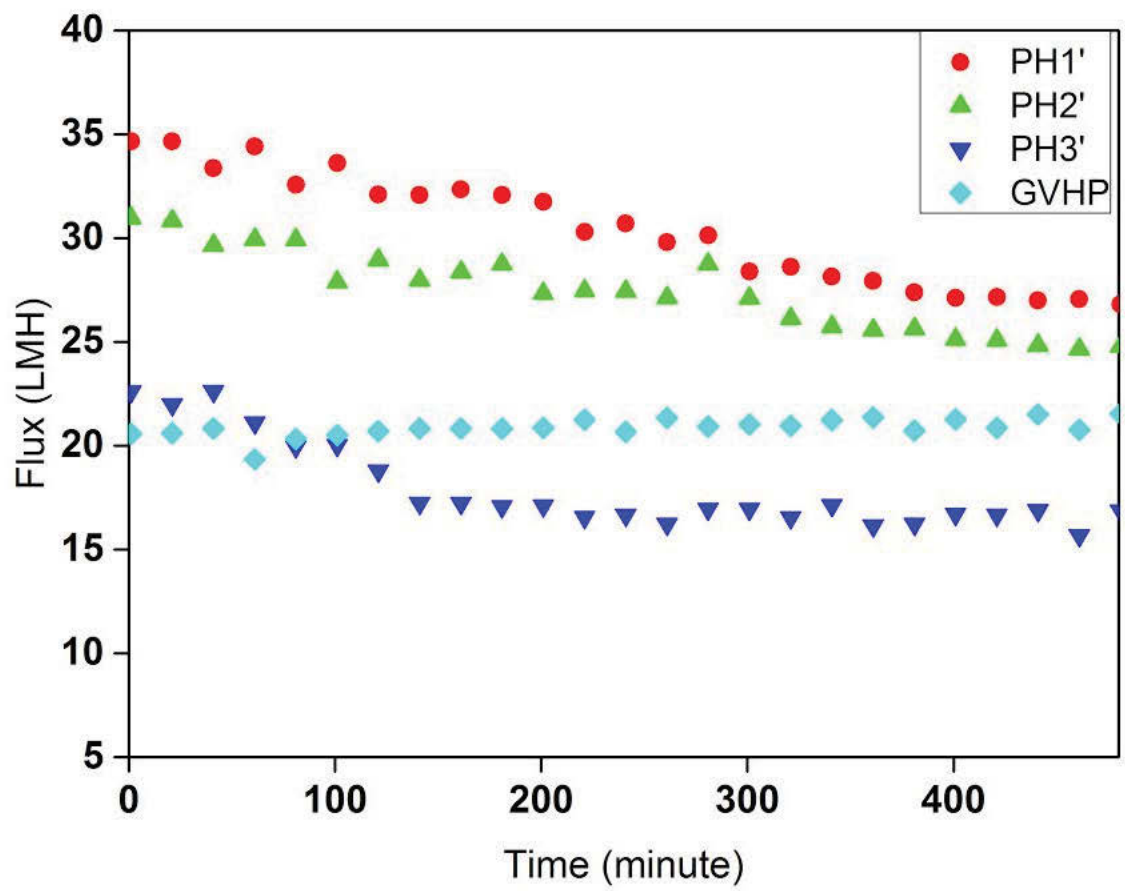


Figure 30-Comparison of DCMD permeation performance of selected membrane samples.

Table 9- Comparison of heat-pressed MD flat-sheet membranes for desalination with commercial PVDF membrane

Membrane	Solvent	Method of heat-press	Mean pore size (μm)	Thickness (μm)	Porosity (%)	Feed solution	Feed velocity (m s ⁻¹)	Feed temperature (°C)	Permeate temperature (°C)	Permeate velocity (m s ⁻¹)	Permeation flux (LMH)	Salt rejection (%)
5% PVDF with LiCl ₂ as additive (Liao et al. 2013b)	DMF/acetone	placed under glass plate in an oven at 170 °C for 1 h	0.21	42	54	3.5 wt% NaCl solution	0.07	50	20	0.14	20.6	-
10% PH (Lalia et al. 2013)	DMAc/acetone	applied iron on both top and bottom surfaces at 200 °C for 1-2 s	0.26	110	55-60%	1 wt% NaCl solution	0.32	50	24	0.32	20-22	98
5% PVDF (Wu et al. 2014)	DMF/acetone	placed under glass plate in an oven at 170 °C for 1 h	-	27-58	80-84%	10 wt% NaCl solution	0.31	65	20	0.31	10-30	-
20% PH1' (in this study)	DMAc/acetone	placed under metal plates in oven at 150 °C for 8 h	0.42	90	86%	3.5 wt% NaCl solution	0.07	60	20	0.07	29	99.99
Millipore GVHP PVDF (in this study)	-	-	0.22	110	-	3.5 wt% NaCl solution	0.07	60	20	0.07	22	99.98

5.4 DCMD performance comparison with other studies using heat-pressed membranes

Table 9 shows a comparison of different electrospun membrane characteristics and DCMD flux performance after subjecting to various heat-press treatment approaches. Compared to other results, PH1' showed very high flux and salt rejection for an 8 h test even it had thicker thickness and running at low flow velocity in both permeate and feed sides. This better performance could be attributed to the slightly wider pore size and high porosity, as both of them were the highest in this table. Considering using the same polymer (PH), heat-press by placing membrane under metal plates in oven at 150 °C for 8 h had much better effects than by applying iron on both top and bottom surfaces at 200 °C for 1-2 s. Heat-press for 8 h in the hot oven could contribute to better modified membrane as it could affect the internal layers of electrospun fibers thoroughly along with less reduction in the porosity. A sufficient duration of heat-press (with adequate temperature and pressure) could change fluffy internal structure of electrospun membrane into reasonably dense and uniform ones (Fig.28c), and hence improve the mechanical properties and LEP greatly, resulting in impressively high salt rejection for long-term MD test. It was also interesting to point out that, in previous studies, relatively low concentration of polymer was applied to obtain membranes with small pore size. However, heat-press treatment could further decrease the pore size and make it lower than optimal range for MD, resulting in low permeate flux. In conclusion, the present result addresses the importance and potential of heat-press on electrospun membrane for improved MD performance.

CHAPTER 6

CONCLUSION AND RECOMMENDATIONS



University of Technology Sydney
FACULTY OF ENGINEERING

6. Conclusion and recommendations

6.1 Conclusions

In the present study, the effects of heat-press conditions (temperature, pressure, and duration) on the electrospun polyvinylidene fluoride-co-hexafluoropropylene (PH) membrane were comprehensively investigated and membranes that had been optimally heat-pressed were tested for DCMD. The following points had been concluded:

(1) Heat-press temperature had crucial effects on the membrane morphology and characteristics. Increase in heat-press temperature could lead to more fibers fused together and improve the PSD, mechanical properties, and LEP, greatly. However, temperature above melting points (155 degree) was not favored as the post-treatment could cause the membrane partially melting so that its internal open network structure could be damaged, which might result in much lower pore size, porosity, and mass transfer coefficient.

(2) Heat-press pressure played less important role in affecting the membrane morphology and characteristics. Increase in pressure could result in more fused fibers, narrower PSD, higher tensile strength, and LEP. However, the improvement was somehow not so great. When the heat-press pressure exceeded certain value, the improvement of characteristics would be ignorable as the membrane had reached its maximum compaction level. Therefore, the permeation performance could not be further improved by increasing the heat-press pressure on the electrospun membranes.

(3) Heat-press duration could affect the morphology and characteristics of membranes greatly. Increase in duration could greatly cause more fibers fused at interlay points, and the PSD was narrowed along with significantly decreased average pore size. With Increase in heat-press duration could increase mechanical strength and LEP greatly also, and the MD efficiency was thus benefited in long-term operation.

(4) Membrane samples with various thicknesses had been heat-pressed at optimal conditions (150 degree, 6.5kPa, and 8 h), and it was found that effects on morphology and characteristics were consistent regardless of the thickness. MD tests with selected membranes were also conducted, and it was found that membranes after heat-press had greatly improved permeation performance while thickness of membrane itself still played an important role in permeation efficiency.

Overall, heat-press treatment with optimal conditions could successfully improve the characteristics of the membranes, and thus permeation and salt rejection performance in MD. It was found that heat-press temperature and duration had dominant roles in the post-treatment, while pressure had a relatively minor role. Thickness of heat-pressed membranes <130 μm was considered as the optimal range due to their relatively high permeability. The benefits of heat-pressed membranes included their relatively small surface pore size, high porosity, CA, and LEP. Thickness of electrospun membrane beyond 200 μm was considered not appropriate due to increased mass transfer resistance. It was estimated that electrospun membranes with other polymers could be improved by heat-press treatment with proper conditions for enhanced membrane morphology, characteristics, LEP and tensile strength. In conclusion, heat-press technique is strongly recommended for electrospun polymer membrane to enhance their morphology and characteristics as required by relative applications including membrane distillation.

6.2 Recommendations

6.2.1 Further study on heat-press conditions

Although heat-press conditions have been extensively investigated by the candidate, there is still some space left that requires further researches. Cooling rate is one of other important factors in heat-press treatment. It was found that various cooling rate could determine the polymer conformation type, crystallization phase, crystal size, and crystallinity (Liu et al. 2011). It was found that faster cooling rate could lead to B conformation, smaller crystal sizes, and relatively lower crystallinity (El Mohajir & Heymans 2001). El Mohajir & Heymans (2001) also stated that, after annealing, polymer (i.e. PVDF) cooled at different rate would have distinctive tensile strength patterns. Treated at fast cooling rate, the stress of the polymer would continue going up after yield when external pressure applied, while treated at slow cooling rate, yield stress was the maximum stress, and then it would decrease and had a necking region prior to rupture. Also, PVDF cooled at quick rate had higher maximum stress and strain around 24% than the ones cooled at slow rate. Therefore, there is a need to optimize the cooling rate after heat-press process, so a better control of the membrane characteristics can be obtained on molecular level (crystallization), and thus suitable characteristics

may be achieved for better MD permeation performance, especially in long-term operation.

6.2.2 Superhydrophobic modification with aerogel powder

One approach that has great potentials to improve MD permeation performance is to incorporate aerogel powder as additive in the polymer solution for electrospinning membrane, which may have lotus effect. Hydrophobic aerogel has some distinguished properties including superhydrophobicity, high shear strength, and low thermal transfer rate. These properties make aerogel powders extremely suitable for MD applications as superhydrophobicity can increase the water resistance of the membrane, benefiting long-term operation. Aerogel powders within size range of 1-5 μm can be added into the polymer solution, and homogenous polymer solution is able to be obtained by sonification followed by mechanical stirring. With incorporation of aerogel powder, it is expected that membranes with much higher LEP and hydrophobicity can be obtained via electrospinning, if the features of aerogel powder can be realized on the nanofiber structures on the electrospun membrane surface.

6.2.3 Optimization of support layer and its adhesion to active layer with electrospinning

Previously being discussed in literature section, support layer had strong effect on the MD permeation process (Shirazi et al. 2014). Support layer with fiber structure had better permeation performance than the ones with non-woven fabric and scrim structures. Therefore, if its mechanical strength could be improved, electrospun membranes will have great potentials to be used as support layers for MD applications, reducing temperature polarization. Also, materials of support layers are essential; normally, polymers with low surface tension energy and high thermal & chemical resistance are favored.

Adhesion between modified hydrophobic active layer and support layer is another challenge, as poor adhesion could result in low robustness of the membrane. Crosslinking is a common method to improve adhesion between the active and support layer. However, adhesive mediums for crosslinking generally are weak against chemical cleaning which are routinely applied in full-scale applications, so its robustness is questionable. Because the solvents had not been fully evaporated during the process, active and support layer both made with electrospinning might be adhered to each other

with the aid of the residue of solvents. Some researchers had successfully electrospun active layer over the substrate layer directly, which was named dual layer electrospun membranes (Woo et al. 2015). Therefore, electrospinning is one of viable approach to solve the weak adhesion issue between active and support layer.

APPENDIX

Thesis related publications and presentations:

Peer-reviewed journal articles:

Yao, M., Woo, Y.C., Tijing, L.D., Shim, W.-G., Choi, J.-S., Kim, S.-H. & Shon, H.K. 2016, 'Effect of heat-press conditions on electrospun membranes for desalination by direct contact membrane distillation', *Desalination*, vol. 378, pp. 80-91.

[doi:10.1016/j.desal.2015.09.025](https://doi.org/10.1016/j.desal.2015.09.025) (This PJA is embedded in the candidate's thesis as part of formal submission)

Conference presentations:

Yao, M., et al., Heat-press effect to electrospun nanofibrous membrane for seawater desalination by membrane distillation, the 7th International Desalination Workshop (IDW), poster, 2014

Yao, M., et al., Effect of heat-press conditions on electrospun membranes for desalination by direct contact membrane distillation, the 8th Challenges in Environmental Science & Engineering (CESE), oral, 2015

REFERENCE

- Acatay, K., Simsek, E., Ow-Yang, C. & Menciloglu, Y.Z. 2004, 'Tunable, superhydrophobically stable polymeric surfaces by electrospinning', *Angewandte Chemie International Edition*, vol. 43, no. 39, pp. 5210-3.
- Adnan, S., Hoang, M., Wang, H. & Xie, Z. 2012, 'Commercial PTFE membranes for membrane distillation application: effect of microstructure and support material', *Desalination*, vol. 284, pp. 297-308.
- Ahmed, F.E., Lalia, B.S. & Hashaikh, R. 2015, 'A review on electrospinning for membrane fabrication: Challenges and applications', *Desalination*, vol. 356, no. 0, pp. 15-30.
- Alkudhiri, A., Darwish, N. & Hilal, N. 2012, 'Membrane distillation: A comprehensive review', *Desalination*, vol. 287, no. 0, pp. 2-18.
- Alkudhiri, A., Darwish, N. & Hilal, N. 2013, 'Treatment of saline solutions using Air Gap Membrane Distillation: Experimental study', *Desalination*, vol. 323, no. 0, pp. 2-7.
- Ataollahi, N., Ahmad, A., Hamzah, H., Rahman, M. & Mohamed, N. 2012, 'Preparation and characterization of PVDF-HFP/MG49 based polymer blend electrolyte', *Int. J. Electrochem. Sci.*, vol. 7, no. 6693, p. e6703.
- Boubakri, A., Hafiane, A. & Bouguecha, S.A.T. 2014, 'Application of response surface methodology for modeling and optimization of membrane distillation desalination process', *Journal of Industrial and Engineering Chemistry*, vol. 20, no. 5, pp. 3163-9.
- Chen, G., Yang, X., Lu, Y., Wang, R. & Fane, A.G. 2014, 'Heat transfer intensification and scaling mitigation in bubbling-enhanced membrane distillation for brine concentration', *Journal of Membrane Science*, vol. 470, pp. 60-9.
- Dong, Z.-Q., Ma, X.-h., Xu, Z.-L., You, W.-T. & Li, F.-b. 2014, 'Superhydrophobic PVDF-PTFE electrospun nanofibrous membranes for desalination by vacuum membrane distillation', *Desalination*, vol. 347, no. 0, pp. 175-83.
- Doshi, D.A., Shah, P.B., Singh, S., Branson, E.D., Malanoski, A.P., Watkins, E.B., Majewski, J., van Swol, F. & Brinker, C.J. 2005, 'Investigating the interface of superhydrophobic surfaces in contact with water', *Langmuir*, vol. 21, no. 17, pp. 7805-11.
- Eda, G., Liu, J. & Shivkumar, S. 2007, 'Solvent effects on jet evolution during electrospinning of semi-dilute polystyrene solutions', *European Polymer Journal*, vol. 43, no. 4, pp. 1154-67.
- El Mohajir, B.-E. & Heymans, N. 2001, 'Changes in structural and mechanical behaviour of PVDF with processing and thermomechanical treatments. 1. Change in structure', *Polymer*, vol. 42, no. 13, pp. 5661-7.
- Essalhi, M. & Khayet, M. 2013, 'Self-sustained webs of polyvinylidene fluoride electrospun nanofibers at different electrospinning times: 1. Desalination by direct contact membrane distillation', *Journal of membrane science*, vol. 433, pp. 167-79.
- Fan, H. & Peng, Y. 2012a, 'Application of PVDF membranes in desalination and comparison of the VMD and DCMD processes', *Chemical Engineering Science*, vol. 79, no. 0, pp. 94-102.

- Fan, H. & Peng, Y. 2012b, 'Application of PVDF membranes in desalination and comparison of the VMD and DCMD processes', *Chemical Engineering Science*, vol. 79, pp. 94-102.
- Fard, A.K., Manawi, Y.M., Rhadfi, T., Mahmoud, K.A., Khraisheh, M. & Benyahia, F. 2015, 'Synoptic analysis of direct contact membrane distillation performance in Qatar: A case study', *Desalination*, vol. 360, pp. 97-107.
- Feng, C., Khulbe, K.C., Matsuura, T., Tabe, S. & Ismail, A.F. 2013, 'Preparation and characterization of electro-spun nanofiber membranes and their possible applications in water treatment', *Separation and Purification Technology*, vol. 102, no. 0, pp. 118-35.
- Francis, L., Ghaffour, N., Alsaadi, A.S., Nunes, S.P. & Amy, G.L. 2014, 'Performance evaluation of the DCMD desalination process under bench scale and large scale module operating conditions', *Journal of Membrane Science*, vol. 455, no. 0, pp. 103-12.
- Francis, L., Maab, H., AlSaadi, A., Nunes, S., Ghaffour, N. & Amy, G. 2013, 'Fabrication of electrospun nanofibrous membranes for membrane distillation application', *Desalination and Water Treatment*, vol. 51, no. 7-9, pp. 1337-43.
- Frenot, A. & Chronakis, I.S. 2003, 'Polymer nanofibers assembled by electrospinning', *Current Opinion in Colloid & Interface Science*, vol. 8, no. 1, pp. 64-75.
- Fürstner, R., Barthlott, W., Neinhuis, C. & Walzel, P. 2005, 'Wetting and self-cleaning properties of artificial superhydrophobic surfaces', *Langmuir*, vol. 21, no. 3, pp. 956-61.
- Ge, J., Peng, Y., Li, Z., Chen, P. & Wang, S. 2014, 'Membrane fouling and wetting in a DCMD process for RO brine concentration', *Desalination*, vol. 344, no. 0, pp. 97-107.
- Geng, H., He, Q., Wu, H., Li, P., Zhang, C. & Chang, H. 2014, 'Experimental study of hollow fiber AGMD modules with energy recovery for high saline water desalination', *Desalination*, vol. 344, no. 0, pp. 55-63.
- Goh, S., Zhang, J., Liu, Y. & Fane, A.G. 2013, 'Fouling and wetting in membrane distillation (MD) and MD-bioreactor (MDBR) for wastewater reclamation', *Desalination*, vol. 323, no. 0, pp. 39-47.
- Guillen-Burrieza, E., Ruiz-Aguirre, A., Zaragoza, G. & Arafat, H.A. 2014, 'Membrane fouling and cleaning in long term plant-scale membrane distillation operations', *Journal of Membrane Science*, vol. 468, pp. 360-72.
- Guillen-Burrieza, E., Servi, A., Lalia, B.S. & Arafat, H.A. 2015, 'Membrane structure and surface morphology impact on the wetting of MD membranes', *Journal of Membrane Science*, vol. 483, no. 0, pp. 94-103.
- Guo, F., Servi, A., Liu, A., Gleason, K.K. & Rutledge, G.C. 2015, 'Desalination by Membrane Distillation using Electrospun Polyamide Fiber Membranes with Surface Fluorination by Chemical Vapor Deposition', *ACS applied materials & interfaces*, vol. 7, no. 15, pp. 8225-32.
- Han, J.T., Xu, X. & Cho, K. 2005a, 'Diverse access to artificial superhydrophobic surfaces using block copolymers', *Langmuir*, vol. 21, no. 15, pp. 6662-5.
- Han, J.T., Zheng, Y., Cho, J.H., Xu, X. & Cho, K. 2005b, 'Stable Superhydrophobic Organic-Inorganic Hybrid Films by Electrostatic Self-Assembly', *The Journal of Physical Chemistry B*, vol. 109, no. 44, pp. 20773-8.
- Hwang, H.J., He, K., Gray, S., Zhang, J. & Moon, I.S. 2011, 'Direct contact membrane distillation (DCMD): Experimental study on the commercial PTFE membrane and modeling', *Journal of Membrane Science*, vol. 371, no. 1-2, pp. 90-8.

- Jeong, S., Lee, S., Chon, H.-T. & Lee, S. 2014, 'Structural analysis and modeling of the commercial high performance composite flat sheet membranes for membrane distillation application', *Desalination*, vol. 349, pp. 115-25.
- Jiang, J., Zhu, L., Zhu, L., Zhu, B. & Xu, Y. 2011, 'Surface characteristics of a self-polymerized dopamine coating deposited on hydrophobic polymer films', *Langmuir*, vol. 27, no. 23, pp. 14180-7.
- Jisr, R.M., Rmaile, H.H. & Schlenoff, J.B. 2005, 'Hydrophobic and Ultrahydrophobic Multilayer Thin Films from Perfluorinated Polyelectrolytes', *Angewandte Chemie International Edition*, vol. 44, no. 5, pp. 782-5.
- Kang, G.-d. & Cao, Y.-m. 2014, 'Application and modification of poly(vinylidene fluoride) (PVDF) membranes – A review', *Journal of Membrane Science*, vol. 463, pp. 145-65.
- Khayet, M. & Matsuura, T. 2011, *Membrane distillation: principles and applications*, Elsevier.
- Koo, J., Han, J., Sohn, J., Lee, S. & Hwang, T.-M. 2013, 'Experimental comparison of direct contact membrane distillation (DCMD) with vacuum membrane distillation (VMD)', *Desalination and Water Treatment*, vol. 51, no. 31-33, pp. 6299-309.
- Kwon, S.-B., Lee, J.S., Kwon, S.J., Yun, S.-T., Lee, S. & Lee, J.-H. 2015, 'Molecular layer-by-layer assembled forward osmosis membranes', *Journal of Membrane Science*, vol. 488, pp. 111-20.
- Lalia, B.S., Guillen-Burrieza, E., Arafat, H.A. & Hashaikeh, R. 2013, 'Fabrication and characterization of polyvinylidene fluoride-co-hexafluoropropylene (PVDF-HFP) electrospun membranes for direct contact membrane distillation', *Journal of Membrane Science*, vol. 428, no. 0, pp. 104-15.
- Lalia, B.S., Guillen, E., Arafat, H.A. & Hashaikeh, R. 2014, 'Nanocrystalline cellulose reinforced PVDF-HFP membranes for membrane distillation application', *Desalination*, vol. 332, no. 1, pp. 134-41.
- Lee, S. 2011, 'Crystal structure and thermal properties of poly (vinylidene fluoridehexafluoropropylene) films prepared by various processing conditions', *Fibers and Polymers*, vol. 12, no. 8, pp. 1030-6.
- Li, X.-M., Reinhoudt, D. & Crego-Calama, M. 2007, 'What do we need for a superhydrophobic surface? A review on the recent progress in the preparation of superhydrophobic surfaces', *Chemical Society Reviews*, vol. 36, no. 8, pp. 1350-68.
- Liao, Y., Loh, C.-H., Wang, R. & Fane, A.G. 2014a, 'Electrospun Superhydrophobic Membranes with Unique Structures for Membrane Distillation', *ACS applied materials & interfaces*, vol. 6, no. 18, pp. 16035-48.
- Liao, Y., Wang, R. & Fane, A.G. 2013a, 'Engineering superhydrophobic surface on poly (vinylidene fluoride) nanofiber membranes for direct contact membrane distillation', *Journal of Membrane Science*, vol. 440, pp. 77-87.
- Liao, Y., Wang, R. & Fane, A.G. 2014b, 'Fabrication of Bioinspired Composite Nanofiber Membranes with Robust Superhydrophobicity for Direct Contact Membrane Distillation', *Environmental Science & Technology*, vol. 48, no. 11, pp. 6335-41.
- Liao, Y., Wang, R., Tian, M., Qiu, C. & Fane, A.G. 2013b, 'Fabrication of polyvinylidene fluoride (PVDF) nanofiber membranes by electro-spinning for direct contact membrane distillation', *Journal of Membrane Science*, vol. 425-426, no. 0, pp. 30-9.

- Liu, F., Hashim, N.A., Liu, Y., Abed, M.R.M. & Li, K. 2011, 'Progress in the production and modification of PVDF membranes', *Journal of Membrane Science*, vol. 375, no. 1–2, pp. 1-27.
- Lu, X., Zhang, J., Zhang, C. & Han, Y. 2005, 'Low-Density Polyethylene (LDPE) Surface With a Wettability Gradient by Tuning its Microstructures', *Macromolecular rapid communications*, vol. 26, no. 8, pp. 637-42.
- Ma, M. & Hill, R.M. 2006, 'Superhydrophobic surfaces', *Current opinion in colloid & interface science*, vol. 11, no. 4, pp. 193-202.
- Ma, M., Hill, R.M., Lowery, J.L., Fridrikh, S.V. & Rutledge, G.C. 2005a, 'Electrospun poly (styrene-block-dimethylsiloxane) block copolymer fibers exhibiting superhydrophobicity', *Langmuir*, vol. 21, no. 12, pp. 5549-54.
- Ma, M., Mao, Y., Gupta, M., Gleason, K.K. & Rutledge, G.C. 2005b, 'Superhydrophobic fabrics produced by electrospinning and chemical vapor deposition', *Macromolecules*, vol. 38, no. 23, pp. 9742-8.
- Manawi, Y.M., Khraisheh, M., Fard, A.K., Benyahia, F. & Adham, S. 2014, 'Effect of operational parameters on distillate flux in direct contact membrane distillation (DCMD): Comparison between experimental and model predicted performance', *Desalination*, vol. 336, no. 0, pp. 110-20.
- Martines, E., Seunarine, K., Morgan, H., Gadegaard, N., Wilkinson, C.D. & Riehle, M.O. 2005, 'Superhydrophobicity and superhydrophilicity of regular nanopatterns', *Nano letters*, vol. 5, no. 10, pp. 2097-103.
- Meng, S., Ye, Y., Mansouri, J. & Chen, V. 2014, 'Fouling and crystallisation behaviour of superhydrophobic nano-composite PVDF membranes in direct contact membrane distillation', *Journal of Membrane Science*, vol. 463, no. 0, pp. 102-12.
- Na, H., Zhao, Y., Zhao, C., Zhao, C. & Yuan, X. 2008, 'Effect of hot-press on electrospun poly (vinylidene fluoride) membranes', *Polymer Engineering & Science*, vol. 48, no. 5, pp. 934-40.
- Nghiem, L.D. & Cath, T. 2011, 'A scaling mitigation approach during direct contact membrane distillation', *Separation and Purification Technology*, vol. 80, no. 2, pp. 315-22.
- Park, S.H., Lee, S.M., Lim, H.S., Han, J.T., Lee, D.R., Shin, H.S., Jeong, Y., Kim, J. & Cho, J.H. 2010, 'Robust superhydrophobic mats based on electrospun crystalline nanofibers combined with a silane precursor', *ACS applied materials & interfaces*, vol. 2, no. 3, pp. 658-62.
- Pelipenko, J., Kristl, J., Janković, B., Baumgartner, S. & Kocbek, P. 2013, 'The impact of relative humidity during electrospinning on the morphology and mechanical properties of nanofibers', *International Journal of Pharmaceutics*, vol. 456, no. 1, pp. 125-34.
- Peñate, B. & García-Rodríguez, L. 2012, 'Current trends and future prospects in the design of seawater reverse osmosis desalination technology', *Desalination*, vol. 284, pp. 1-8.
- Prince, J.A., Rana, D., Matsuura, T., Ayyanar, N., Shanmugasundaram, T.S. & Singh, G. 2014, 'Nanofiber based triple layer hydro-philic/-phobic membrane - a solution for pore wetting in membrane distillation', *Sci. Rep.*, vol. 4.
- Properties 2015, Sigma-aldrich, viewed 11/06/2015 2015, <<http://www.sigmaaldrich.com/catalog/product/aldrich/427179?lang=en®ion=AU>>.

- Razmjou, A., Arifin, E., Dong, G., Mansouri, J. & Chen, V. 2012, 'Superhydrophobic modification of TiO₂ nanocomposite PVDF membranes for applications in membrane distillation', *Journal of Membrane Science*, vol. 415, pp. 850-63.
- Shang, H., Wang, Y., Limmer, S., Chou, T., Takahashi, K. & Cao, G. 2005, 'Optically transparent superhydrophobic silica-based films', *Thin Solid Films*, vol. 472, no. 1, pp. 37-43.
- Shirazi, M.M.A., Kargari, A. & Tabatabaei, M. 2014, 'Evaluation of commercial PTFE membranes in desalination by direct contact membrane distillation', *Chemical Engineering and Processing: Process Intensification*, vol. 76, pp. 16-25.
- Song, Z.W. & Jiang, L.Y. 2013, 'Optimization of morphology and performance of PVDF hollow fiber for direct contact membrane distillation using experimental design', *Chemical Engineering Science*, vol. 101, no. 0, pp. 130-43.
- Tian, R., Gao, H., Yang, X., Yan, S. & Li, S. 2014a, 'A new enhancement technique on air gap membrane distillation', *Desalination*, vol. 332, no. 1, pp. 52-9.
- Tian, R., Gao, H., Yang, X.H., Yan, S.Y. & Li, S. 2014b, 'A new enhancement technique on air gap membrane distillation', *Desalination*, vol. 332, no. 1, pp. 52-9.
- Tijing, L.D., Choi, J.-S., Lee, S., Kim, S.-H. & Shon, H.K. 2014a, 'Recent progress of membrane distillation using electrospun nanofibrous membrane', *Journal of Membrane Science*, vol. 453, no. 0, pp. 435-62.
- Tijing, L.D., Woo, Y.C., Johir, M.A.H., Choi, J.-S. & Shon, H.K. 2014b, 'A novel dual-layer bicomponent electrospun nanofibrous membrane for desalination by direct contact membrane distillation', *Chemical Engineering Journal*, vol. 256, pp. 155-9.
- Tomaszewska, M., Gryta, M. & Morawski, A.W. 1994, 'A study of separation by the direct-contact membrane distillation process', *Separations Technology*, vol. 4, no. 4, pp. 244-8.
- Vogelaar, L., Lammertink, R.G. & Wessling, M. 2006, 'Superhydrophobic surfaces having two-fold adjustable roughness prepared in a single step', *Langmuir*, vol. 22, no. 7, pp. 3125-30.
- Wang, P. & Chung, T.-S. 2015, 'Recent advances in membrane distillation processes: Membrane development, configuration design and application exploring', *Journal of Membrane Science*, vol. 474, pp. 39-56.
- Warsinger, D.E., Swaminathan, J. & Maswadeh, L.A. 2015, 'Superhydrophobic condenser surfaces for air gap membrane distillation', *Journal of Membrane Science*, vol. 492, pp. 578-87.
- Woo, Y.C., Tijing, L.D., Park, M.J., Yao, M., Choi, J.-S., Lee, S., Kim, S.-H., An, K.-J. & Shon, H.K. 2015, 'Electrospun dual-layer nonwoven membrane for desalination by air gap membrane distillation', *Desalination*.
- Wu, H.Y., Wang, R. & Field, R.W. 2014, 'Direct contact membrane distillation: An experimental and analytical investigation of the effect of membrane thickness upon transmembrane flux', *Journal of Membrane Science*, vol. 470, no. 0, pp. 257-65.
- Xiao, T., Wang, P., Yang, X., Cai, X. & Lu, J. 2015, 'Fabrication and characterization of novel asymmetric polyvinylidene fluoride (PVDF) membranes by the nonsolvent thermally induced phase separation (NTIPS) method for membrane distillation applications', *Journal of Membrane Science*, vol. 489, pp. 160-74.
- Xie, Q., Fan, G., Zhao, N., Guo, X., Xu, J., Dong, J., Zhang, L. & Zhang, Y. 2004, 'Facile Creation of a Bionic Super-Hydrophobic Block Copolymer Surface', *Advanced materials*, vol. 16, no. 20, pp. 1830-3.

- Yang, C., Li, X.-M., Gilron, J., Kong, D.-f., Yin, Y., Oren, Y., Linder, C. & He, T. 2014, 'CF 4 plasma-modified superhydrophobic PVDF membranes for direct contact membrane distillation', *Journal of Membrane Science*, vol. 456, pp. 155-61.
- Zhang, J., Gray, S. & Li, J.-D. 2013a, 'Predicting the influence of operating conditions on DCMD flux and thermal efficiency for incompressible and compressible membrane systems', *Desalination*, vol. 323, no. 0, pp. 142-9.
- Zhang, J., Li, J.-D. & Gray, S. 2011, 'Effect of applied pressure on performance of PTFE membrane in DCMD', *Journal of Membrane Science*, vol. 369, no. 1-2, pp. 514-25.
- Zhang, J., Xu, Z., Shan, M., Zhou, B., Li, Y., Li, B., Niu, J. & Qian, X. 2013b, 'Synergetic effects of oxidized carbon nanotubes and graphene oxide on fouling control and anti-fouling mechanism of polyvinylidene fluoride ultrafiltration membranes', *Journal of Membrane Science*, vol. 448, pp. 81-92.
- Zhang, J., Yin, G.-P., Wang, Z.-B., Lai, Q.-Z. & Cai, K.-D. 2007, 'Effects of hot pressing conditions on the performances of MEAs for direct methanol fuel cells', *Journal of Power Sources*, vol. 165, no. 1, pp. 73-81.
- Zhang, P. & Lv, F.Y. 2015, 'A review of the recent advances in superhydrophobic surfaces and the emerging energy-related applications', *Energy*, vol. 82, pp. 1068-87.
- Zhang, P., Zhao, X., Zhang, X., Lai, Y., Wang, X., Li, J., Wei, G. & Su, Z. 2014, 'Electrospun doping of carbon nanotubes and platinum nanoparticles into the β -phase polyvinylidene difluoride nanofibrous membrane for biosensor and catalysis applications', *ACS applied materials & interfaces*, vol. 6, no. 10, pp. 7563-71.
- Zhu, L., Xiu, Y., Xu, J., Tamirisa, P.A., Hess, D.W. & Wong, C.-P. 2005, 'Superhydrophobicity on two-tier rough surfaces fabricated by controlled growth of aligned carbon nanotube arrays coated with fluorocarbon', *Langmuir*, vol. 21, no. 24, pp. 11208-12.